AD-A242 843

NAVAL POSTGRADUATE SCHOOL
Monterey, California

THESIS

SOURCE OF COLD WATER IN MONTEREY BAY
OBSERVED BY AVHRR SATELLITE IMAGERY

by

Dan E. Tracy

December 1990

Thesis Advisor: Leslie K. Rosenfeld
Co-Advisor: Newell Garfield
Co-Advisor   Franklin B. Schwing

Approved for public release; distribution unlimited.

91-16268

Unclassified
Security Classification of this page

REPORT DOCUMENTATION PAGE

1a Report Security Classification Unclassified		1b Restrictive Markings			
2a. Security Classification Authority		3 Distribution Availability of Report			
2b Declassification/Downgrading Schedule		Approved for public release; distribution is unlimited.			
4 Performing Organization Report Number(s)		5 Monitoring Organization Report Number(s)			
6a Name of Performing Organization Naval Postgraduate School	6b Office Symbol *(If Applicable)* OC	7a Name of Monitoring Organization Naval Postgraduate School			
6c Address *(city, state, and ZIP code)* Monterey, CA 93943-5000		7b Address *(city, state, and ZIP code)* Monterey, CA 93943-5000			
8a Name of Funding/Sponsoring Organization	8b Office Symbol *(If Applicable)*	9 Procurement Instrument Identification Number			
8c Address *(city, state, and ZIP code)*		10 Source of Funding Numbers			
		Program Element Number	Project No	Task No	Work Unit Accession No
11 Title *(Include Security Classification)* SOURCE OF COLD WATER IN MONTEREY BAY OBSERVED BY AVHRR SATELLITE IMAGERY					
12 Personal Author(s) Tracy, Dan E.					
13a Type of Report Master's Thesis	13b Time Covered From To	14 Date of Report *(year, month,day)* 1990, December	15 Page Count 137		
16 Supplementary Notation The views expressed in this thesis are those of the author and do not reflect the official policy or position of the Department of Defense or the U.S. Government.					

17 Cosati Codes			18 Subject Terms *(continue on reverse if necessary and identify by block number)*
Field	Group	Subgroup	Monterey Bay, Currents, AVHRR satellite imagery, upwelling, jets, plumes, eddies

19 Abstract *(continue on reverse if necessary and identify by block number)*

A one year record of AVHRR satellite images, beginning October 1, 1988, was processed and evaluated to determine the source of cold, nutrient-rich water in Monterey Bay. Wind records indicated a strong correlation with the intensity of upwelling at Año Nuevo and Point Sur as seen in numerous satellite images. Close quantitative agreement between satellite derived multi-channel sea surface temperature and in situ observation of sea surface temperature by oceanographic research ships support remote sensing as a valid tool for observing thermal gradients.

During upwelling events in the spring and summer, offshore plumes of cold water appear at Año Nuevo and Point Sur. In addition, southward flow at both locations is inferred from satellite images and from vertical temperature profiles. One jet of cool water, approximately 10 km wide and 30 m deep originates at Año Nuevo and flows south across the mouth of the Monterey Bay, effectively isolating the Bay from oceanic surface circulation. Cool surface water is injected into the middle and southern Bay resulting in a generally cyclonic flow inside the Bay. Offshore, a warm core, anticyclonic eddy persists with a radius of 30 km. It is bounded on the north and south by the previously mentioned offshore plumes and on the east by the southward flow from Año Nuevo.

During wind relaxation and/or reversal, the upwelling ceases, the southward jet also ceases, and oceanic water from the warm core eddy rushes into the Bay with circulation that appears to be anticyclonic. This revelation of surface circulation in the Bay seems to agree with most historical observations, but does not support the historical interpretations of Monterey Submarine Canyon induced upwelling, or northward flow of upwelled water from Point Sur into the Bay. The cold water observed in Monterey Bay is clearly related to the recently upwelled water advected southward from Año Nuevo.

20 Distribution/Availability of Abstract [X] unclassified/unlimited [ ] same as report [ ] DTIC users Unclassified	21 Abstract Security Classification Unclassified	
22a Name of Responsible Individual Leslie K. Rosenfeld	22b Telephone *(Include Area code)* (408) 646-3226	22c Office Symbol OC/Ro

DD FORM 1473, 84 MAR   83 APR edition may be used until exhausted   security classification of this page
All other editions are obsolete

Unclassified

Source of Cold Water in Monterey Bay Observed by AVHRR Satellite Imagery.

by

Dan E. Tracy
Commander, NOAA Corps
B.S., San Jose State University, 1968
M.S., San Jose State University, 1971

Submitted in partial fulfillment of the requirements
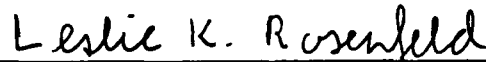for the degree of

MASTER OF SCIENCE IN PHYSICAL OCEANOGRAPHY

from the
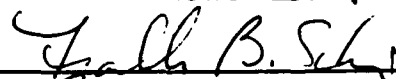
NAVAL POSTGRADUATE SCHOOL
December, 1990

Author: _____
Dan E. Tracy

Approved by: _____
Leslie K. Rosenfeld, Thesis Advisor

_____
Newell Garfield, Co-Advisor

_____
Franklin B. Schwing, Co-Advisor

_____
Curtis A. Collins, Chairman, Department of Oceanography

ii

ABSTRACT

A one year record of AVHRR satellite images, beginning October 1, 1988, was processed and evaluated to determine the source of cold, nutrient-rich water in Monterey Bay. Wind records indicated a strong correlation with the intensity of upwelling at Año Nuevo and Point Sur as seen in numerous satellite images. Close quantitative agreement between satellite derived multi-channel sea surface temperature and in situ observation of sea surface temperature by oceanographic research ships support remote sensing as a valid tool for observing thermal gradients.

During upwelling events in the spring and summer, offshore plumes of cold water appear at Año Nuevo and Point Sur. In addition, southward flow at both locations is inferred from satellite images and from vertical temperature profiles. One jet of cool water, approximately 10 km wide and 30 m deep originates at Año Nuevo and flows south across the mouth of the Monterey Bay, effectively isolating the Bay from oceanic surface circulation. Cool surface water is injected into the middle and southern Bay resulting in a generally cyclonic flow inside the Bay. Offshore, a warm core, anticyclonic eddy persists with a radius of 30 km. It is bounded on the north and south by the previously mentioned offshore plumes and on the east by the southward flow from Año Nuevo.

During wind relaxation and/or reversal, the upwelling ceases, the southward jet also ceases, and oceanic water from the warm core eddy rushes into the Bay with circulation that appears to be anticyclonic. This revelation of surface circulation in the Bay seems to agree with most historical observations, but does not support the historical interpretations of Monterey Submarine Canyon induced upwelling, or northward flow of upwelled water from Point Sur into the Bay. The cold water observed in Monterey Bay is clearly related to the recently upwelled water advected southward from Año Nuevo.

iii

TABLE OF CONTENTS

LIST OF FIGURES

ACKNOWLEDGMENTS

I. INTRODUCTION

Monterey Bay is located on the central California coast (36.8°N, 122.0 ฬ)
approximately 100 km south of San Francisco. The Bay is oriented north-south and is
open to the Pacific Ocean on the west. The dimensions of the Bay are 36 km north-south
and 20 km east-west (Figure 1). The Bay is shallow, with 82 percent of the area which lies
inside the Bay shallower than 100 m (Breaker and Broenkow 1989).

The Bay is divided equally into a northern and a southern bight by the Monterey
Submarine Canyon. The Canyon's axis is east-west and its depth (Figure 2) is similar to
the relief of the Grand Canyon (Shepard 1966). The Canyon descends rapidly to a depth
of 2000 m inside the Bay and begins to meander southward outside the Bay as it continues
to descend below 3000 m. The steep, rocky walls of the Canyon reach heights of almost
1500 m. The Canyon floor widens from a narrow channel at the head to a 5 km width at a
depth of 1900 m.

Occasional AVHRR satellite images of Monterey Bay show an isolated cold water
cell located over the middle of the Bay. Hydrographic stations also indicate cold surface
water in the mid-Bay. A natural question to ask is, "What is the source of this cold water?"
Is the upwelling the result of local processes or advection from a remote source? Local
production could be the result of upwelling from the Monterey Submarine Canyon caused
by local wind shear, convergence of submarine currents, interaction of internal waves with
topography, or other forcing parameters. Remote sources are the known upwelling sites
located north of the Bay at Año Nuevo and south at Point Sur.

Since the question was initiated by viewing an AVHRR satellite image, perhaps the
solution may also be found using satellite imagery. A one year historical record of low
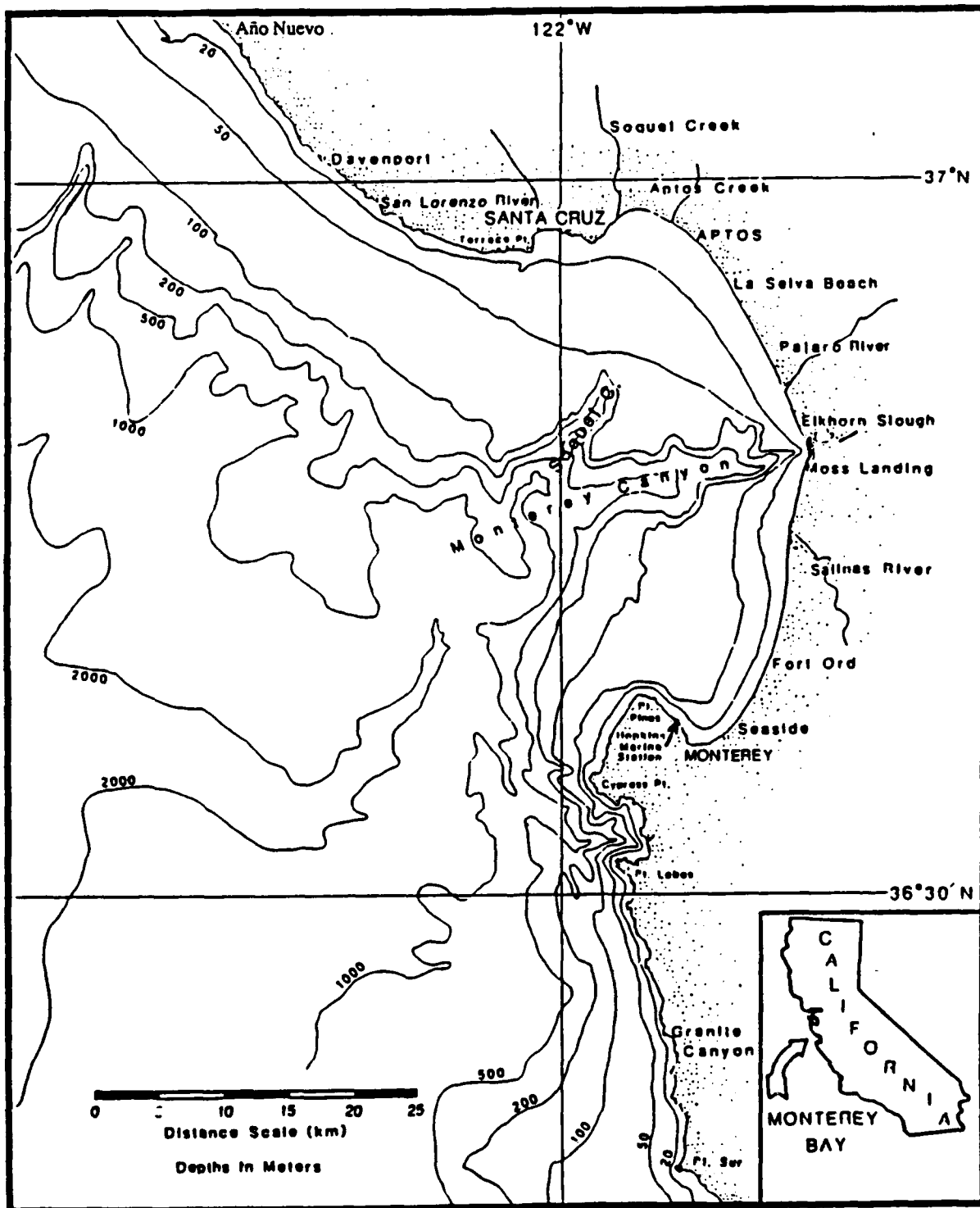
Figure 1.   Chart of Monterey Bay and surrounding area (Breaker and Broenkow 1989)
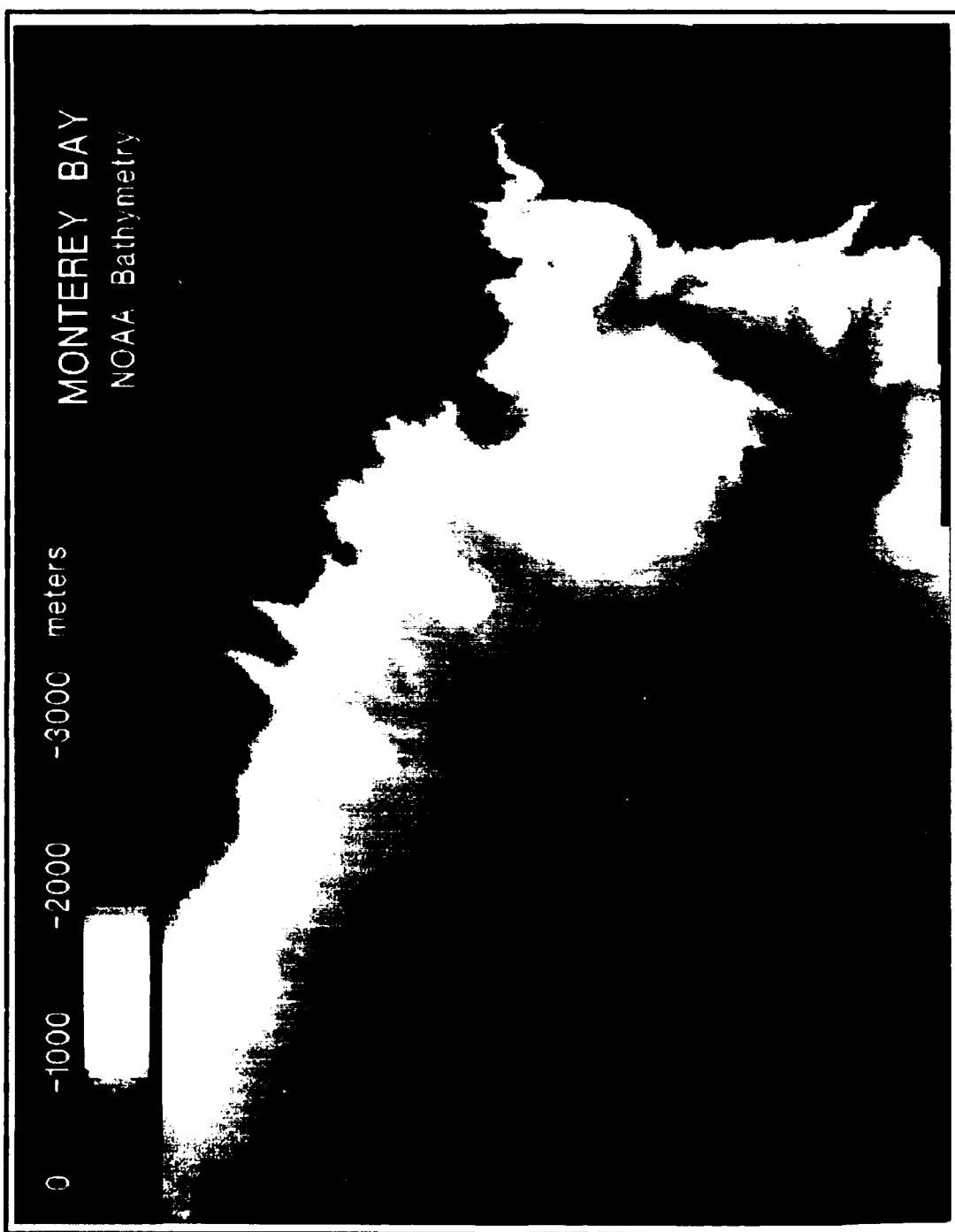
Figure 2. NOAA bathymetry of Monterey Submarine Canyon plotted using TerraScan software. The contour interval is 50 m with a range from sea level (red) down to 3,500 m (Violet).

3

THIS PAGE INTENTIONALLY LEFT BLANK

resolution AVHRR hard copy images, beginning October 1, 1988, was reviewed to identify the dates of cloud free satellite coverage of Monterey Bay. Subsequently, 112 AVHRR high resolution images were processed and analyzed to help determine the source of cold, nutrient-rich surface water in the Bay and its subsequent effect on circulation.

Satellite observations, during the 1988-89 winter, indicated that uniformly cold surface water existed both inside and outside the Bay. The thermal uniformity reduced the information extractable from the satellite imagery to infer surface currents. During the spring, the surface temperature along the Central California Coast increased, thus providing a greater thermal contrast between the cold upwelled water near Monterey Bay and the warm water unaffected by upwelling. The thermal gradients in a satellite image allow the viewer to infer circulation - especially if concurrent vertical temperature profiles and transections are available.

A sequential series of images gives a much better perspective than a single image by placing unique features in context of the total implied surface circulation pattern. Persistent features are more noticeable and dynamic features become quite obvious. Several days of sequential satellite images during spring upwelling and relaxation events show evidence of a dominant circulation pattern related to wind forcing.

Wind records show that northwesterly winds are dominant near Monterey which generate an upwelling circulation regime. If the winds relax and/or reverse direction, currents can reverse direction, potentially impacting the various activities in the Bay.

Previous oceanographic studies conducted in Monterey Bay have not considered the coastal wind field, primarily because long land-based observations are not indicative of the coastal winds and wind data from the Monterey meteorological buoy 46042 has only become available since 1987. Tidal currents have been studied using drogues, but Lagrangian drifters have not been of sufficient duration to resolve synoptic scale events.

Fixed current meter moorings have been deployed over longer periods of time, but the spatial coverage was very limited. Satellite imagery provides broad spatial coverage and at least daily images when clouds do not obscure the Bay.

Environmental data were available from sources other than satellite imagery. A long term meteorological mooring just outside the mouth of Monterey Bay provided coastal wind data. During part of the year, several oceanographic research vessels were in the greater Monterey Bay area collecting hydrographic data. As a result, surface temperature observations from satellite were confirmed by shipboard measurement and vertical temperature structure provided a more complete interpretation of the circulation in Monterey Bay.

This circulation in Monterey Bay is of broad interest. It has great impact on primary productivity, fishery recruitment, pollution dispersal, search and rescue, sediment transport (erosion), fishing, and recreation. During the upwelling season, synoptic winds appear to be the primary driving force for circulation in the Bay. Also, circulation near Monterey Bay is an important consideration in establishing offshore petroleum lease sites and the boundaries of the proposed Monterey Bay Marine Sanctuary. This thesis develops a conceptual model for circulation in the greater Monterey Bay.

II. HISTORICAL OBSERVATIONS

A. SURFACE CIRCULATION OUTSIDE MONTEREY BAY

1. California Current

Since the Bay is open to oceanic forcing on the west, the effects of oceanic circulation near Monterey may be important to circulation within the Bay. The eastern Pacific flow is dominated by the effects of the California Current System, which is generally described as the southward return flow from the North Pacific gyre and occurs within 1000 km of the eastern boundary of United States (Hickey 1979). This broad diffuse current is fed by the North Pacific Current and transports Subarctic water southward with the addition of Subtropical water offshore of Monterey.

Using California Cooperative Oceanic Fisheries (CALCOFI) data, Wyllie (1966) produced monthly coastal maps of geostrophic flow at the surface relative to 500 db by averaging over the years 1950-1965. The 500 db reference was based on the deepest common depth of data rather than a level of no motion. These maps indicate that a permanent counterclockwise gyre exists off San Francisco and southward about half the distance to Point Conception. This eddy produces northward flow within 100 km of the coast. The flow is strongest from November to January, much weaker during spring, and becomes southward during April.

On the other hand, drift bottles released close to shore generally indicate a southward flow (Schwartzlose 1963; Crowe and Schwartzlose 1972). Hickey (1979) concludes the drift bottle results could be consistent with the dynamic topographies from CALCOFI if there was a southward current very near the coast that was not resolved by the large station spacing of CALCOFI.

7

Similarly, ship drift data indicate a southward current field near Monterey Bay (Nelson 1976). Nelson further observes the southward flow generally has an offshore (cross-isobath) component which he attributed to wind effects (i.e., Ekman drift) being a substantial part of the velocity measured by ship drift.

In addition, currents were measured at 11 current meter locations along the central California coast from February 1984 to July 1985 in the Central California Coastal Circulation Study (CCCCS) (Chelton *et al.* 1987). Moorings were installed at the 100 m and 250 m isobaths with two moorings located near Point Sur and two moorings located halfway between Monterey and San Francisco.

Chelton *et al.* observed generally poleward and offshore flow near Point Sur, but north of Monterey the nearshore flow was generally equatorward. Similar results were seen from his hydrographic sections north of Monterey; nearshore flow was equatorward with poleward flow offshore. Their map of surface dynamic topography for July 1984 indicated an anticyclonic warm core eddy just offshore of Monterey Bay (Figure 3). Chelton *et al.* observed considerable variability in alongshore shelf currents and concluded that the variance was most likely due to local wind forcing.

Skogsberg (1936) suggested that a deep southward current across the mouth of Monterey Bay acted as an eastern boundary for upwelling as northwesterly winds transported surface water further offshore, thus bringing cold water to the surface which then flowed into the Bay.

2. California Undercurrent

Below 150 m, the California Undercurrent (CUC) flows northward (Hickey 1979). The CUC veers to the right due to the Coriolis force and is trapped against the coast as it continues to flow northward. The CUC is further constrained to flow at a depth determined by the density of the warm, saline water compared with the surrounding water.

Wickham, Bird, and Mooers (1987) found the CUC to have a jet-like core near Cape San Martin (60 km south of Point Sur) with velocities in excess of 15 cm/s. Hickey points out that the flow is generally confined to the upper 300 m of the water column and to within 30 km of the coast. The variability is predominantly annual with a maximum poleward flow in May-June. However, Wyllie (1966) observed that the CUC reaches a minimum between
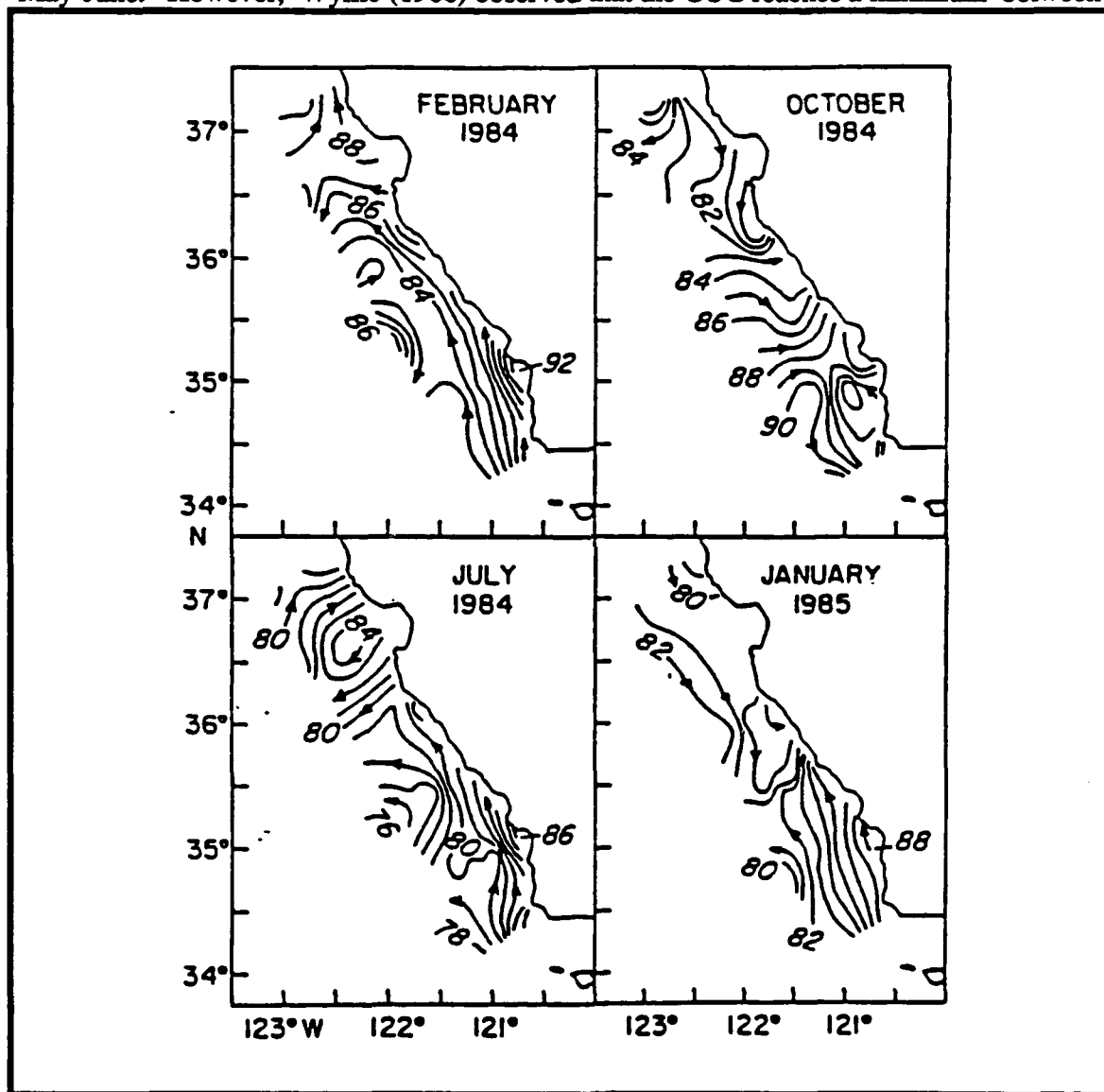
Figure 3. Surface dynamic topography relative to 500 m (1 dyn-cm contour interval) for each of four CTD surveys. CCCCS station spacing was 50 km, along-shore, and 20 km, cross-shore, within 100 km of shore. (After Chelton et al. 1987)

March and May. Obviously, there is great variability in the CUC and the dynamics are not well understood.

3.   Davidson Current

Generally, as the subtropical high dissipates in the fall and winter, the northwesterly winds subside, upwelling decreases, and a northward flowing, nearshore current becomes established that may in fact be the surface manifestation of the CUC. This current is called the Davidson current (Hickey 1979).

B.   CIRCULATION INSIDE MONTEREY BAY

1.   Indirect Measurements

Breaker and Broenkow (1989) noted that most studies of Monterey Bay circulation have been highly focussed, only considering certain limited aspects of the circulation within the Bay. No systematic long-term current measurements have been made throughout the interior of the Bay to determine its general circulation and primary driving forces. It seems there are offshore studies (e.g., CALCOFI, CCCCS, etc.) and Monterey Bay studies, but no comprehensive studies that measure the interaction of the coastal circulation with that of the Bay.

Bigelow and Leslie (1930) conducted the first hydrographic survey of any consequence in Monterey Bay. Temperature and salinity measurements were taken at 21 stations broadly spaced throughout the Bay between June 30 and July 24, 1928 (Figure 4). Vertical spacing of samples was fine in the upper 25 m, but coarse in the deeper measurements. Sample depths were not uniformly fixed and the limitation of their Nansen bottle sampling required considerable interpolation between measurement depths for vertical cross-sections of temperature.

Since the observed mean surface temperature throughout the Bay was 13.4°C and the maximum deviation was 2.4°C, Bigelow and Leslie observed "great

10

regional uniformity which is evidently characteristic of Monterey Bay." Bigelow and Leslie assumed the Bay was quiescent and considered the survey to be synoptic. Thus, although the survey took over three weeks to complete, they compared data between stations taken weeks apart. They also neglected the effects of high frequency temporal variability on the vertical temperature distribution.
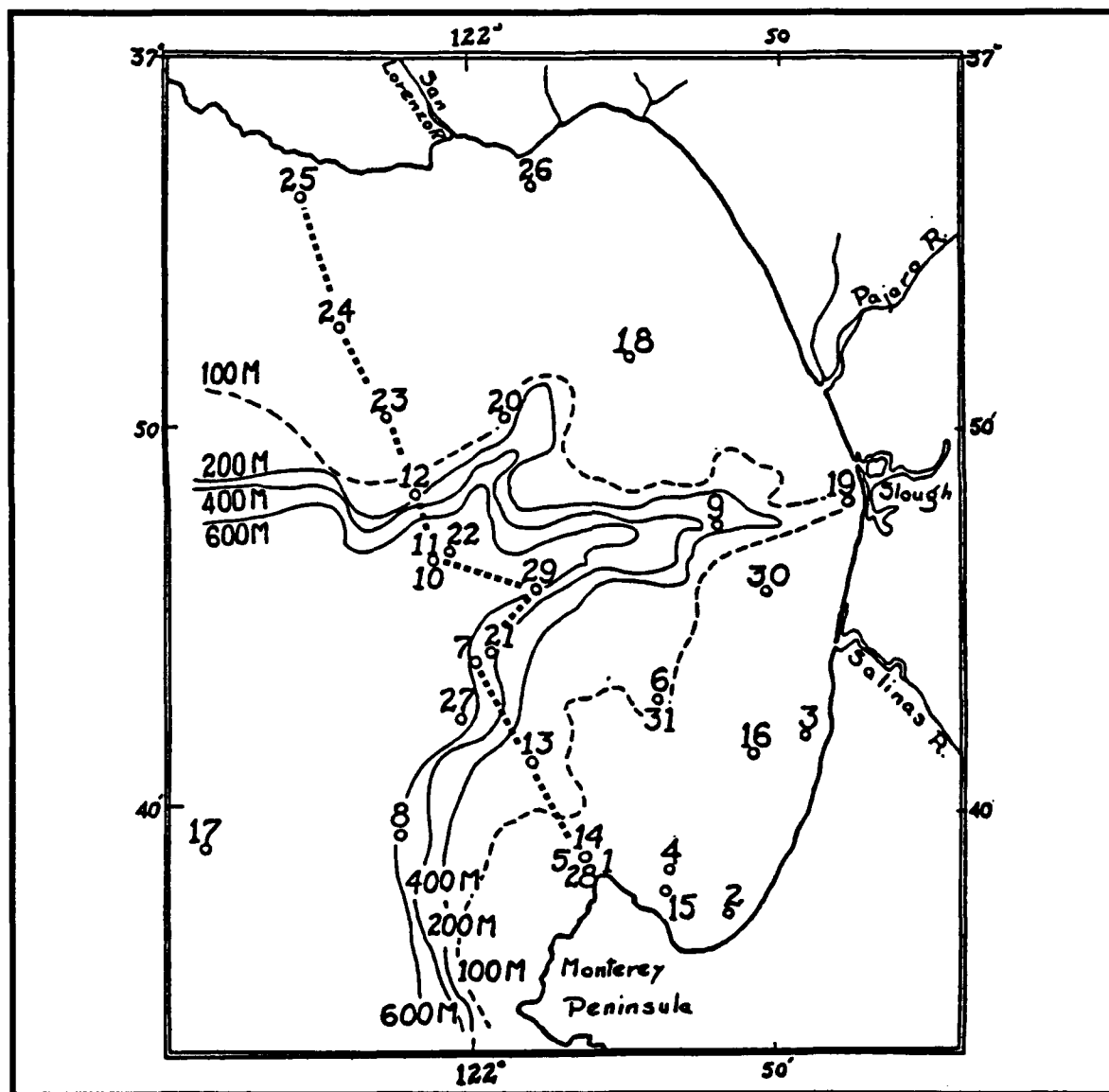
Figure 4. Chart of Monterey Bay, showing locations of stations, and bottom contours for depths of 100, 200, 400, and 600 m (Bigelow and Leslie 1930)

Along Bigelow and Leslie's cross-canyon transection (Figure 5) warm deep water was found in the central Canyon at station 29 compared to cool deep water at stations 10 and 7, located on either side of station 29. The cold water on either side of the Canyon axis was interpreted as upwelling along the Canyon walls. In fact, this argument appears to be the major historical justification for the theory of canyon-induced upwelling inside Monterey Bay, and has become a widely distributed concept throughout the literature today.
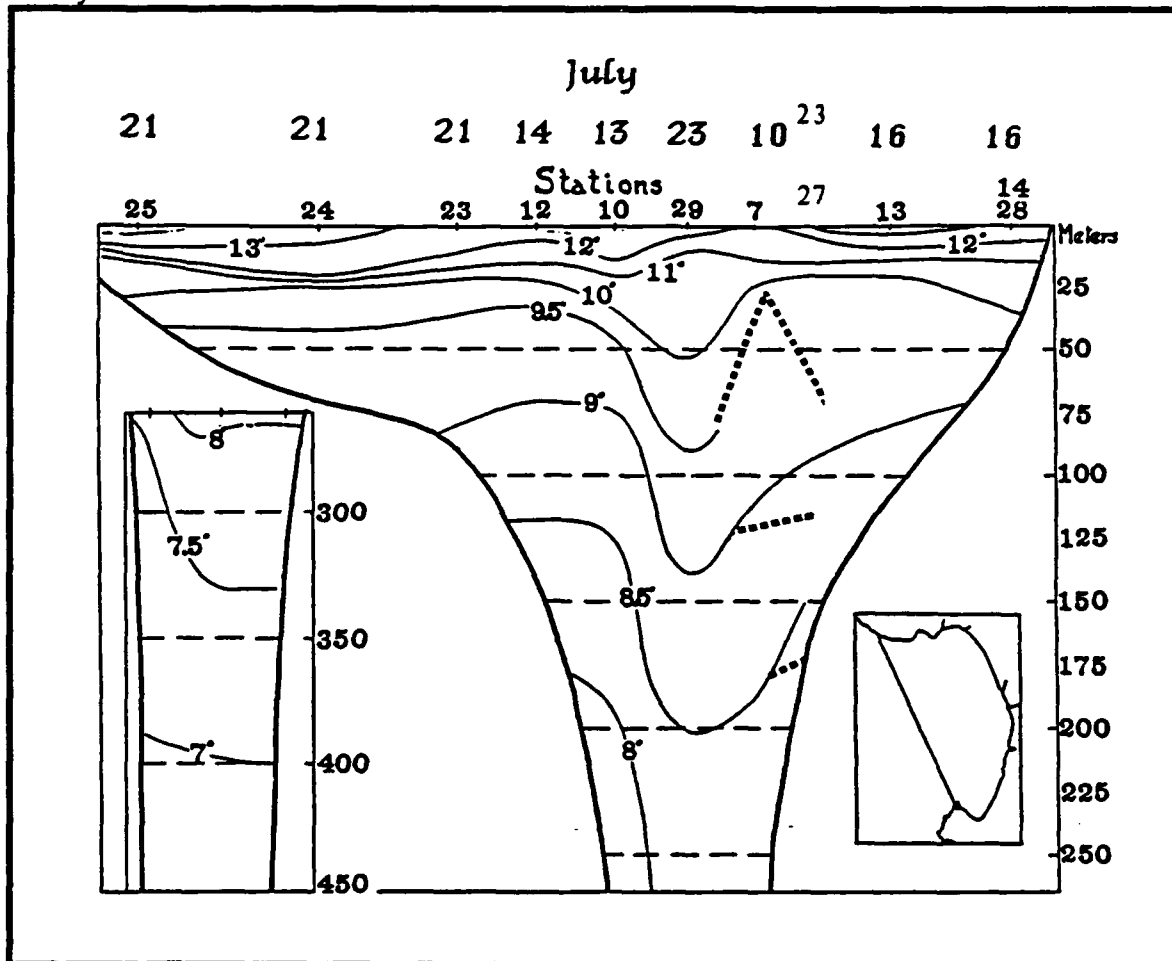
Figure 5. Hydrographic transection across the mouth of Monterey Bay during July, 1928. Date of station is indicated above station number. Descending isotherms at station 29 promote the concept of upwelling over canyon walls (Bigelow and Leslie 1930). However this station was taken almost two weeks after the stations on either side. Dashed lines show the results of including station 27.

It must be pointed out, however, that station 29 was observed 10 days later than station 10. Continuing across the transection, station 27 lies just south of station 7, again observations were separated by 10 days. Station 27 also shows warmer deep water like station 29 (see dashed line on Figure 5), but was not included in the vertical transection provided by Bigelow and Leslie. Clearly, stations 29 and 27 are similar in vertical temperature distribution but much warmer than the adjacent stations 7, 10, and 13 taken almost two weeks earlier. This supports the notion that there is significant temperature variability in the Bay over time, and places great skepticism on Bigelow and Leslie's claim for upwelling in the Canyon.

Taking a closer look at the data from the mouth of the Bay, station 10 had a surface temperature of 13.1 °C, but 10 days later, the temperature had dropped to 12.5 °C at nearby station 29. Also, the 100 m depth temperature measurements at these respective stations show 8.7 and 9.4 °C. It is precisely this 0.7 °C temperature difference which is claimed to indicate upwelling in the Canyon.

Skogsberg (1936) observed great variability over a short time in vertical temperature profiles, and stated that Bigelow and Leslie's field procedure was not valid in the Bay. Shea and Broenkow (1982) observed large (120 m) vertical excursions of isotherms due to internal tides. Koehler (1990) also found great temporal variability in vertical temperature structure in the Bay.

Obviously it is difficult to intercompare data when sample depths are not held constant and the survey is not synoptic. Bigelow and Leslie (1930) provided a good baseline survey of Monterey Bay considering their inadequate spatial sampling, insufficient shiptime, and their scant knowledge of the circulation in the Bay. However, their interpretation of upwelling along the Canyon walls must be critically analyzed in light of more recent research in the Bay.

13

Skogsberg (1936) conducted an extended oceanographic study of the southern Monterey Bay primarily by vertical temperature measurements during 1929 - 1933. His survey provided weekly observations at several locations including stations 4 and B (Figure 6). Initial temperature measurements demonstrated that the hydrographic situation of the southern end of the Bay was ever changing and he hypothesized that the changes were caused by forces outside of Monterey Bay. It became evident that the field technique used by Bigelow and Leslie (inter-comparison of vertical temperature measurements from stations taken at different times) should under no circumstances be applied to this region.

By combining the weekly temperature averages for five years of data from stations 4 and B, Skogsberg presented the "normal annual rhythm" for the upper 100 m in Monterey Bay. There appeared to be three hydrographic seasons related to his perception of water source (Figure 7). The "upwelling period" extended from mid-February through August, the "oceanic period" extended from September through October, and the "Davidson Current period" which extended from November until mid-February. Notice most of his stations were in the south Bay.

Later Skogsberg redefines these three periods to represent the type of water in the Bay. The "cold water phase" extended from mid-February through November, a "warm water phase" extended from mid-August to mid-October and a "low thermal gradient phase" which extended from December to mid-February. Skogsberg attributed the "cold water phase" to upwelled water; 9 °C water was elevated from below 100 m depths to as high as 30 m inside the Bay.

The effects of upwelling were quite variable in time and amplitude. Upwelling didn't begin at the same time each year and there were strong, moderate, and weak years. The onset of upwelled water in the upper 200 m was quite rapid and highly correlated with the wind.

14
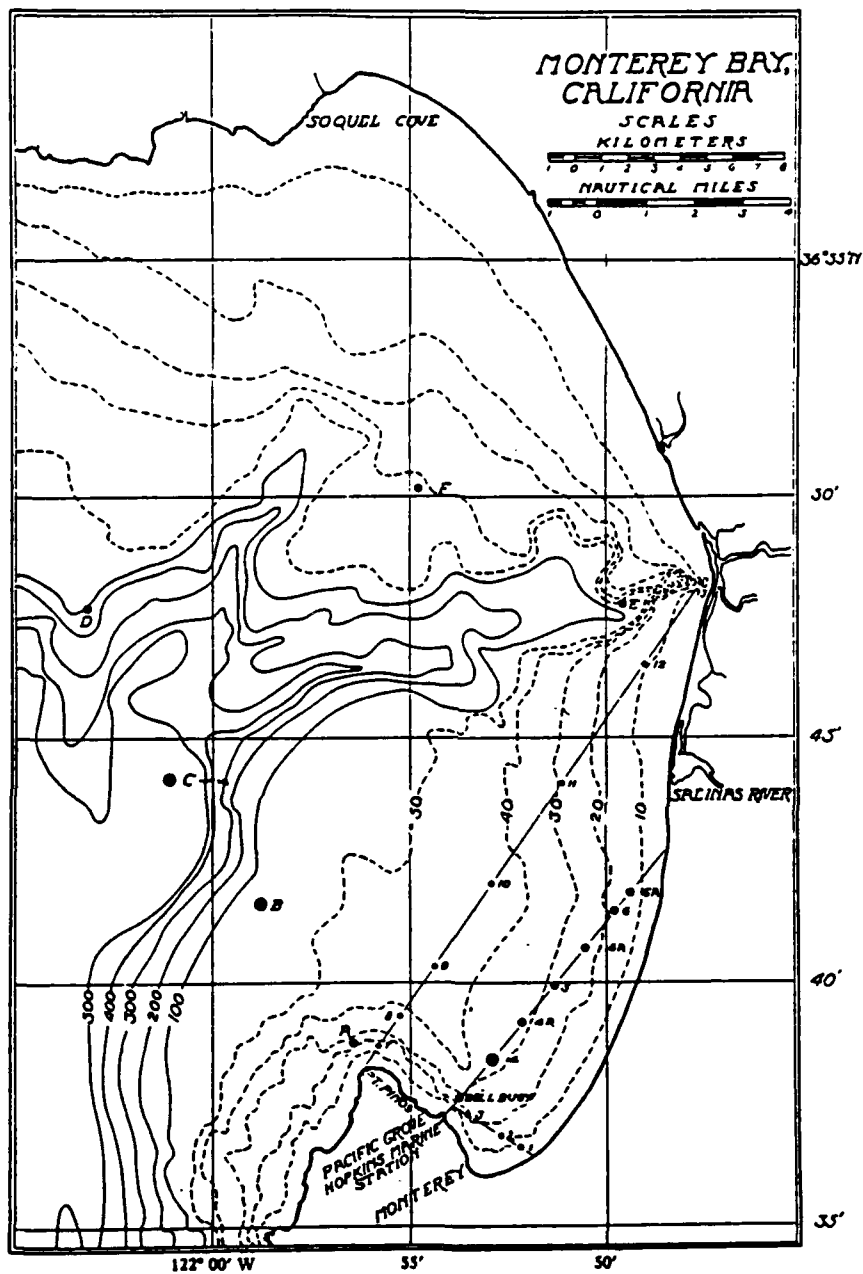
Figure 6.   Map of Monterey Bay CTD stations investigated by Skogsberg (1929-1933). Large dots indicate stations which were treated most extensively. Notice most of his stations were in the south Bay.
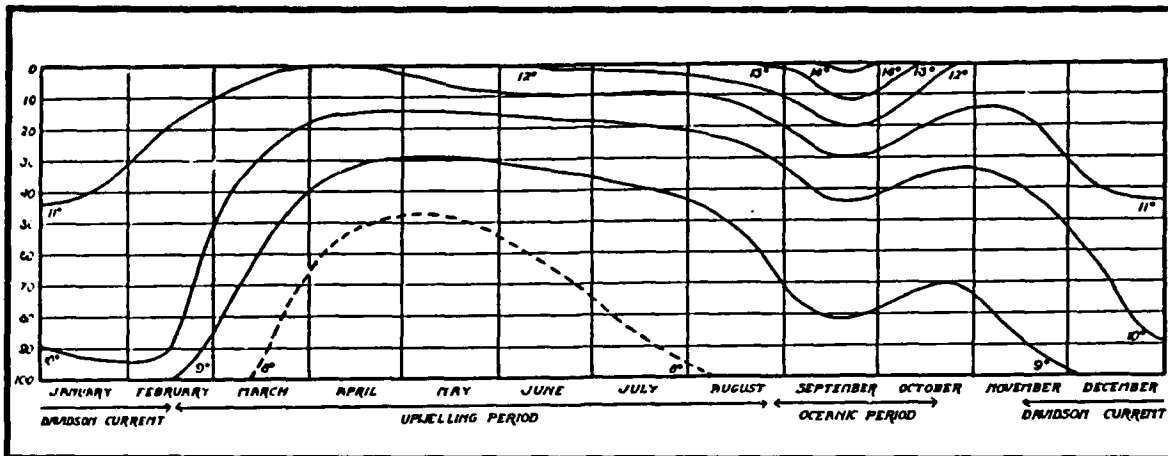
Figure 7. Normal annual rhythm of the temperatures in the upper 100 m, in Monterey Bay, obtained by the combination of the thermal rhythms of 1929-1933. Skogsberg (1936) defines the "upwelling period" from mid-February through August, the "oceanic period" from August through October and the "Davidson Current period" from November to mid-February. Isotherms are plotted above as a function of depth in meters (vertical axis) and month of the year (horizontal axis).
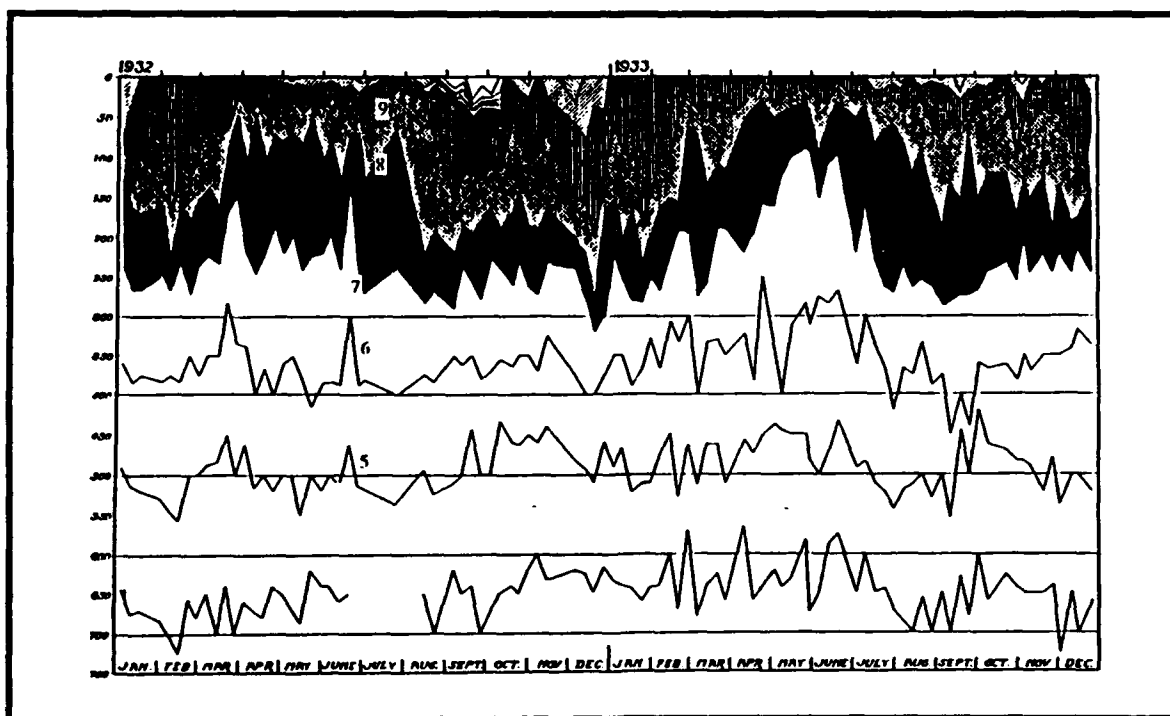
Figure 8. Thermal conditions in the upper 750 m at station C in 1932 and 1933. The swelling of the 7-8°C isotherm (black level) is an indication of advection into the Bay rather than upwelling. Isotherms are plotted above as a function of depth in meters (vertical axis) and month of the year (horizontal axis). (Skogsberg 1936).

16

Another peculiarity of the cold water rhythm is the irregular swelling and shrinking of the various thermal strata; e.g., in the summer of 1932, the thickness of the 7°C to 8°C water layer showed a pronounced expansion (Figure 8). This phenomenon appears to suggest that the actual upwelling had taken place on these occasions at some distance outside the Bay rather than against the continental slope. Advection allows the cold water layer to expand vertically, whereas upwelling from the Canyon would cause the cold layer to rise toward the surface while maintaining a constant vertical thickness.

Over a longer time scale, Skogsberg observed limited upwelling over the Canyon from as deep as 200-500 m depending on the year. When Skogsberg mentions upwelling, he is observing cold water at a higher level. This is not necessarily limited to local upwelling at the exclusion of advection of recently upwelled water along the surface. Also, he found considerable interannual variability in the intensity of upwelling in the Bay.

Skogsberg attributes the "warm water phase" to onshore movement of oceanic water associated with the California Current, which corresponded to the period of weaker and variable winds. The "low thermal gradient phase" coincided with the local occurrence of the northward flowing Davidson Current. Southerly winds during this period produced surface convergence near the coast and thus were responsible for the observed lower thermal gradients in the upper 50 to 100 m.

Skogsberg inferred that coastal waters moved through the Bay sometimes in a northward direction and sometimes in a southward direction, thus stressing the irregularity of Bay circulation and rapidity of change. The shortcoming of these measurements, obviously, was the lack of direct current observations.

Direct observations of the current may provide a more accurate measurement at a few specific locations. But without a comprehensive framework for circulation, it is not clear what accurate measurement of currents in a specific locations indicate.

Skogsberg and Phelps (1946) presented additional results on the hydrography of Monterey Bay for the years 1934-1937. Their earlier results were essentially confirmed, except the three oceanographic seasons were not as distinct. The annual temperature cycle, during 1936 and 1937, is shown (Figure 9) for the upper 100 m at a point 7.5 km NNW of Point Piños, near the southern edge of the Canyon. Upwelling is apparent, starting in February or March and weakening in July. Upwelling was particularly pronounced during March and April 1937, where apparent vertical velocities for the 9, 10, 11 °C isotherms were 3 to 4 m/day. Skogsberg and Phelps, however, did not include the effects of mixing or advection in computing these vertical velocities.
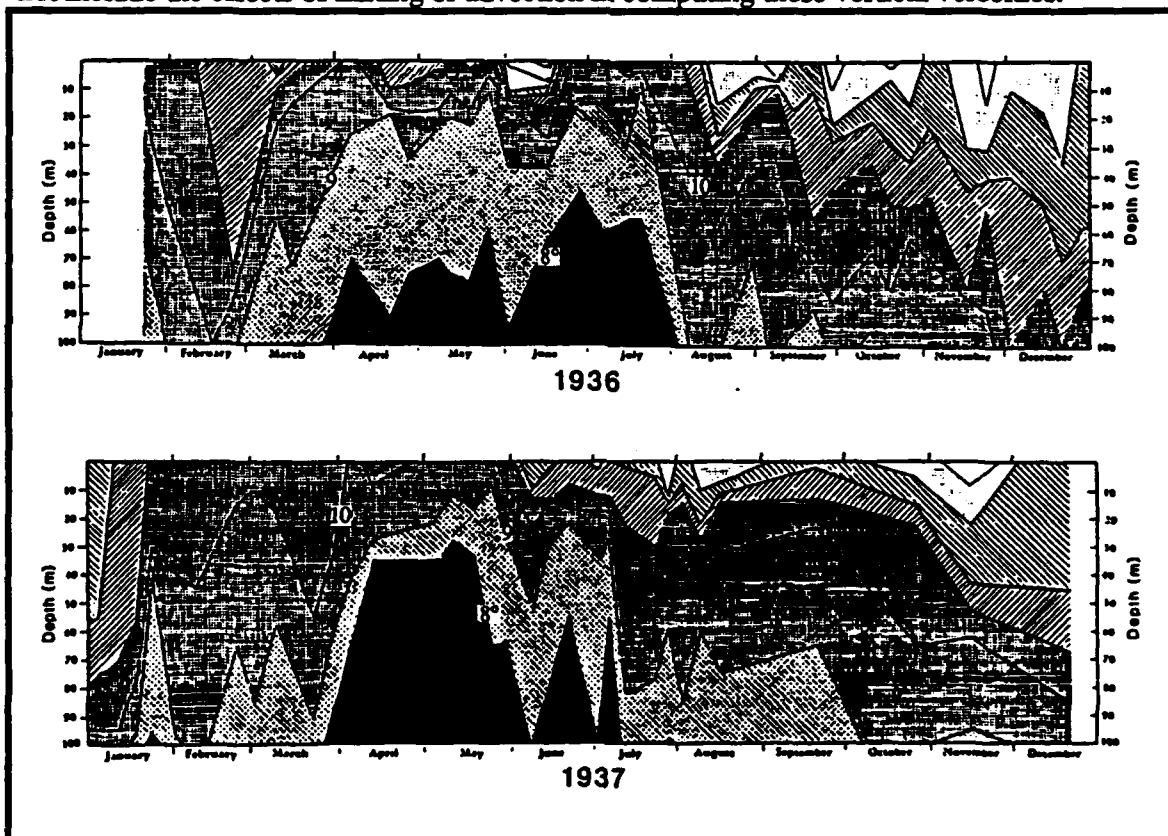
Figure 9   Thermal conditions in the upper 100 m over the entrance of Monterey Bay during 1936 (upper) and 1937 (lower). 7-8°C water is black. Pronounced upwelling occurred during March and April, 1937 with 9, 10 and 11°C isotherms rising at 3 to 4 m/day (Skogsberg and Phelps 1946).

A Progress Report from the California Cooperative Fisheries Investigation (CALCOFI 1958) shows a conceptual model of Monterey Bay circulation (Figure 10) derived from six hydrographic stations during July 7, 1955. Based on temperature, salinity, and wet volume of phytoplankton, there appeared to be a source of cold, saline, low plankton water upwelled from the Submarine Canyon located centrally along the mouth of the Bay. Using an increase in temperature, a decrease in salinity, and an increase in plankton volume, the authors inferred that the circulation was shoreward and southward in the south Bay, and shoreward and northward in the north Bay. Apparently advection of cold, saline water from outside the Bay was not considered as a source of this upwelled water.

Bolin and Abbott (1963) conducted hydrographic and phytoplankton sampling along the central California coast from 1954 until 1960. Weekly observations of temperature at six CALCOFI stations in Monterey Bay were averaged by month and compared to the weekly maximum and minimum values during the month. A large separation of maximum and minimum temperatures was considered an indication of upwelling during the month. Their results were in general agreement with Skogsberg's (1936) three annual seasons. They also found rapid changes in temperature in the Bay and observed large interannual variability as well.

Breaker and Broenkow (1989) reference Anderson (1971) as providing a source of data which indicates that upwelling occurred within the upper 25 m or so across the entrance of the Bay. In fact, the vertical temperature transections from Anderson clearly showed nearshore upwelling in a cross-shore transection at Point Sur. But the cold water observed just outside the Bay in the up-canyon transection appeared to be from horizontal advection because the 11 °C isotherm was essentially level at 25 m across the mouth of the Bay, where warmer surface water is seen both nearer to shore and further offshore.

19

JULY 7, 1955

Temperature (°C)
Salinity (‰)
Wet volume (cc) of phytoplankton

13.88

34.00 2.5
F

35

11.41

34.09
D

36

11.73

34.09
E

10.26 34.14 4
A

MAJOR LOCAL
AREA OF
UPWELLING

20

10.94 4

34.09
B

32

12.38

33.75
C
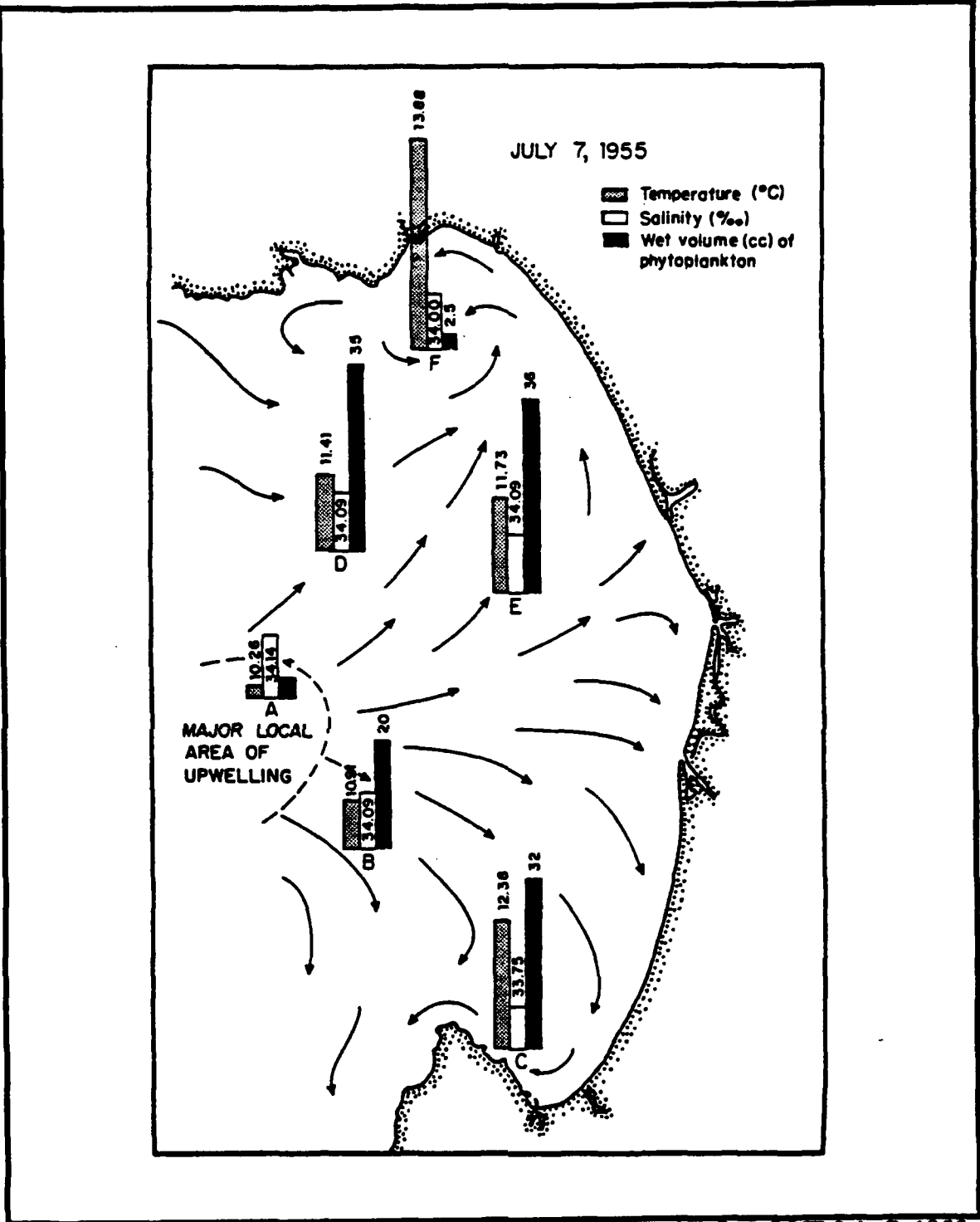
Figure 10. Monterey Bay hydrographic station locations for CALCOFI July 7, 1955. Surface values are given at each station for temperature, salinity, and plankton volume. A major area of local upwelling is sited in mid-Bay with cold water entering at mid-Bay. (CALCOFI Report 1958)

20

Based on the displacement of nutrients and other hydrographic fields in Monterey Bay, Lasley (1977) inferred that the net flow in the Bay was to the north. He presumed a northward flow of water past Point Piños into the Bay, continuing northward within the Bay, and finally exiting past Point Santa Cruz at the north end of the Bay. He observed the greatest spatial changes in water property distributions near Point Piños, with weaker gradients observed in the central and northern portions of the Bay. By observing distributions of temperature, nitrate, and salinity, Broenkow and Smethie (1978) interpreted that cool, high-nitrate waters penetrate into the Bay from the south around Point Piños one-third of the time.

During non-upwelling periods, Shea and Broenkow (1982) claimed that internal tides were capable of transporting cold, nutrient-rich waters to the surface. Using hourly CTDs they observed extremely large vertical oscillations of temperature during a tidal cycle. Internal wave amplitudes of 50 - 120 m were amplified by the narrowing and shoaling of the Canyon near the head. The steeper waves eventually broke and caused mixing of nutrients toward the surface.

Shea and Broenkow's research in the northern bight also showed 12 °C water rising with the internal tide and flooding the shelf. As the tide receded, most of the 12 °C water retreated down-canyon leaving a lens of water along the shelf of the northern bight (Figure 11). However, they did not provide a reason for the 16 °C surface water which appeared as the internal tide recedes. It seems that cross-shore advection of warm water during an ebbing tide should be considered as a mechanism to provide both the warm surface water as well as the 12 °C water over the shelf.

2.   Direct Measurements

Results from a drift-bottle study in the southern bight of Monterey Bay over a 14-month period between April 1963 and May 1964, indicated that surface flow is
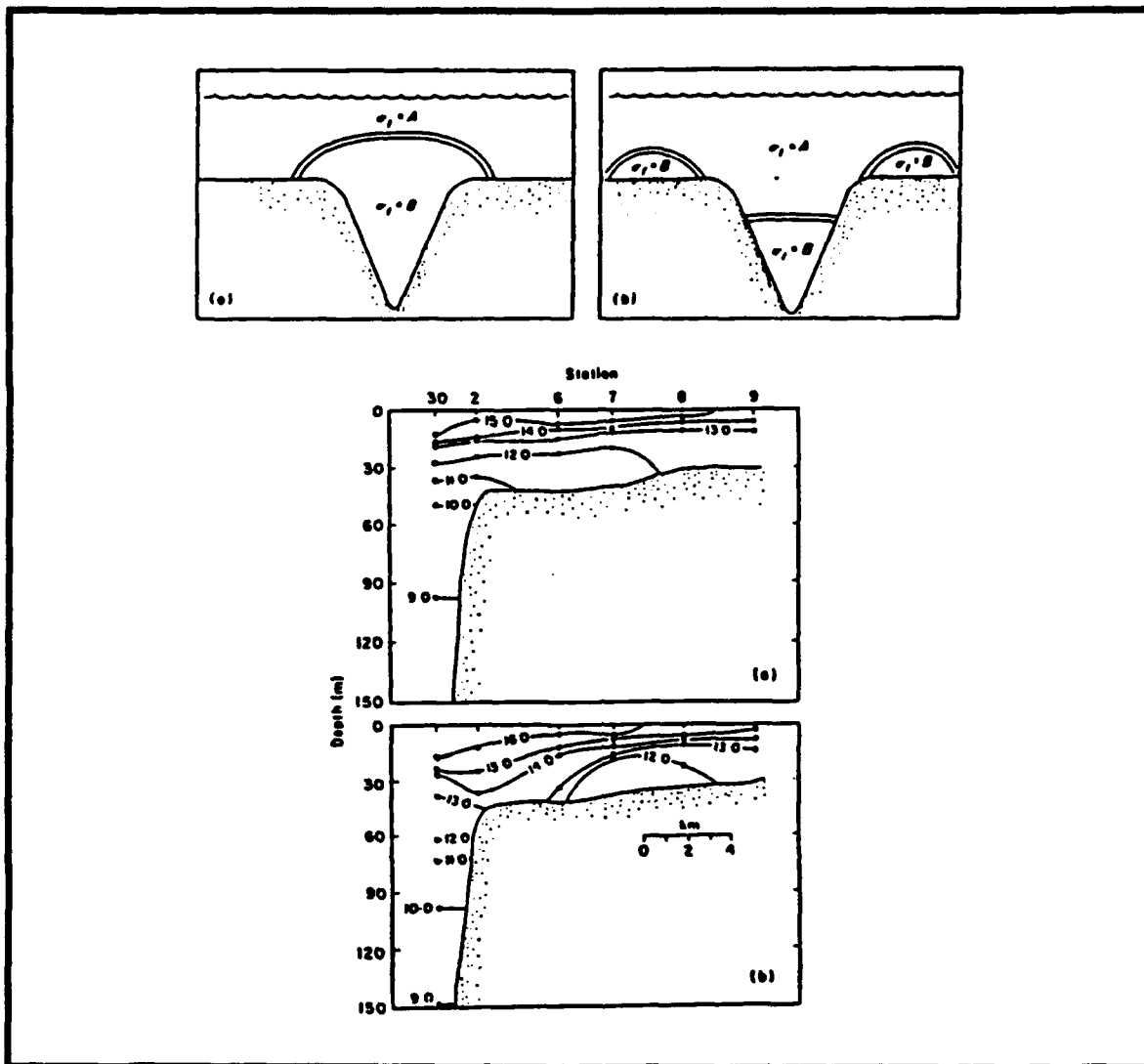
Figure 11. Conceptual model (top) of temperature distributions (bottom) near the edge of the Monterey Canyon. Top figures show the simple 2-level model used by Shea and Broenkow (1982) to describe how denser water from within the Canyon is lifted out of the Canyon at high internal tide (a), then pinched off onto the shelves during low internal tide (b). Bottom figures show actual temperature cross sections along the shelf during high (a) and low internal tides (b) (Shea and Broenkow 1982).

generally cyclonic (Reise 1973). Stoddard (1971) deployed 38 drogues in Monterey Bay over a four month period, August - November, 1970. He did not consider the wind record from Moss Landing to be representative of the Bay, and thus he did not use the Moss Landing winds when considering windage on those drogues deployed in mid-Bay. Tidal

22

effects were seen increasing in magnitude toward shore. Since these drogues were rarely tracked longer than 24 hours, larger scale currents were not resolved. Stoddard deployed groups of drogues, which gave an indication of the net surface current drift when the drogue trajectories were integrated over the full period of deployment. Most of the drogue deployments showed onshore drift in the mid-Bay, a counter-clockwise flow in the northern bight, and clockwise flow in the southern bight.

Moomy (1973) compared drogue trajectories with contours of surface density to provide a consistent picture of cyclonic surface circulation in Monterey Bay with flow to the north across the central portion of the Bay (Figure 12). Hydrographic data were acquired during August 28-30, 1972. The drogues were deployed at 12 m depth and tracked over a two-day period from August 30-31, 1972. The observed flow pattern was generally cyclonic with onshore flow in the south Bay and offshore flow in the north Bay.

Drogues were deployed near the mouth of the Salinas River during 1976-77 by Engineering Sciences, Inc. (1978). The flow was generally northward, however, there were occasions when the flow was weak or southward. Current meter measurements during the same period near the Salinas River indicated northward flow 65% of the time and southward flow 35% of the time. The northward flow showed intermittent bursts of current to the south occasionally lasting several days. During 1980, current meters were installed near the Pajaro River mouth by ECOMAR, Inc. (1981). The monthly mean flow was consistently northward.

In the northern bight, just south of Terrace Point, long-term current meters were installed from May, 1976 until January, 1977 (Brown and Caldwell 1977). A large tidal signal was observed, but between June and September, the flow was predominantly toward the west, consistent with northward flow within the interior of the Bay and continuity of surface flow. During periods of weak winds, the drogues deployed over the

23

Canyon by Broenkow and Smethie (1978) indicated a divergence near the head of the Canyon with currents speeds on the order of 5 cm/sec. In the southern bight, current meter measurements near the Monterey Bay Aquarium show weak westward flow (Breaker and Broenkow 1989). Again, a strong tidal component was observed.

These studies show little evidence that the Canyon affects surface currents. According to the baroclinic model results of Klinck (1989), when the width of a canyon is
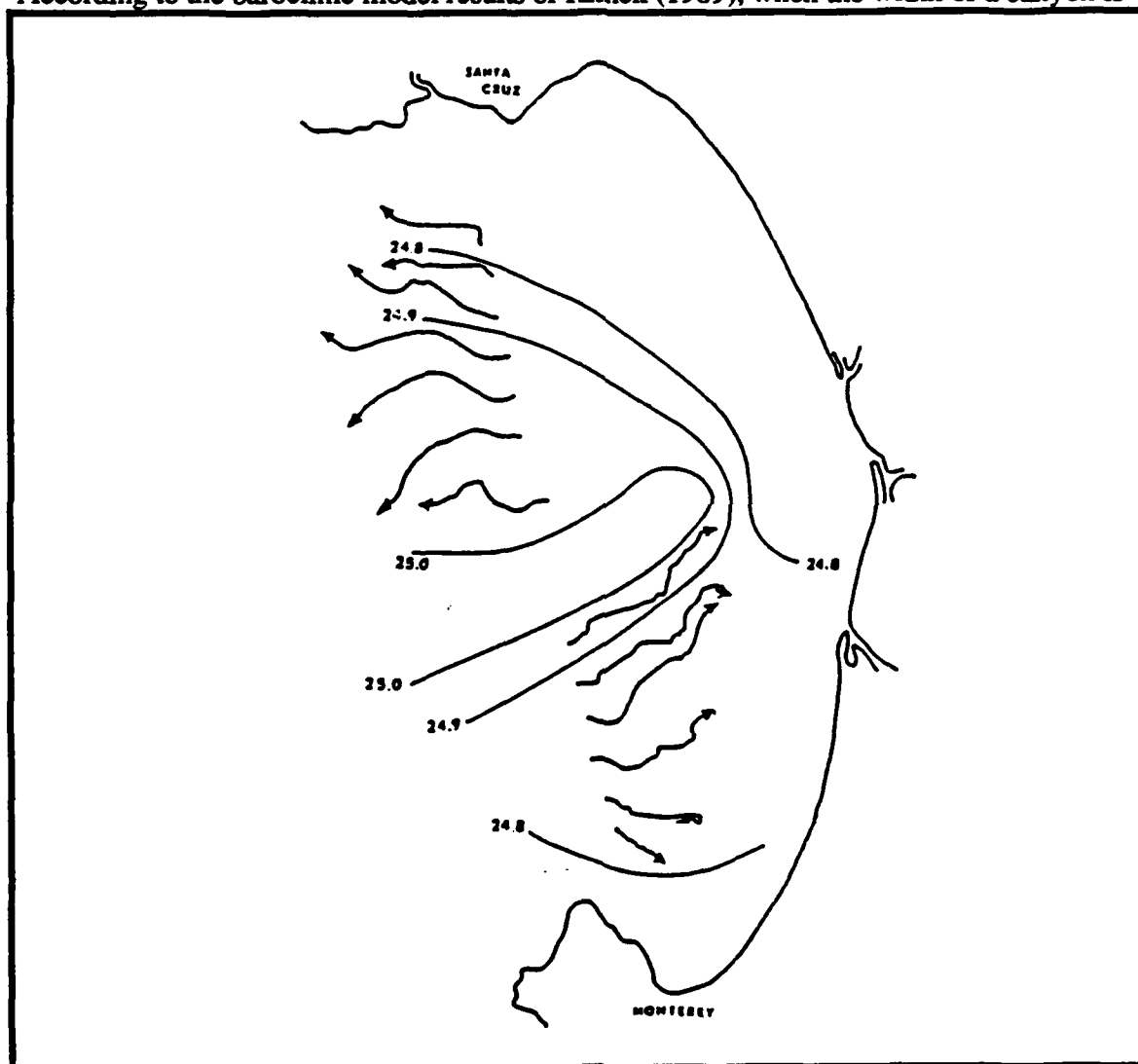
Figure 12. Drogue trajectories at 12 m for 30 to 31 August 1972, and contours of surface density based on hydrographic data acquired between 28 and 30 August 1972 (Moomy 1973).

relatively small compared to the first internal Rossby radius, the bathymetric effect on surface flow is greatly reduced. His results also indicated that a narrow canyon greatly inhibits upwelling due to vortex stretching. Calculations by Koehler (1990) demonstrate that the Monterey Submarine Canyon is narrower in a baroclinic sense than the Rossby radius.

3. Satellite Observations

Remote sensing observations have been applied to infer circulation in Monterey Bay. Pirie and Stellar (1974) used visual imagery of sediment plumes to interpret current patterns using aircraft overflights along with two visible channels on LANDSAT (nee ERTS-1), which had an 18 day repeating cycle. They developed monthly composite maps showing great detail of eddies in the Bay and coastal meanders. Given the difficulty in determining the predominant direction of flow from these composite images, such a detailed interpretation of the flow field doesn't seem warranted.

Working with individual images, certain aspects of Pirie and Stellar's work are quite clear. An ERTS-1 satellite image on January 22, 1973 shows a pattern of suspended sediment originating from the mouth of the Salinas River and flowing northward along the shore. From March through July (except April) Pirie and Stellar inferred southward flow along the California coast.

Breaker and Broenkow (1989) observed cold water associated with intense coastal upwelling from Point Piños south along the central California coast from AVHRR infra-red imagery for March 16, 1980. Cooler waters just north of Monterey Bay indicated that coastal upwelling may have just started in that area as well. From other images, they observed that during periods of active coastal upwelling, a band of cold water sometimes crosses the entrance of Monterey Bay. Thus, a continuous cold-water tongue often connected the upwelling center near Año Nuevo, to the north, with that originating near

Point Sur, to the south. In some cases, it appeared that cold water which originates at Año Nuevo was advected south across the entrance of the Bay.

In the absence of a coastal boundary, Breaker and Broenkow proposed that upwelling in the surface layer near the mouth of Monterey Bay may be the result of Ekman pumping due to wind stress curl which may be enhanced by cyclonic circulation over the Canyon.

There are several features common to the satellite AVHRR images of the Bay according to Breaker and Broenkow. The temperatures inside Monterey Bay are generally warmer than near the mouth, suggesting that coastal upwelling may not occur to any appreciable extent inside the Bay, and that local heating is important.

Offshore of the Bay, a meander originating in the California Current frequently takes the form of an anti-cyclonic, warm-core eddy centered roughly 50 km WNW of Point Piños. Breaker and Broenkow estimated the diameter of this eddy to be 50 to 100 km and speculated that its existence and location may be related to the presence of the Canyon. They suggested that the clockwise circulation associated with this eddy may at times enhance the southerly flow of cold upwelled water across the entrance of Monterey Bay. This feature is indicated in a map of surface dynamic topography (Figure 3) for July, 1984 by Chelton *et al.* (1987). The depth of this eddy was observed by CTD transection which indicated depression of isotherms down to 800 m (Tisch 1990).

C.   TIDAL EFFECTS

The tidal currents, as observed by many drogue deployments, appear weak. Shomaker (1983) used an implicit, two-dimensional model to analyze homogeneous barotropic tidal forcing of the Bay. Resulting height fields showed the clear progression of the tides into the Bay. The inferred currents into and out of the Bay associated with these heights were relatively weak. Consequently, other effects, such as wind forcing and

offshore currents, were determined to dominate the flow field, rather than barotropic tidal influences.

D.   VARIABILITY IN TIME AND SPACE SCALES

A basic problem when trying to infer the circulation of Monterey Bay from hydrographic parameters is the interpretation of the spatial structure of these parameters in light of the great temporal variations that occur at a given location. The vertical temperature profile can change significantly in several hours as reported by Skogsberg (1936), Breaker (1983), and Koehler (1990).

Estimating adequate sampling rates is far more difficult in coastal areas than in the deep ocean due to the variety, complexity, and interaction of physical processes that typically exist in coastal regions. In coastal areas, there is greater sensitivity to local winds, tides, and boundary effects. Internal waves also contribute to variability near the coast. The combined effects of these processes will result in considerably shorter space-time scales in coastal areas than in the deep ocean (Breaker 1983).

Monterey Bay is distinctly different from most bays and estuaries bordering the continental United States. It has little freshwater input, a large submarine canyon running through it and a very broad opening to the ocean. As such, it reflects much of the variability that occurs in the coastal ocean outside the Bay. A wide spectrum of forcing affects the Bay, resulting in highly non-stationary circulation.

The significant length scale in any given situation is the one that provides the minimum value (Huthnance 1981). Using reasonable estimates of time and space scales, dynamical space scales can be derived from the equations of motion. Most research has shown that the processes which affect circulation in Monterey Bay have very short time scales (i.e., hours to days). Space scales are also short in both the vertical and horizontal dimension (i.e., meters in vertical and kilometers in horizontal).

III. CIRCULATION DYNAMICS

There are several dynamic effects which appear to be operative in Monterey Bay. Ekman transport driven by northwesterly winds is a primary factor in creating centers of upwelling. Geostrophic adjustment establishes a balanced flow in response to Ekman transport. During wind relaxation events, low mixing in combination with solar heating can cause rapid changes in sea surface temperature. Offshore of Monterey Bay, a warm core eddy is a dominant, persistent feature which affects circulation in the Bay upon reversal of the upwelling favorable winds.

A.   EKMAN TRANSPORT

At the air-sea interface, energy is frictionally transferred from the wind to the water surface. The vertical structure of surface currents driven by this wind is such that each deeper layer of water moves slightly to the right of the one above. The result is a current spiral with the net transport at 90 degrees to the right of the wind (Ekman 1905).

Assuming a steady-state, homogeneous ocean with a flat surface, so that there are no horizontal pressure gradients, and neglecting non-linear terms, the equations of motion reduce to:

$$f \, u = A_z \, \frac{\partial^2 v}{\partial z^2} = \frac{1}{\rho} \frac{\partial \tau^y}{\partial z} \qquad (1)$$

$$-f \, v = A_z \, \frac{\partial^2 u}{\partial z^2} = \frac{1}{\rho} \frac{\partial \tau^x}{\partial z} \qquad (2)$$

28

Where f is the Coriolis parameter, (u,v) are the cross-shelf and along-shelf components of velocity, z is the vertical direction (positive up) and A is the eddy viscosity. The wind stress τ^y is taken to be in the along-shelf direction only. Integrating (1) and (2) from the surface (z=0) down to a depth z, beyond which the effect of wind stress is negligible, results in the cross-shelf Ekman transport (M^X).

$$M^X = \int_{-z}^{0} \rho \, u \, dz = \frac{\tau^y}{f} \tag{3}$$

When the wind blows equatorward along eastern boundaries, the Ekman transport is offshore $(M^X < 0)$. Continuity requires that the surface water transported away from shore be replaced. This results in colder water, often nutrient-rich, being raised to the surface near the shore. These regions of upwelling are among the richest biological areas in the world. Northwesterly wind-generated upwelling occurs quite frequently along the California coast. Off central California, offshore transport and upwelling seem to be concentrated north and south of Monterey Bay at Año Nuevo and Point Sur, respectively.

Ekman transport of surface water away from the coast raises the water level offshore and leaves a low water level nearshore. In addition, the upwelling of cold water along the coast causes the isotherms to rise toward shore.

B.   COASTAL UPWELLING

Northwesterly winds occur quite frequently throughout the year near Monterey, as indicated by the wind record between 10/1/88 - 9/30/89, provided by D. Husby, NOAA/ NMFS (Figure 13a and 13 b). During the spring and summer along the central California coast, the subtropical high pressure cell generates coastal winds from the northwest (Reid, Roden, and Wyllie 1958) (Figure 14). Northwesterly winds are stronger and more persistent during this period than during the fall and winter, when winds are lighter and

reverse direction more frequently. Consider the case of spatially uniform winds blowing along an eastern coastal boundary. Offshore Ekman transport produces upwelling of cold nutrient-rich water along the coastal boundary as described by Brink (1983) (Figure 15).

DAILY BUOY WINDS - 1988

0.308E-02
MAXIMUM VECTOR

46013 - BODEGA BAY

46012 - HALF MOON BAY

46042 - MONTEREY BAY

| 210 | 240 | 270 | 300 | 330 |

DAY OF YEAR
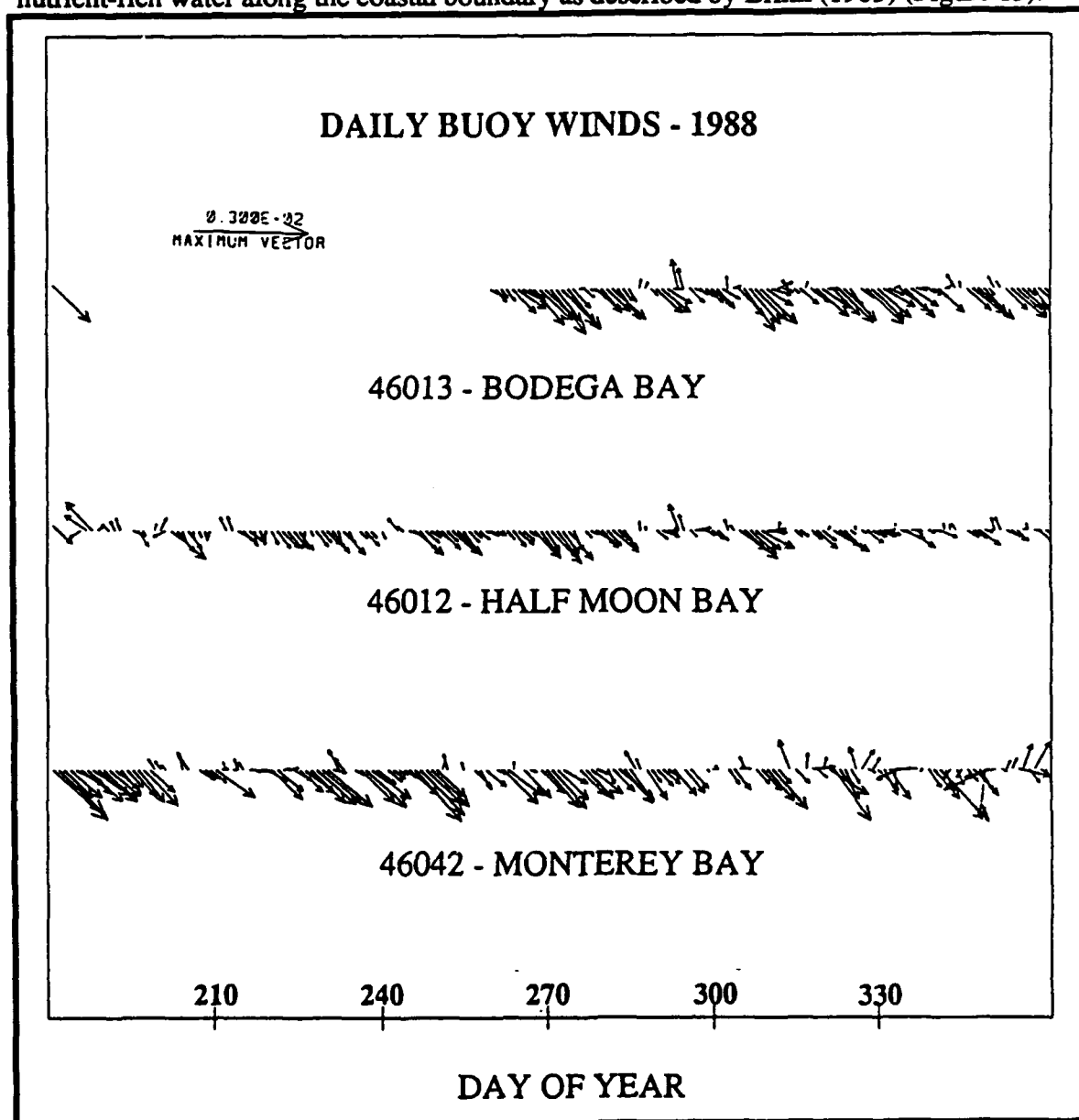
Figure 13a. Daily average winds from NDBC Buoys at: Monterey Bay (36.8°N, 122.4°W), Half Moon Bay (37.4°N, 122.7°W), and Bodega Bay (38.2°N, 123.3°W). Winds from JD 183-366, 1988 are represented by stick plots showing the direction to which the wind is blowing. The maximum wind vector is 30 m/s. Monterey winds are predominantly northwesterly.

30

DAILY BUOY WINDS - 1989

0.300E-02
MAXIMUM VECTOR

46013 - BODEGA BAY

46012 - HALF MOON BAY

46042 - MONTEREY BAY

30   60   90   120   150

DAY OF YEAR
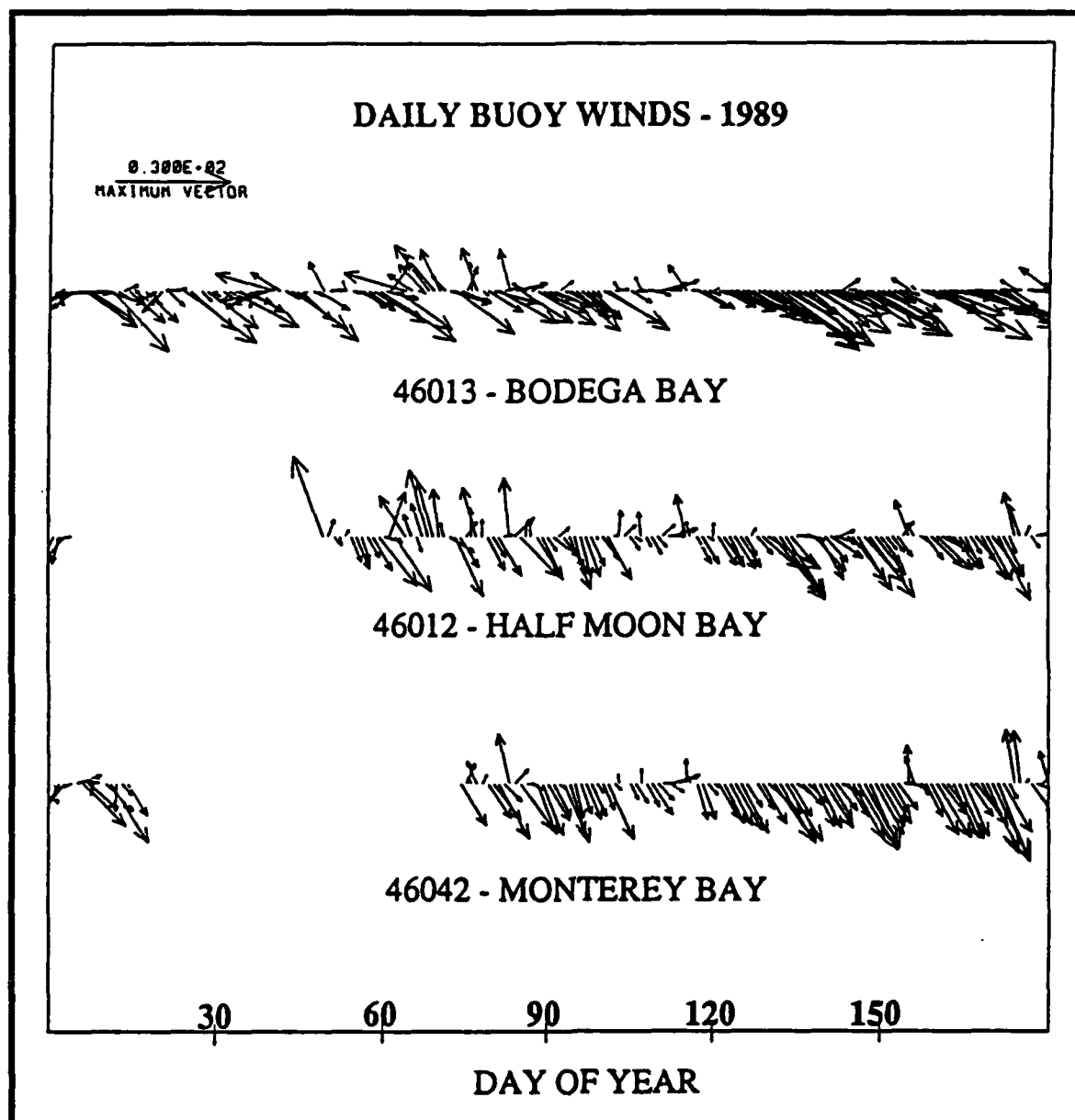
Figure 13b. Daily average winds from Monterey Bay (36.8°N, 122.4°W), Half Moon
Bay (37.4°N, 123.3°W), and Bodega Bay (38.2°N, 123.3°W). Winds from
JD 1-181, 1989, except for a gap from mid-January to mid-March, are
represented by stick plots showing the direction to which the wind is
blowing. The maximum wind vector is 30 m/s. Monterey winds are
predominantly northwesterly and became stronger in May and June.

Coastal upwelling has a major impact on nearshore circulation and provides strong thermal gradients during spring and summer. If the coastline is straight with a constant bathymetric slope, the thermal gradient would be uniform and increase from cold water near shore to warmer water offshore. However, there are numerous capes along the California coast, and it should not be surprising that centers of intense upwelling occur. Cold nutrient rich water is frequently found equatorward of these capes (e.g., Año Nuevo, Point Sur).
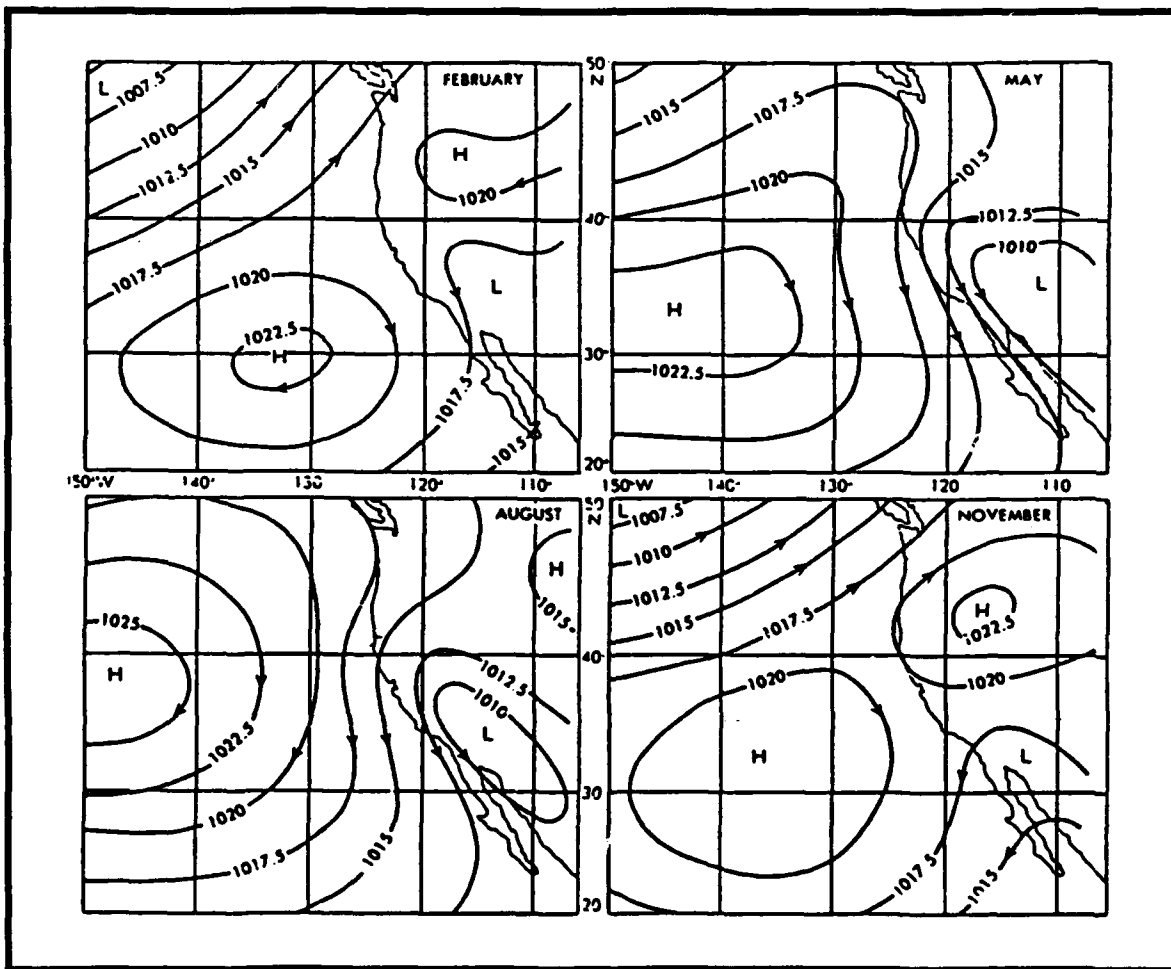
Figure 14. Average monthly atmospheric sea level pressure(in mb) over the eastern North Pacific Ocean and the western coast of North America during four months of the year, (reproduced from Reid, Roden and Wyllie 1958.)

32
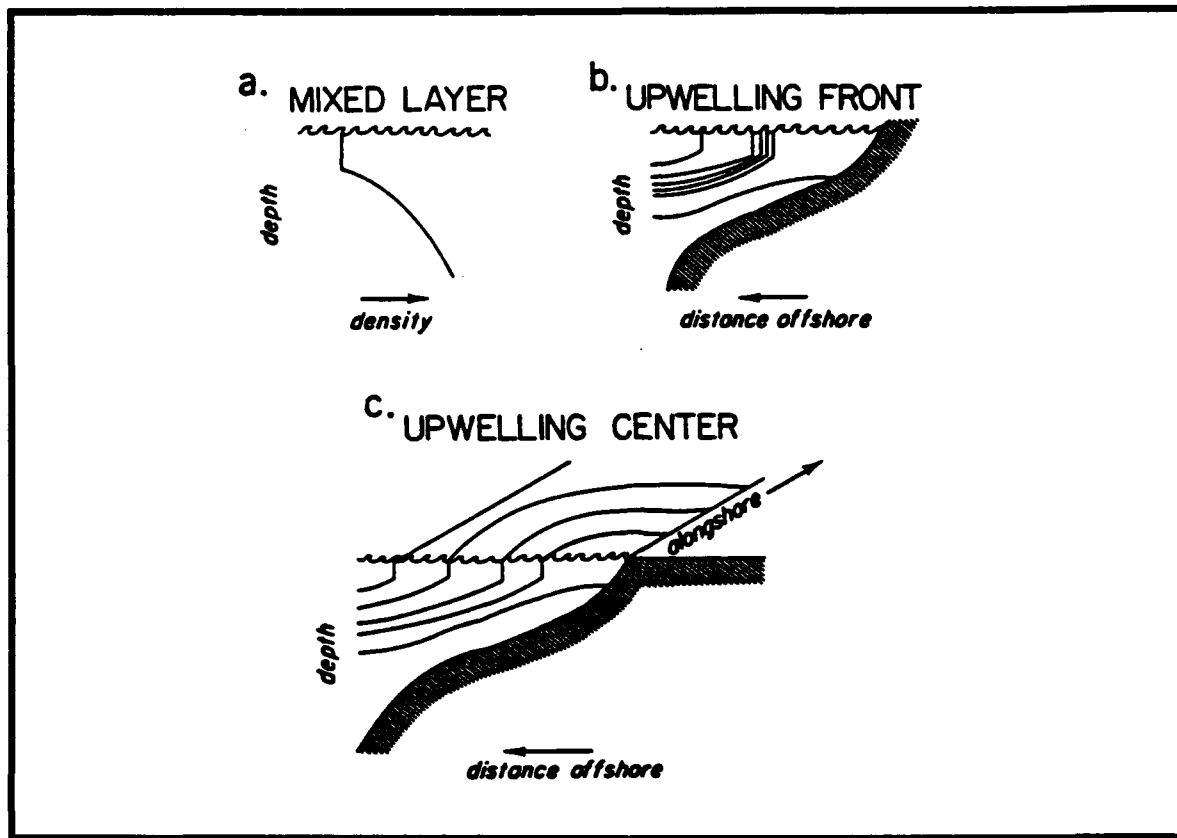
Figure 15. A schematic indicating the density structures associated with some near-surface features of coastal upwelling. (a) The mixed layer: density vs. depth. (b) The surface upwelling front: density contours drawn in a vertical, cross-shelf plane. (c) The coastal upwelling center: contours drawn in three dimensions. (reproduced from Brink 1983)

1. Upwelling Intensification near Capes

Arthur (1965) describes local intensification of upwelling equatorward of capes. He begins with the total vorticity equation and uses a scaling argument to neglect small terms. The resulting relation for vorticity (ζ) is:

$$f \frac{dw}{dz} = \frac{d\zeta}{dt} + \beta v \qquad (4)$$

where w is the upward velocity, v is velocity positive northward, f is the Coriolis parameter and β is the change in the Coriolis parameter with latitude, which is always positive. Using the northwestern boundary of Monterey Bay (Figure 16) as an example:

33
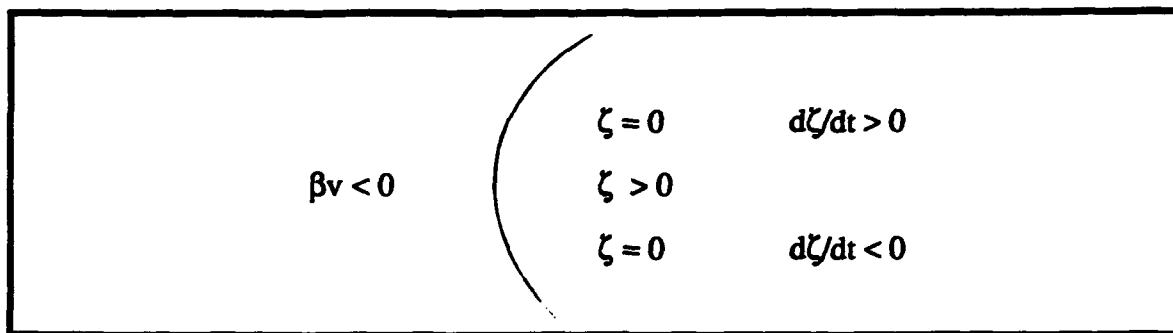
Figure 16. Southward current flow around a cape has positive vorticity when compared to the flow along a straight coastline. Poleward of the cape, the change in vorticity following a particle is positive. Equatorward of the cape, the change is negative. Since the flow is equatorward and β is always positive, both terms are negative so that upwelling is enhanced equatorward of the cape.

for the case of upwelling with southward flow, the two terms $d\zeta/dt$ and β v have the same sign (i.e., negative) and thus enhancement of upwelling occurs equatorward of the cape.

2. Topographic Effects on Upwelling

Peffley and O'Brien (1976) suggest that bottom relief is more important than coastline curvature in causing localized upwelling. A great degree of variability in the north-south lower layer flow is explained by variations in the longshore pressure gradient induced by the topographic β effect. Topography-induced variations in the longshore flow excite irregularities in the barotropic onshore-offshore flow on scales exceeding that of the sloping topography. Their model results show the computed elevation of the pycnocline to be greater with bottom relief than with no relief which confirms the importance of submarine topography. The observed tendency for enhanced upwelling at capes may then be caused by the general correspondence to submarine ridges.

3. Undercurrent Effect on Upwelling

Preller and O'Brien (1980) suggest that intensified upwelling at the observed location is only obtained when a realistic poleward flow (opposite to the sense of the local wind stress) exists in the lower layer. This undercurrent accelerates in order to

cross a submarine ridge, thus requiring an alongshore pressure gradient which is created by doming of the model interface equatorward of the ridge. This may account for the enhanced upwelling centers which are seen at Año Nuevo and Point Sur. Since the undercurrent is observed closer to shore near Point Sur than Año Nuevo, this may also explain why the Point Sur upwelling appears to have greater intensity.

C.   GEOSTROPHIC ADJUSTMENT

Geostrophic flow is the balance of the pressure gradient force with the Coriolis force. The process of initiating this flow equilibrium is called geostrophic adjustment. Consider upwelling along the coast with the sea level elevated offshore (west) representing a high pressure cell. Conversely, the lower sea level nearshore (east) represents a low pressure cell. The pressure gradient force (PGF), then is from high to low with the flow to the right (south). The Coriolis force is to the right of the flow and opposite in direction to the PGF. When the geostrophic flow reaches equilibrium, the PGF balances the Coriolis force and the established flow is equatorward.

The calculated dynamic height for warm offshore water is greater than the dynamic height for the cold inshore water, along the mouth of Monterey Bay, when referenced to an assumed level of no motion. The difference in dynamic height indicates a downward slope of the sea surface toward shore which agrees with the previous argument for an equatorward jet in geostrophic balance. When facing in the direction of the flow, light water is seen on the right.

D.   WIND MIXING AND SURFACE HEATING

Wind conditions are quite variable and steady state rarely occurs in the surface mixed layer of the ocean. To approach equilibrium, the wind mixing and the surface heat

flux must balance. At the surface, heat is primarily removed by latent and sensible heat flux and added by solar insolation.

Wind stress drives mechanical turbulent mixing at the surface of ocean, while surface cooling or heating can either subtract or add stability, respectively, by decreasing buoyancy or adding stratification. At the bottom of the mixed layer, turbulence is dissipated by entraining cold water upward into the mixed layer. Cold water from the lower layer is more dense than the warmer water from the upper layer; as the two water masses are mixed, the resulting center of gravity is raised and the turbulent kinetic energy is converted to potential energy.

The mixed layer depth approaches a constant level when mechanical mixing energy is exactly balanced by heating. When the wind is strong and evaporation is cooling the surface, both mechanical and buoyant turbulence combine to form a deep mixed layer. On the other hand, when the wind is calm, there is little mechanical turbulence a shallow, warm mixed layer can form from solar insolation.

During relaxation of upwelling favorable winds, the mixed layer depth decreases and is defined by the Monin-Obukhov length scale (L) where mechanical and turbulent production have equivalent magnitudes (Stull 1988). (See Appendix B for more details of calculations and definitions of symbols.)

$$L = \frac{C_1 \, \rho_0 \, C_p \, w_*^3}{C_2 \, \alpha \, g \, Q_0} \qquad (5)$$

By measuring the wind stress and assuming a climatological value for heat flux, the prognostic equation for temperature can be solved (See Appendix B.)

$$\frac{dT}{dt} = \frac{Q_0}{\rho \, C_p \, L} \qquad (6)$$

For a 2 m/s wind and a daily average $Q_0 = 100$ W/m^2, the Obukhov length scale is less than a meter and the one-day change in temperature due to solar heating is 3.1 °C. This is an approximate value since the true heat flux is much larger during a clear day in Monterey, but for clear water, half of the solar energy is transmitted below one meter, and for turbid coastal water 80 percent of the incoming solar energy is absorbed in the top meter of water.

Light winds and surface heating occur occasionally in Monterey Bay and allow dramatic increases in surface temperature. This effect along with advection of warm oceanic water into the Bay provide thermal changes in the Bay which may have significant effect on biota within the Bay.

E.   WARM CORE EDDY DYNAMICS

Eddies are frequently associated with strong currents, such as the Gulf Stream, but eddy-like features are found throughout the ocean. Eddy formation is usually attributed to either baroclinic or barotropic flow instability. Warm core rings in geostrophic balance exhibit clockwise rotation with light water on the right in the northern hemisphere. Freely rotating eddies associated with the Gulf Stream have been observed to propagate westward on the order of 5 km/day. Eddy dissipation is generally through Rossby wave radiation to the west.

An anticyclonic warm core eddy is a semi-permanent feature offshore of Monterey Bay (Breaker and Broenkow 1989). Recall that there is an offshore upwelling plume located at Año Nuevo, to the north of Monterey Bay, and a similar upwelling plume offshore at Point Sur, to the south of the Bay. Also there is an equatorward jet from Año Nuevo flowing across the mouth of the Bay (Skogsberg 1936). These features border the eddy to the north, south and east, respectively.

There are three possible arguments for the observed warm-core eddy located offshore of Monterey Bay. First, the eddy may be a meander of the warm, poleward flow of the California Current System which has become trapped against the upwelling jet and plumes. Since the eddy does not appear to propagate westward, there must be some, as yet undefined dynamic balance, possibly between the southward jet along the coast with cross-shelf changes in density that holds the eddy onshore. In fact, when the upwelling winds relax, the warm eddy is quickly forced onshore and into the Bay.

A second explanation of the eddy formation and maintenance may be an instability caused by vertical shear produced by the California Undercurrent. Once generated, the eddy is again trapped as explained in the previous argument.

A third hypothesis is that the equatorward jet from Año Nuevo and the offshore plume from Point Sur generate and maintain the eddy. The jet and plume have strong shear at the edge of the eddy and impart negative vorticity which generates and maintains an anticyclonic eddy. This eddy is held in place by the offshore flow to the north and south. There still exist some undefined onshore pressure gradient force holding the eddy to the eastern boundary (southward jet).

IV. DATA ACQUISITION AND PROCESSING

As mentioned before, a one-year record of AVHRR satellite images between 10/1/88 and 9/30/89 was reviewed to determine which days were cloud-free in the vicinity of Monterey Bay. Subsequently, 112 images were processed and analyzed. The most interesting features were observed on a series of four sequential images from 5/23 - 5/26. Another sequence of interest began on 6/17 and ended on 6/24. Wind records during the May - June period were processed from four locations near the Bay. In addition, four oceanographic research ships were collecting CTD data at locations both inside and outside the Bay during May and June, 1989.

A. WIND

1. NDBC Buoy 46042

Coastal wind records were available from the National Data Buoy Center (NDBC) buoy 46042 located just outside Monterey Bay at 36.8 °N, 122.4 °W. The winds were measured at a height of 5 m above the sea surface. (The raw data, listing hourly averages of wind speed and direction, were provided by David Husby, NOAA/NMFS). Daily averages were computed and presented on the corresponding satellite image to the nearest 2 m/s. The one-year record of wind (Figure 13a and 13b) had a two-month gap from mid-January until mid-March, 1989.

2. Monterey Bay Aquarium

The Monterey Bay Aquarium (MBA) winds were measured at 21 m above sea level and are available as 5 minute average values or as daily mean speed and direction. Meteorological and oceanographic data are available from the MBA archive via telephone modem. The location of the MBA station is 36.6°N, 121.9°W.

3. Moss Landing Marine Laboratory

Wind data were available from Moss Landing Marine Laboratory (MLML) located at 36.8 °N, 121.8 °W. A record of daily average winds at MLML was provided by William Broenkow.

4. Granite Canyon Shellfish Laboratory

Wind data were observed daily near sea level and hand logged. Wind speed and direction represent instantaneous values rather than a daily average. Dave Husby also provided these data and stick plots of the wind records.

B. AVHRR SATELLITE IMAGERY

To view the surface distribution of cold surface water in Monterey Bay, one satellite multi-channel sea surface temperature (MCSST) image was chosen for each cloud-free day. These images were augmented by CTD observations to further investigate the cold water distribution and infer the circulation pattern in the Bay.

Quite frequently, Monterey Bay is covered to some extent with fog or clouds. Under these conditions, visual and infrared satellite sensors measure the albedo and brightness temperature of the clouds instead of the sea surface. To obtain useful MCSST, I reviewed the hardcopy archive of both visible and infrared satellite imagery from the NOAA Weather Service Forecast Office at Redwood City, CA. During the period, 10/1/88 - 9/30/89, 110 images appeared cloud free over Monterey Bay (Figure 17).

West coast AVHRR imagery was obtained from three archives: Naval Oceanographic and Atmospheric Research Laboratory - East (NOARL), Scripps Satellite Oceanography Center (SSOC), and Sea Space (a private company).

The TIROS-N satellites are sun-synchronous, polar orbiting and cover the same location on the Earth twice a day. This section summarizes AVHRR sensor and satellite

```
          ..        ....        P      P c        .         .P        . ..   OS
      p.        pc..           .      . c       c          ..        . ..   PS
          ..        ....              .    . P      .          ..        . ..   MB
          ..        ....              .      . c      .          ..        . ..   AN
OO....KK.....KKJK............J...K.K.....K.....OKK.....JOKK
1    5    10    15    20   25   30    5    10   15   20   25   30
               OCTOBER                              NOVEMBER

. P P .     c c.              .       . .. c       .. ...c.          .      c  · OS
. . . .       . cp            .       . .. c       .. ...c          .      .    PS
. P . .       . cp            .       . .. P       .. .**..          .      .    MB
. c . .       . cc            .       . .. c       .. ...PP          .      .    AN
K.KOJ.IK...I.II..........O.....I.II.I....II.IIIIJ.......I...I.
1    5    10    15    20   25   30    5    10   15   20   25   30
               DECEMBER              1989       JANUARY

      ...   ccc.c .    c             .         c cp-     c     c c.        OS
      ...   c.c.c .    .             .         . cp-     c     . ..        PS
      ...   .c... .    .             .         . .p-     .     . cc        MB
      ...   ppccc .    c             .         . cp-     c     c c.        AN
....III..IIIII.I...J..........I..........I.III....I....I.IJ.
1    5    10    15    20   25   1    5    10   15   20   25   30
               FEBRUARY                             MARCH

  c c..              ..    P c      c      pcc p         ....  ppc  OS
  c c..              PP    c .      .      ccc .         ...c  c.c  PS
  c c..              ..    P .      c      ..p .         ....  ..p  MB
  c c..              ..    x c      .      ..c p         ....  c.c  AN
..I.JJJ.............II...I.J....I......III.I......IIII...III
1    5    10    15    20   25   30    5    10   15   20   25   30
               APRIL                                MAY

      c cc.cff... ..cp      c..   .        .c          c.c c.  OS
      c ....ff... ..cc      ...   .        .c          p.. cc  PS
      . ...cff... ....      ...   c        .c          ccc p.  MB
      c cc.cff...   c.      p.p  c        .c          cc. c.  AN
........I.IIIJJOIII.JIII......JII..I......IJ...........III.II
1    5    10    15    20   25   30    5    10   15   20   25   30
               JUNE                                 JULY

.c                    c                              ..     OS
.c                    .                              ..     PS
.P                    .                .             p.     MB
.c                    c                              c.     AN
II................I..OO....O.......O.......O..O......OII....
1    5    10    15    20   25   30    5    10   15   20   25   30
               AUGUST                               SEPTEMBER

Key:   . = clear     p = partly cloudy   AN = Ano Nuevo   OS = Offshore
       f = fog       c = cloudy          PS = Point Sur   MB = Monterey Bay

       I = NOAA 11      J = NOAA 10       K = NOAA 9    O = No image, clear
```
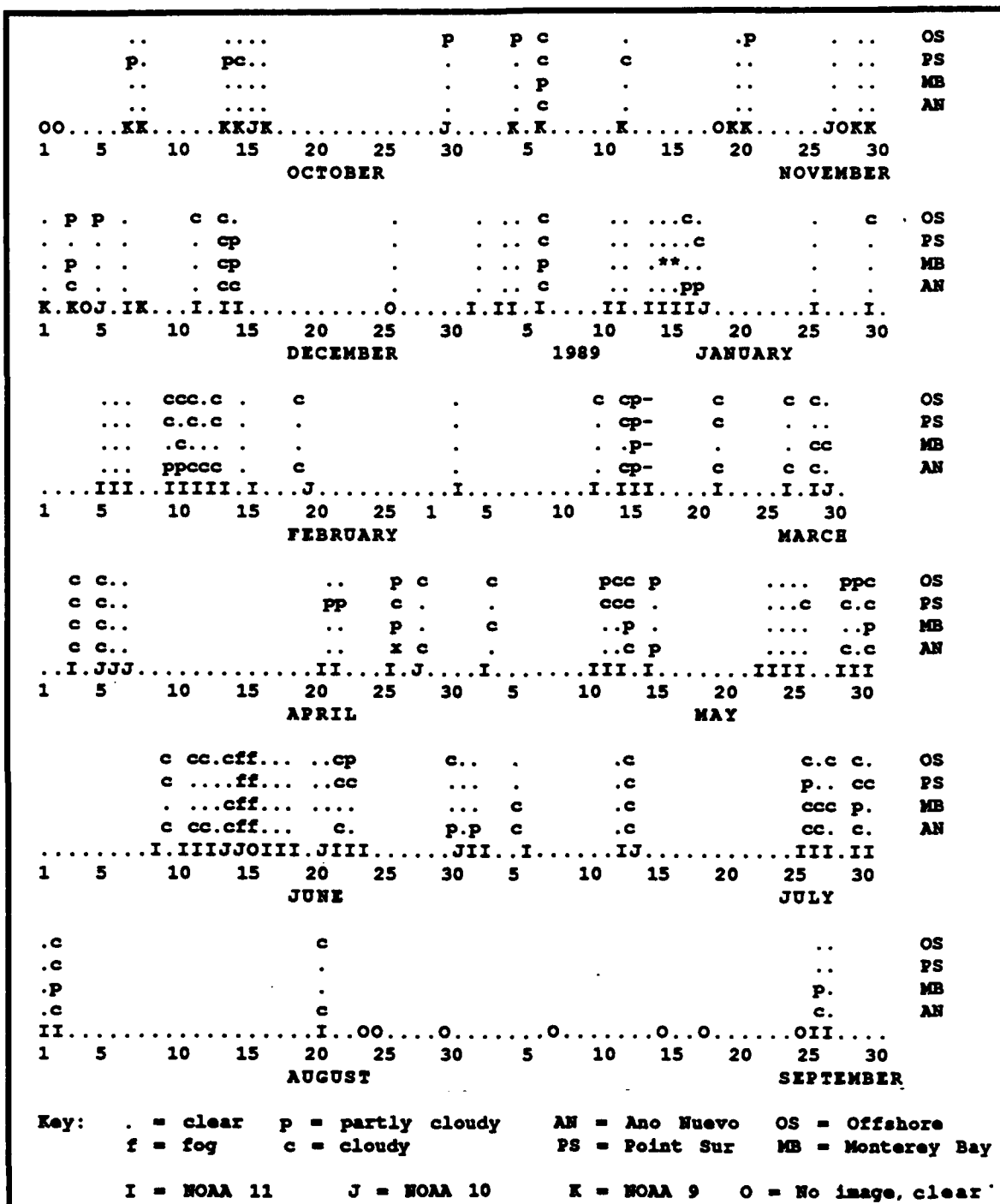
Figure 17. A calendar of AVHRR satellite images for the period beginning 10/1/88 to 9/30/89. Satellite passes are identified by code: I=NOAA-9, J=NOAA-10 and K=NOAA-11. One of these codes lies on a date if a satellite pass was processed. Cloud cover is labeled by c=cloudy, p=partly cloudy, f=fog and dot(.)=clear. Cloud cover was recorded in four locations: AN=Año Nuevo, MB=Monterey Bay, PS=Point Sur and OS=offshore.

41

specifications which are elaborated upon by Bernstein (1982) and McClain (1985). Three TIROS-N satellites are presently operational and using the Advanced Very High Resolution Radiometer (AVHRR) sensor. NOAA 10 has only the four channel radiometer, while NOAA 9 and 11 carry the five channel sensor which can be used to correct for atmospheric effects of water vapor. Spatial resolution of the AVHRR sensor is 1.1 x 1.1 km directly below the satellite, and 1.5 km along track by 4.0 km cross track at the swath edges due to curvature of the earth. The five-channel AVHRR measures radiation in the visible (0.6-0.7 um), near infrared (0.7-1.1 um), and thermal infrared (3.5-3.9 um, 10.5-11.5 um, and 11.5-12.5 um) wavelength bands (Bernstein, 1982).

The five spectral bands of the AVHRR are digitized to 10-bit resolution in equal increments of energy. The calibrations for the first two bands are based entirely on prelaunch tests and are expressed in terms of percent solar albedo. The noise in the first two channels is less than the least significant bit, and thus their data are only limited by least count noise. The 10-bit resolution corresponds to 0.1% in albedo.

The remaining three bands in the thermal infrared are radiometrically calibrated every scan line. On every rotation of the scan mirror, the optics scan the earth below followed by a view of a deep space, blackbody target. The target temperature is measured by four platinum-resistance temperature probes embedded in it. The noise equivalent difference temperature (NEΔT) is the sum of inherent and least count noise, amounting to 0.07 °C for channel 4 and 5. Channel 3 is contaminated by sensor noise, and during the day, is affected by reflected solar radiation.

Dense, wide-spread clouds completely block infrared radiation from the sea. Thick clouds can usually be detected by their high albedo compared to the dark ocean. Although they restrict the number of observations, they introduce no errors. On the other hand, thin clouds or undetected small clouds can lower the apparent MCSST by 1.0 °C or more.

Infrared radiation emitted from the ocean surface is partially absorbed by the atmosphere and re-emitted at colder cloud temperature. The net effect for a satellite radiometer is that it observes a blackbody equivalent ocean surface temperature which is usually colder than the actual surface.

Satellite infrared observations measure the ocean skin temperatures of the upper 1 mm, while ship and buoy measurements are bulk temperatures of the upper few meters. By regressing the satellite observations against the ship and buoy measurements, an algorithm can be developed to predict bulk temperatures from satellite observations.

The difference between the actual and observed temperature, which is a function of wavelength, has been estimated by Deschamps and Phulpin (1980). The infrared channels 3, 4, and 5 were selected to fall in the atmospheric 'window' where the absorption effect on temperature is relatively low (McClain, 1985). The atmospheric absorption in these channels occurs primarily near the ocean surface and thus the observed temperature is considered to be the same for each channel. In fact, this temperature is nearly that of the sea surface.

Furthermore, the difference in temperature between the sea surface and the measured radiance is a linear function in each channel due only to the absorption effects by water vapor. The accuracy is improved by correcting for the solar zenith angle (sza) and using the split-window (two channel, $T(11)$ is centered at 11 μm and $T(12)$ is centered at 12 μm) algorithm for bulk MCSST (McClain):

$$MCSST = A * T(11) + [T(11)\text{-}T(12)][B + C * (SEC(sza) - 1)] + D$$

$$A = 1.01345, \quad B = 2.659762, C = 0.520056, D = -288.67 \qquad (7)$$

These constants change for each sensor and can be modified for different atmospheric conditions.

Raw satellite data are organized into a sensor-level data set containing remotely sensed, earth-view data along with enough information to earth locate and calibrate these data. Raw data (10-bit) are transmitted by the satellite in real time and received by an earth station while the satellite is above the horizon.

The initial ground data processing results in a sensor-level data set called "Level 1b" which consists of one scan line per record with quality control information, calibration coefficients for each channel, and earth positions for selected data landmarks appended to each scan line.

Level 1b AVHRR satellite data from Sea Space and Scripps were delivered in standard high resolution picture transmission (HRPT) format. The NOARL data were delivered in Local Area Coverage (LAC) format which is essentially the HRPT format, but stored on magnetic tape in condensed format without a header for every record.

The TERASCAN image processing system, installed at NOARL - West in Monterey, CA, was used to obtain the series of atmospherically corrected, co-registered images used for this analysis. The TERASCAN system runs on an Hewlett-Packard minicomputer using the UNIX operating system, allowing the user to manipulate files with UNIX commands. Additional processing details are included in Appendix A.

C. CTD DATA

Although satellite observations provide good spatial coverage of the surface temperature distribution, the vertical temperature structure must be considered to fully interpret these images. Several ships were operating in Monterey Bay during May - June, 1989. The USNS DeSTEIGUER recorded numerous CTD transections during May 11-26. The NOAA ship DAVID STAR JORDAN performed CTD transections on May 14-16, May 25-28 and June 4-6 (Figure 18). The Monterey Bay Aquarium Research Institute (MBARI) vessel POINT LOBOS occupied CTD stations on May 4, June 14, June 20 and

Figure 18 AVHRR satellite image of Monterey Bay on 5/24/89. CTD station locations from DeSteiguer and DAVID STARR JORDAN (5/23-5/26) are labeled numerically. MBARI stations begin with C, M, or H, while UCSC stations begin with S. The sea surface temperature is color enhanced, where violet is cold (9 C) and red is warm (16 C). The latitude and longitude are drawn at 8' increments.

48

THIS PAGE INTENTIONALLY LEFT BLANK

June 29. The UCSC vessel DAVID JOHNSTON conducted a CTD transection on May 24.

The USNS DeSTEIGUER was equipped with a Neil Brown Instrument Systems (NBIS) Mark IIIB CTD Probe. Water samples were taken at the bottom of each cast and sea surface temperature measurements were obtained from bucket measurements. Pressure offset (the pressure recorded by the CTD while sitting on deck) values were recorded just prior to deploying, and upon recovery of, the instrument. Finally, to insure accurate salinity measurements, the conductivity probe was rinsed with fresh water and covered after each hydrocast.

Calibrations were conducted prior to the cruise by checking the CTD conductivity, temperature, and pressure readings against standards in the laboratory. Differences obtained in this manner were then averaged and fit to a linear regression scheme in order to obtain the coefficients necessary to adjust the measurements made by the CTD to the reference standards. Temperature coefficients had a slope of 0.999363 and an intercept of 0.003435 while the pressure slope was calculated to be 1.000000.

VARIABLE	RANGE	ACCURACY	RESOLUTION
Pressure	0 to 3200 db	+/- 3.2 db	0.05 db
Temperature	-3 to 32 °C	+/- 0.005 °C	0.0005 °C
Conductivity	1 to 65 mmho	+/- 0.005 mmho	0.001 mmho

The Monterey Bay Aquarium Research Institute (MBARI) CTD measurements were made with a Sea-Bird model SBE 9/11 unit. The temperature and conductivity sensors were calibrated at the Northwest Regional Calibration Center (NRCC). The errors are estimated to be +/-0.01 psu for salinity and +/- 0.02 °C for temperature.

The DAVID STARR JORDAN used a Sea Bird model SBE 9/11 with annual calibration at NRCC. An intercomparison between the two Sea Bird CTDs and the DeSteiguer CTD was performed at station H3, located in mid-Bay. The CTD comparison was conducted after the fact, with close agreement in temperature at 200 m, well within the observed spatial variability of Bay water. The temperature at 200 m has a small vertical gradient and is not significantly affected by internal waves.

V. OBSERVATIONS

A. WIND

At NDBC Buoy 46042, the coastal wind, from 10/88 - 9/89 (Figure 13a and 13b) was predominantly northwesterly with relaxation and reversals at approximately 10 - 15 day intervals. Although the winds were lighter at Half Moon Bay, NDBC Buoy 46012, there was a strong correlation in direction, which is expected along the relatively straight coast between Monterey and San Francisco. The NDBC Buoy 46042, Moss Landing, Monterey Bay Aquarium (MBA), and Granite Canyon wind records for May - June, 1989 are plotted on an expanded scale in Figure 19. During this period, the winds were northwesterly with occasional relaxations and reversals. The MLML winds were primarily westerly, perhaps due to a thermal gradient caused by heating in the Salinas Valley. In general the MBA winds were more rectilinear and lower in magnitude due to topographic effects near MBA. The Granite Canyon winds were also rectilinear due to topographic effects. Wind reversals at Granite Canyon were much larger in magnitude than observed at the Buoy.

Two cloud-free periods have been outlined on Figure 19. During the period in May, to be described later in more detail, the winds were favorable for upwelling until 5/23 when a slight relaxation occurred. The winds increased for the next three days until 5/26.

During the next cloud-free period, strong northwesterly winds were sustained beginning on 6/17 and continuing through 6/20. The winds began to relax on 6/21 and actually reversed to a southerly flow on 6/23 and 6/24.

B. SATELLITE IMAGERY

The satellite images of Monterey Bay are centered at 36.6 °N, 122.2 °W with a spatial coverage of 200 x 200 km. Latitude and longitude grid lines at 30 minute intervals,
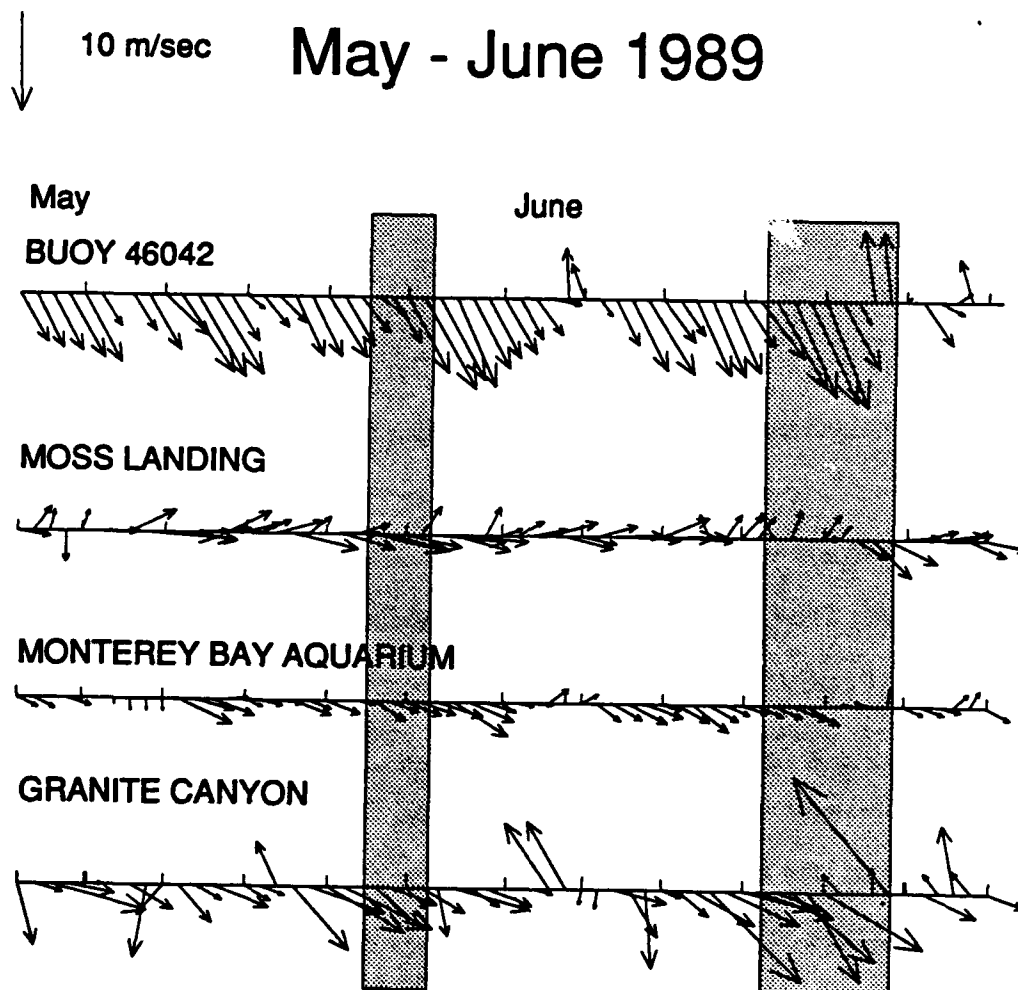
Figure 19. Monterey Bay Winds for May-June, 1989. Sequential satellite images of Monterey Bay were available for the dates indicated by the shaded areas. Winds were primarily northwesterly during the observation period, but relaxations and/or reversal events occur every week or two.

50

coastline and bathymetric contours at 50, 200, and 1000 meters are superimposed on each AVHRR image. The location of the oceanographic/meteorological buoy 46042 at 36.8 °N, 122.4 °W is denoted by a small white square. On the right side, a 9-16 °C color bar relates the color of the ocean surface to temperature. Average daily wind speed and direction is indicated in the upper right corner of each image with arrows showing the direction of the wind and each arrow point representing 2 m/s. The indicated winds are averaged for the 24 hours preceding the afternoon satellite pass and may be slightly different from the daily average winds of Figure 19, which are averaged to midnight. The land mass has been blacked out. Other black areas over the ocean are due to clouds or fog.

There were two series of satellite images (5/23 - 5/26 and 6/17 - 6/24) which seem to characterize the response of waters in and near Monterey Bay to upwelling and relaxation wind events. These dates were selected because sequential images were relatively clear of clouds and concurrent hydrographic data were available.

The wind was moderate and from the northwest at the beginning of the May sequence (Figure 20). The oceanic water was about 3 °C warmer than that found near the coast, and the shape of the oceanic thermal structure outside the Bay suggested a warm core, anticyclonic eddy or meander. There were two centers of cold water; one was found north of Monterey Bay near Año Nuevo, the other south off Point Sur. Notice that cold water appeared to extend southward from Año Nuevo across the mouth of the Bay. A tongue of cold water from Point Sur also extended offshore.

On the next day, 5/24 (Figure 18) the features were generally the same as on the previous day. The two cold water centers still exist, although Point Sur water extended further offshore. The cold band across the mouth of the Bay was slightly broader. A close look at temperature difference shows a cool cell just outside the mouth of the Bay to the north on 5/23 which progressed southward to mid-Bay on 5/24.

51

The wind increased on 5/25 (Figure 21) and the warm offshore feature extended further offshore from Point Piños allowing the band of cold water across the mouth of the Bay to join the cold tongue offshore of Point Sur. The Nearshore water warmed in the south and mid-Bay.

The wind continued to increase on 5/26 (Figure 22) which apparently caused the cold tongue extending southward from Año Nuevo to broaden and become colder. The cold water near Point Sur also became colder and extended further offshore. The nearshore water in northern Monterey Bay became very warm. The oceanic eddy feature continued to move offshore.

Even though the next few days were clear, satellite coverage was not available due to the orbital position of the satellite. The retrograde precession of the sun synchronous satellite orbit causes a two day gap in coverage every ten days. Clouds were present over the Bay for the next two weeks.

On 6/17 (Figure 23) the wind was northwesterly and cold centers were established near Año Nuevo and Point Sur similar to the previous surface temperature pattern. The cold tongue extended southward from Año Nuevo. Warm water was found nearshore, especially in the north Bay. The oceanic feature was warm and appeared to be an eddy attached to a warm offshore structure.

The wind continued from the northwest on 6/18 (Figure 24). The cold centers at Año Nuevo and Point Sur cooled by 1°C. The southward tongue from Año Nuevo has a cold central axis and a greater cooling effect on the Bay. Nearshore heating continued. The cold water tongue from Point Sur also tends southward and doesn't appear to affect the circulation in Monterey Bay. Heating continued in the nearshore region.

The wind continued from the northwest on 6/19 (Figure 25). The temperature distribution was generally the same as on the previous day with slight warming of the
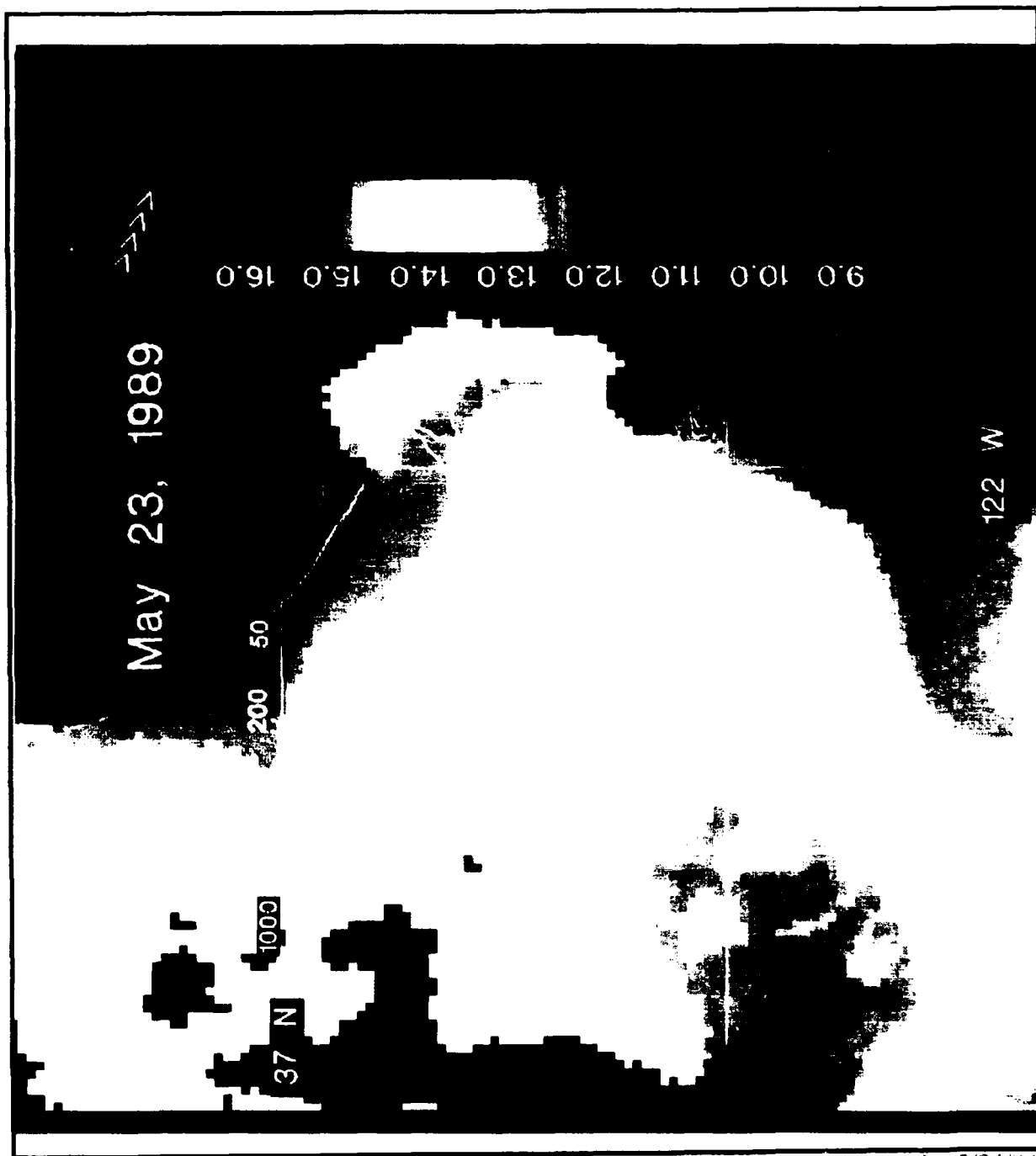
Figure 20   AVHRR satellite image of Monterey Bay on 5/23/89. The image for 5/24/89 was presented earlier as Figure 18. Each arrow point represents 2 m/s wind speed in the indicated direction.
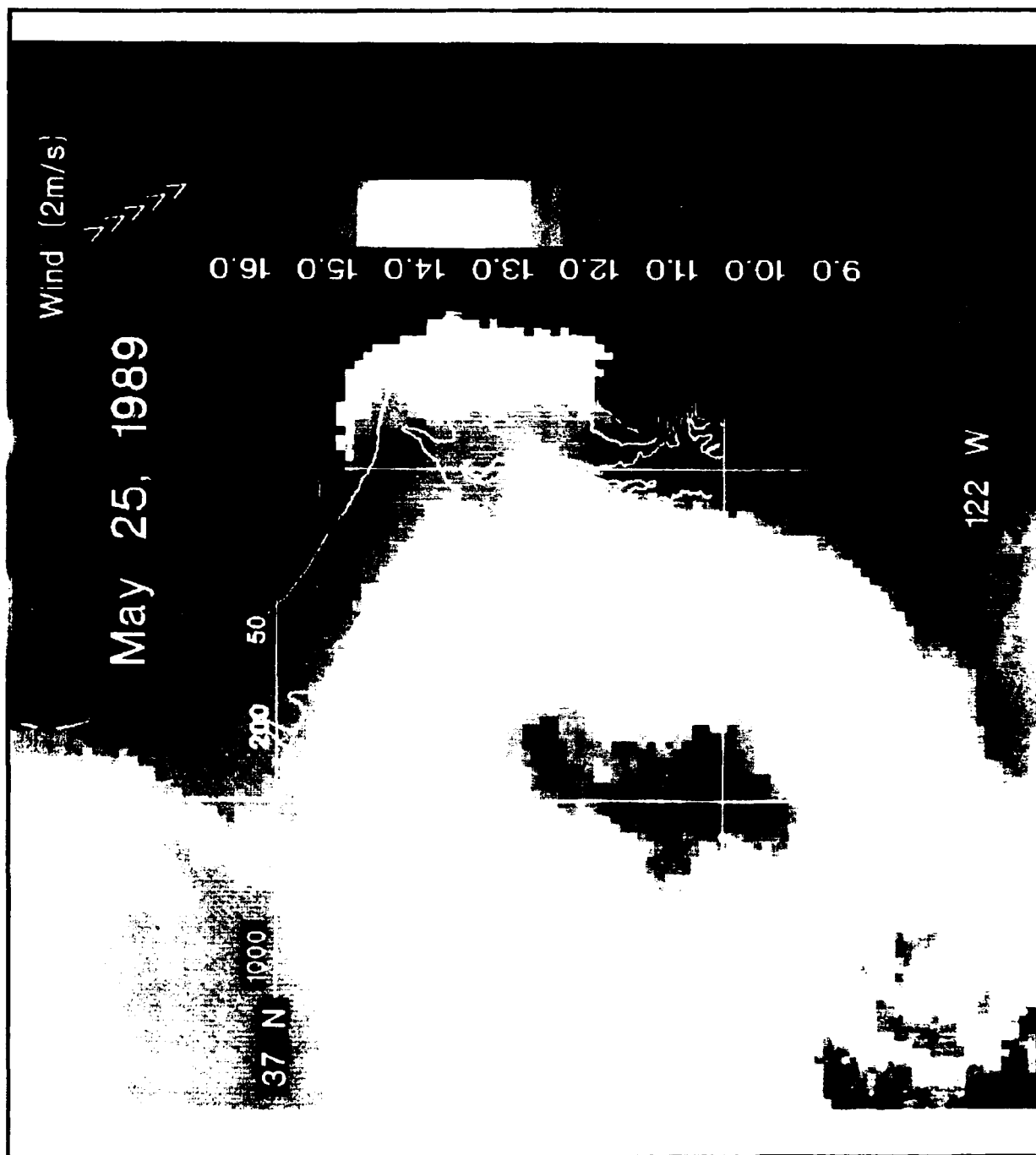
THIS PAGE INTENTIONALLY LEFT BLANK

Figure 21. AVHRR satellite image of Monterey Bay on 5/25/89.
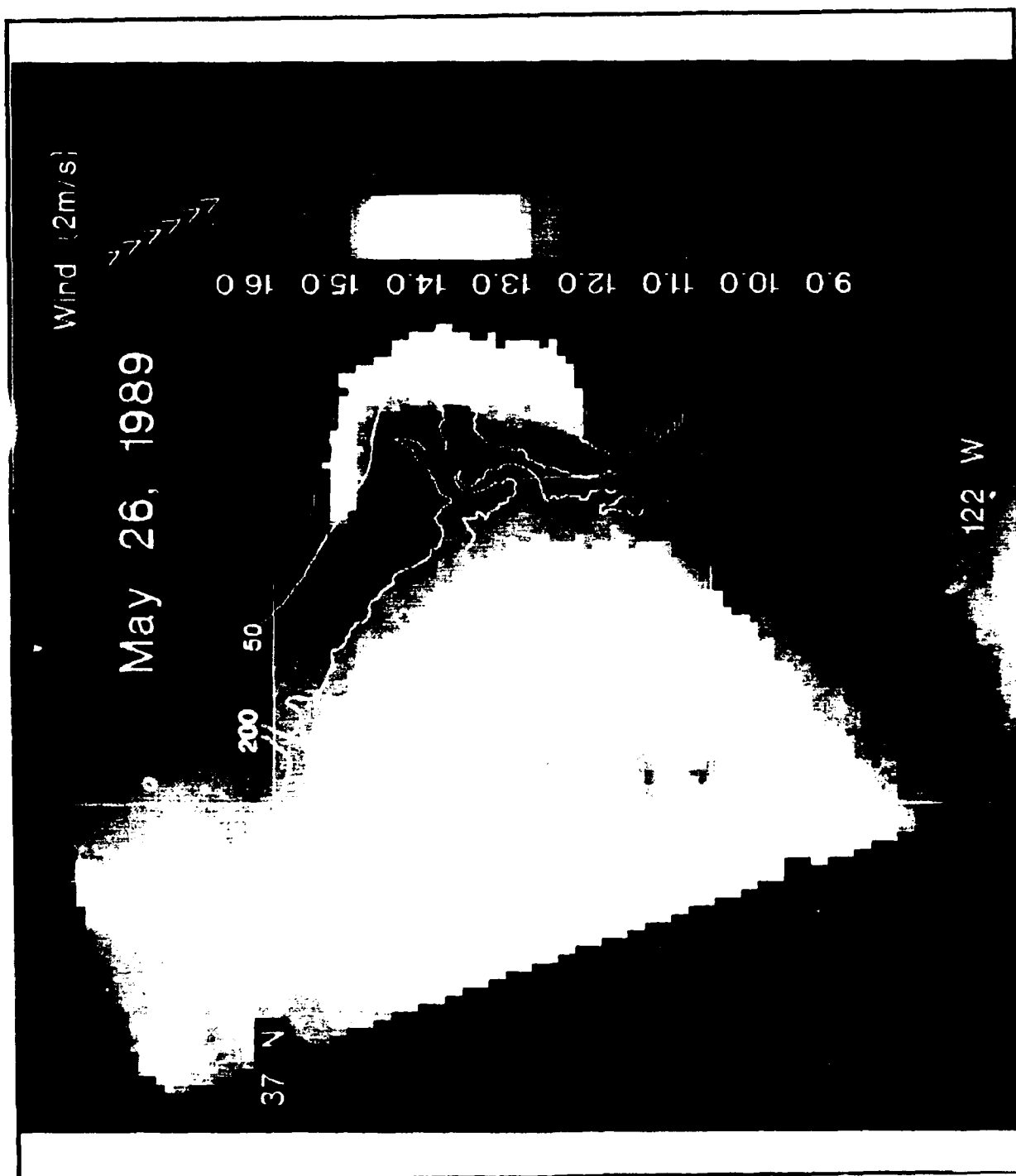
THIS PAGE INTENTIONALLY LEFT BLANK

Figure 22. AVHRR satellite image of Monterey Bay on 5/26/89.
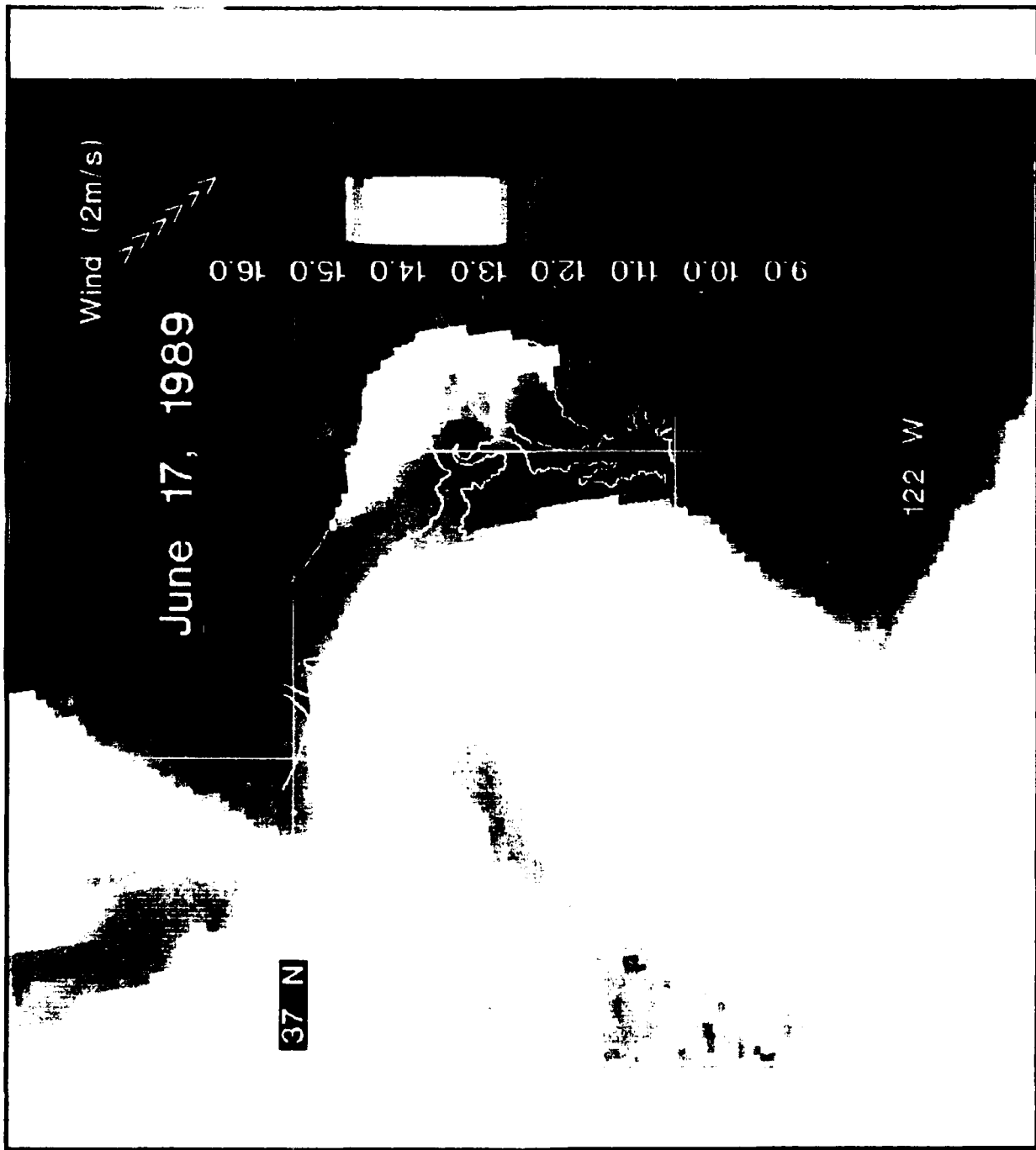
THIS PAGE INTENTIONALLY LEFT BLANK

Figure 23. AVHRR satellite image of Monterey Bay on 6/17/89. Beginning of the second sequence

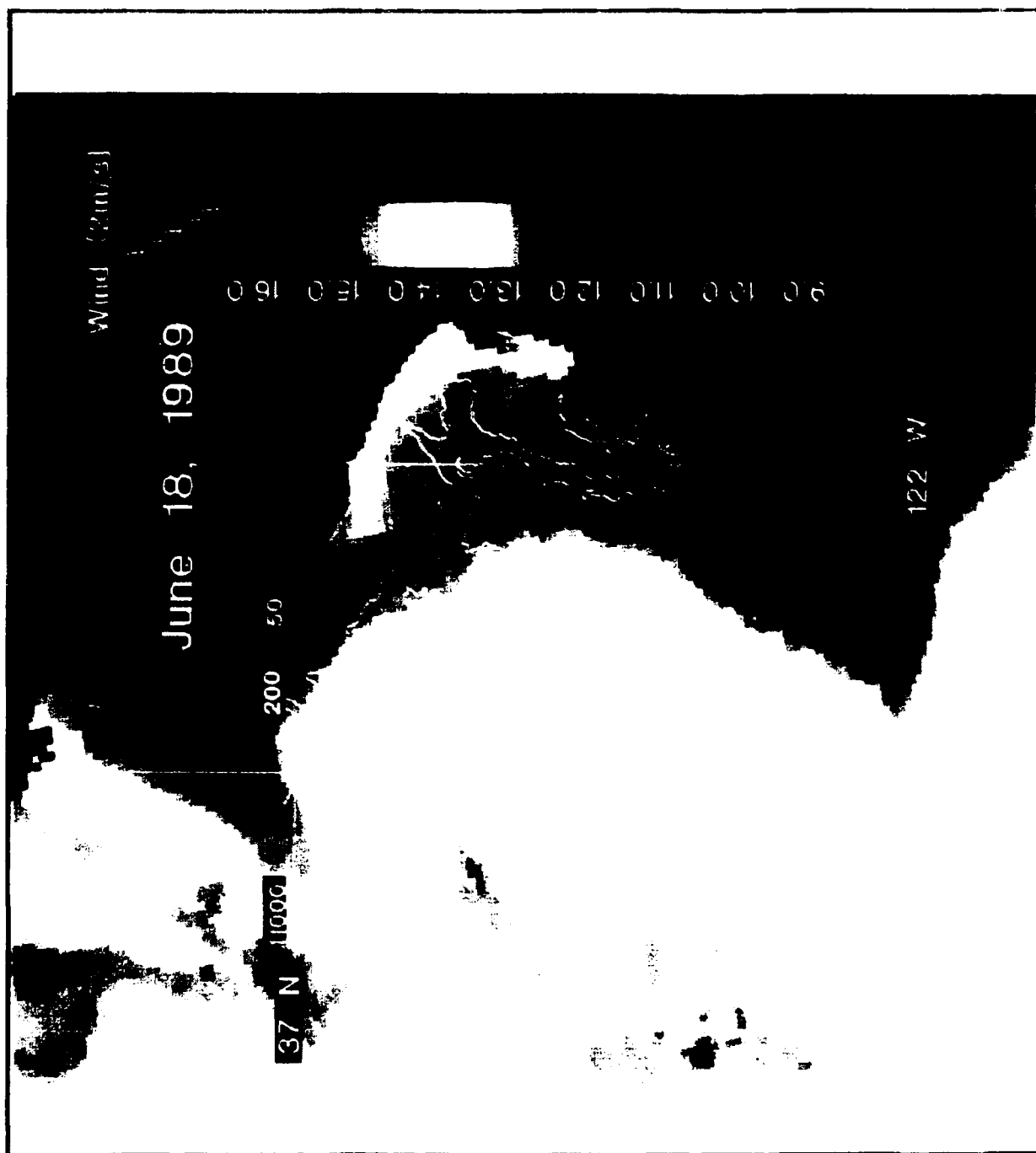THIS PAGE INTENTIONALLY LEFT BLANK

Figure 24. AVHRR satellite image of Monterey Bay on 6/18/89.

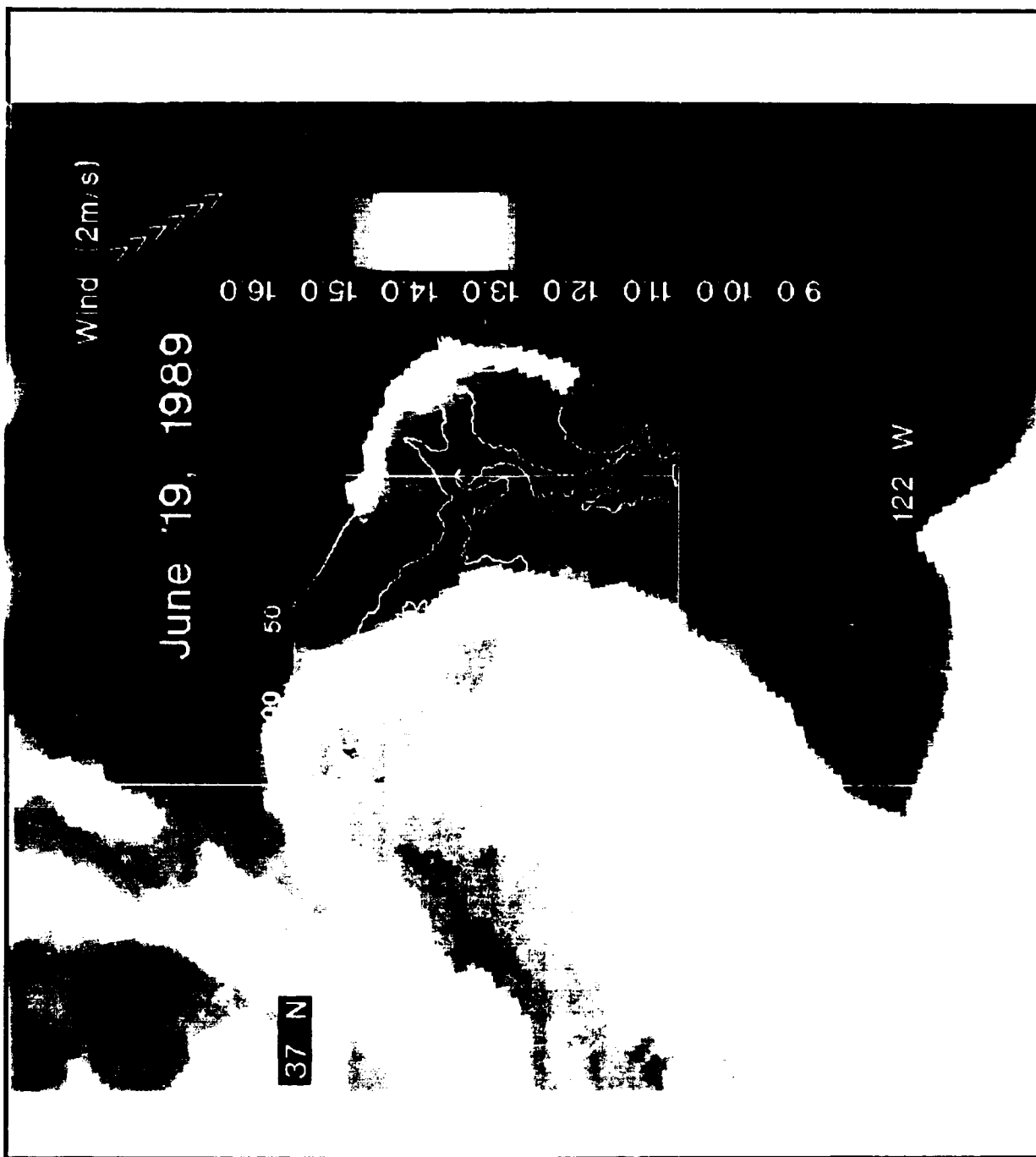THIS PAGE INTENTIONALLY LEFT BLANK

Figure 25   AVHRR satellite image of Monterey Bay on 6/19/89

THIS PAGE INTENTIONALLY LEFT BLANK

oceanic eddy. The cold water near Point Sur extended 10 km further offshore. Warm water stayed within the 50 m contour.

NOAA 11 images were not available on 6/20 and 6/21 due to the position of the satellite orbit. The image on 6/21 is from the NOAA 10 satellite, which only has one infrared channel. Even though the SST accuracy is reduced, the precision of the sensor is the same as that of NOAA 11 The temperature was also registered to the buoy 46042 at the time of the overpass. A composite image for 6/20 (Figure 26) was created from 6/19 and 6/21 (Figure 27) by averaging the temperatures from both images at each pixel location. The wind was still from the northwest, but it had relaxed significantly. The cold centers were not as cold as before, although the cold tongue off Point Sur extended further offshore.

NOAA 11 coverage returned on 6/22 (Figure 28) and shows that a radical change took place. The wind was light and had backed to warmer southerly flow, allowing considerable heating over the entire scene. Oceanic water warmed 2-3 °C and moved toward shore in a northeastward direction until the oceanic feature intersected with the northern boundary of the Bay. Warming occurred in the northern Bay due to a combination of effects, including: surface heating, reduced vertical mixing and advection of the warm oceanic water.

Compared with the previous image, a retroflection feature at the bottom of the scene appeared to move shoreward with clockwise rotation until the feature impacted the shore. This onshore flow was observed near Point Sur by Farrell, Bracher, and Roughgarden (1990) when four recruitment pulses of intertidal barnacle populations occurred during a period of relaxation in alongshore winds and cessation of coastal upwelling. In each case, recruitment ended when strong equatorward winds reappeared and reinitiated upwelling.

65

Notice the warming of the cold tongue off Point Sur. There was an extremely warm 16.8 °C plume offshore oriented north-south along 122° 50'W. The low albedo indicates that this was a true oceanic feature and not a layer of fog which warmed above the water temperature.

There was considerable cloud cover offshore of Monterey Bay on 6/23 (Figure 29). The wind remained southerly and increased in strength. Buoy 46042 was covered by clouds during the satellite pass so the registration of the image was approximated by a nearby pixel temperature. This is reasonable since the surface temperature was fairly uniform near the buoy on 6/22 and appeared uniform again on 6/23. In general, there was cooling of the surface, but warming nearshore at the south end of the Bay. Cold water remained near Point Sur.

The southerly wind continued on 6/24 (Figure 30) with clouds approaching from the south. The Bay and oceanic water appeared uniformly warm. The cold cell located near Point Sur on 6/23 was located further north on 6/24.

Unfortunately, clouds obscured Monterey Bay during the next two days as the wind veered to northwesterly becoming favorable for upwelling again.

C. CTD OBSERVATIONS

Since there was considerable variability in the vertical and horizontal structure of the Bay, this study has not relied completely on CTD data, but used temperature data in support of MCSST from AVHRR satellite imagery. Since the winds were consistently favorable to upwelling during 5/18-25, the CTD transections were considered synoptic. Several sources of hydrographic data were studied to supplement the AVHRR imagery.

1. Surface Temperature Contours

The NOAA Ship DAVID STARR JORDAN made numerous CTD casts near Monterey Bay during 5/14-6/13, as part of the Southwest Fisheries Science Center's
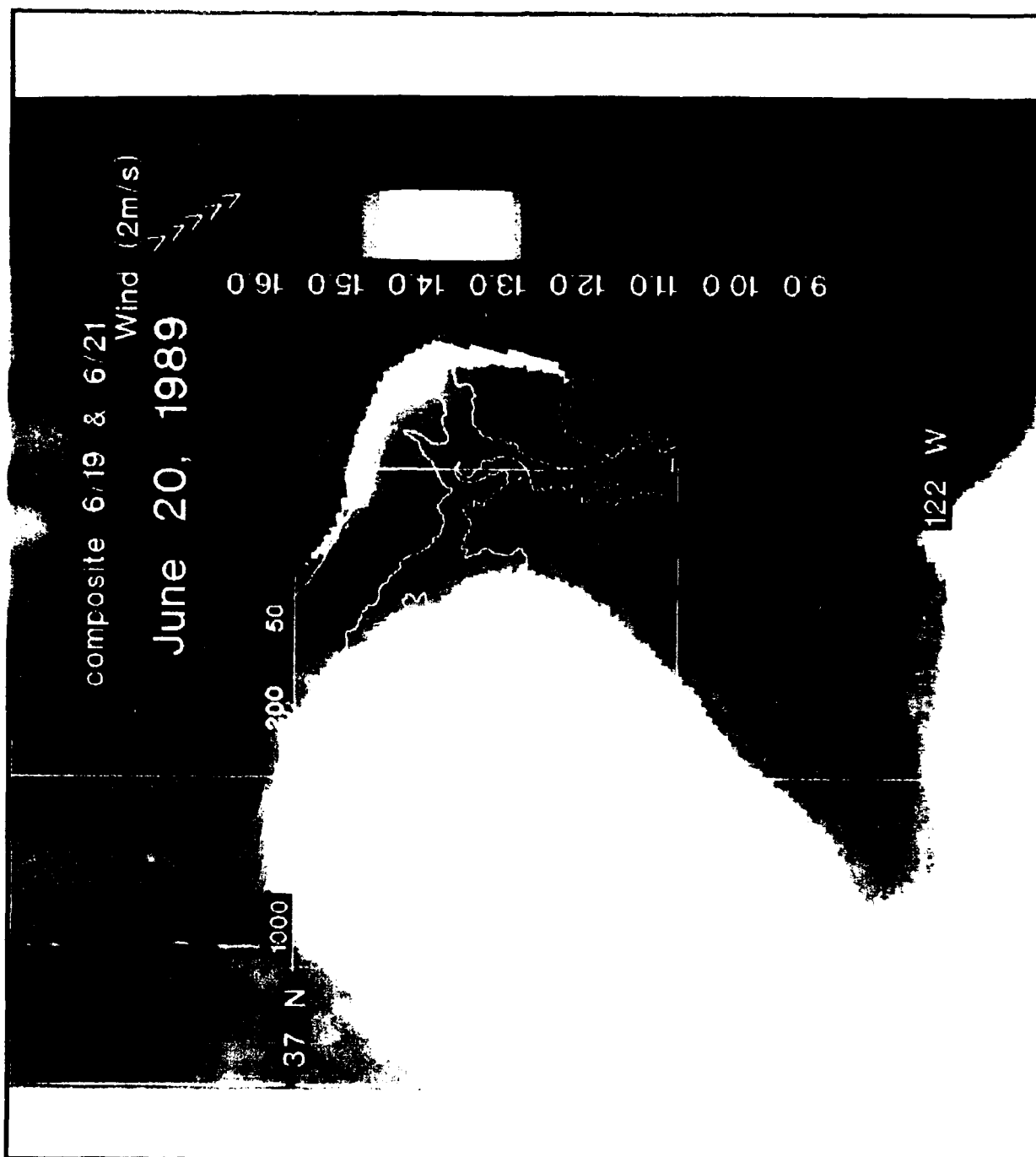
Figure 26   AVHRR satellite 6/20/89 composite image of Monterey Bay from 6/19 and
6/21
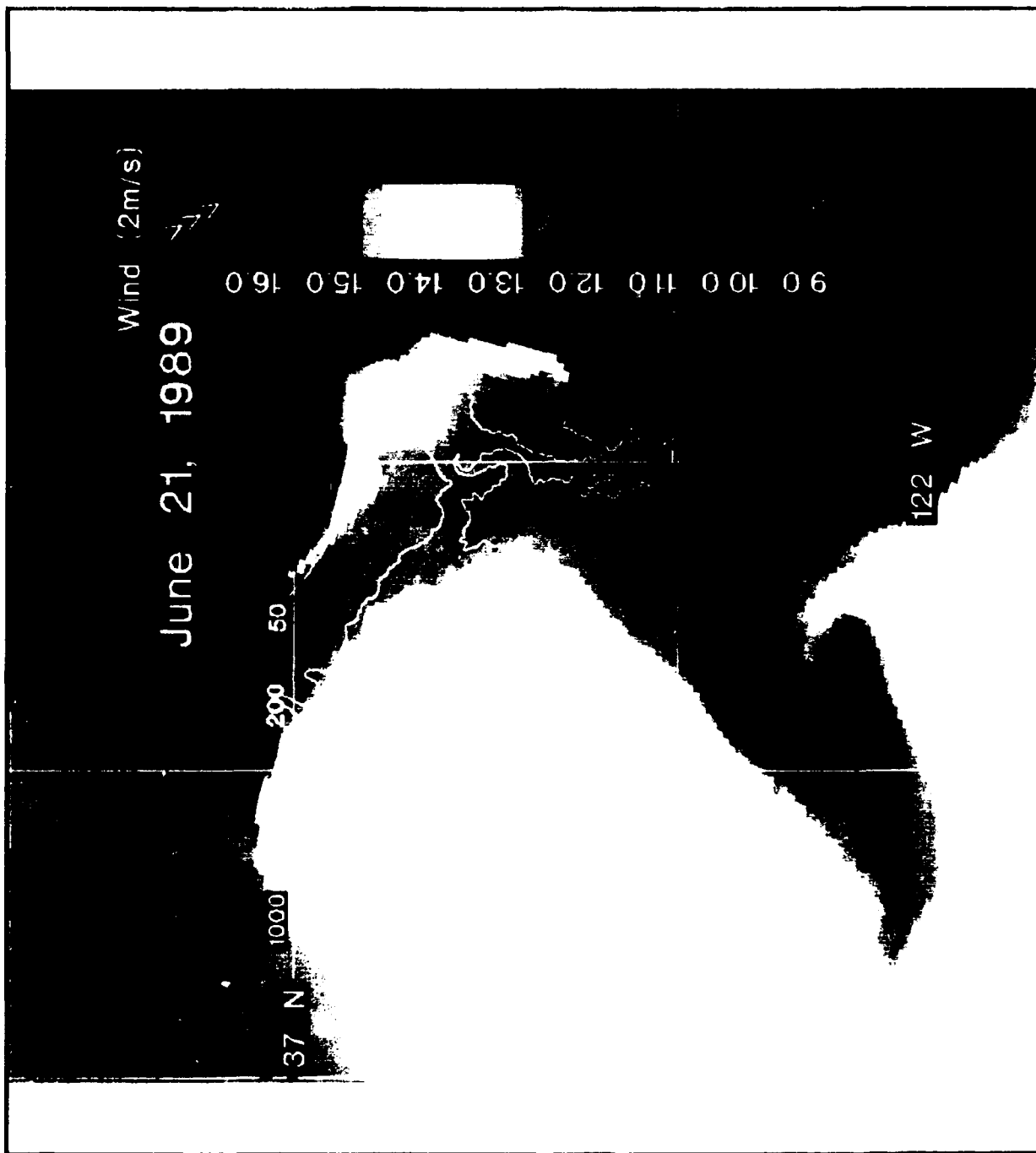
THIS PAGE INTENTIONALLY LEFT BLANK

Figure 27 AVHRR satellite image of Monterey Bay on 6/21/89.

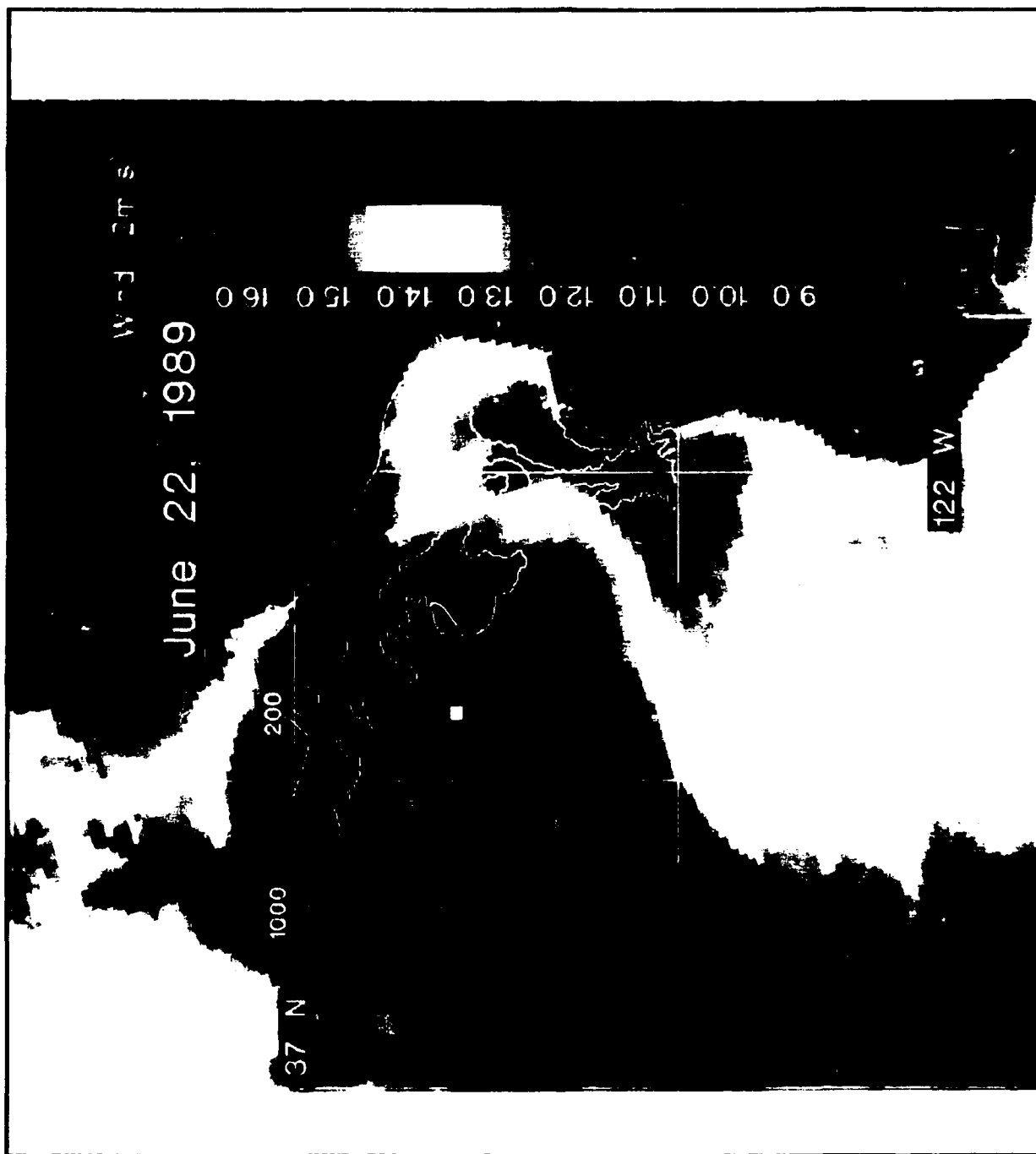THIS PAGE INTENTIONALLY LEFT BLANK

Figure 28. AVHRR satellite image of Monterey Bay on 6/22/89.
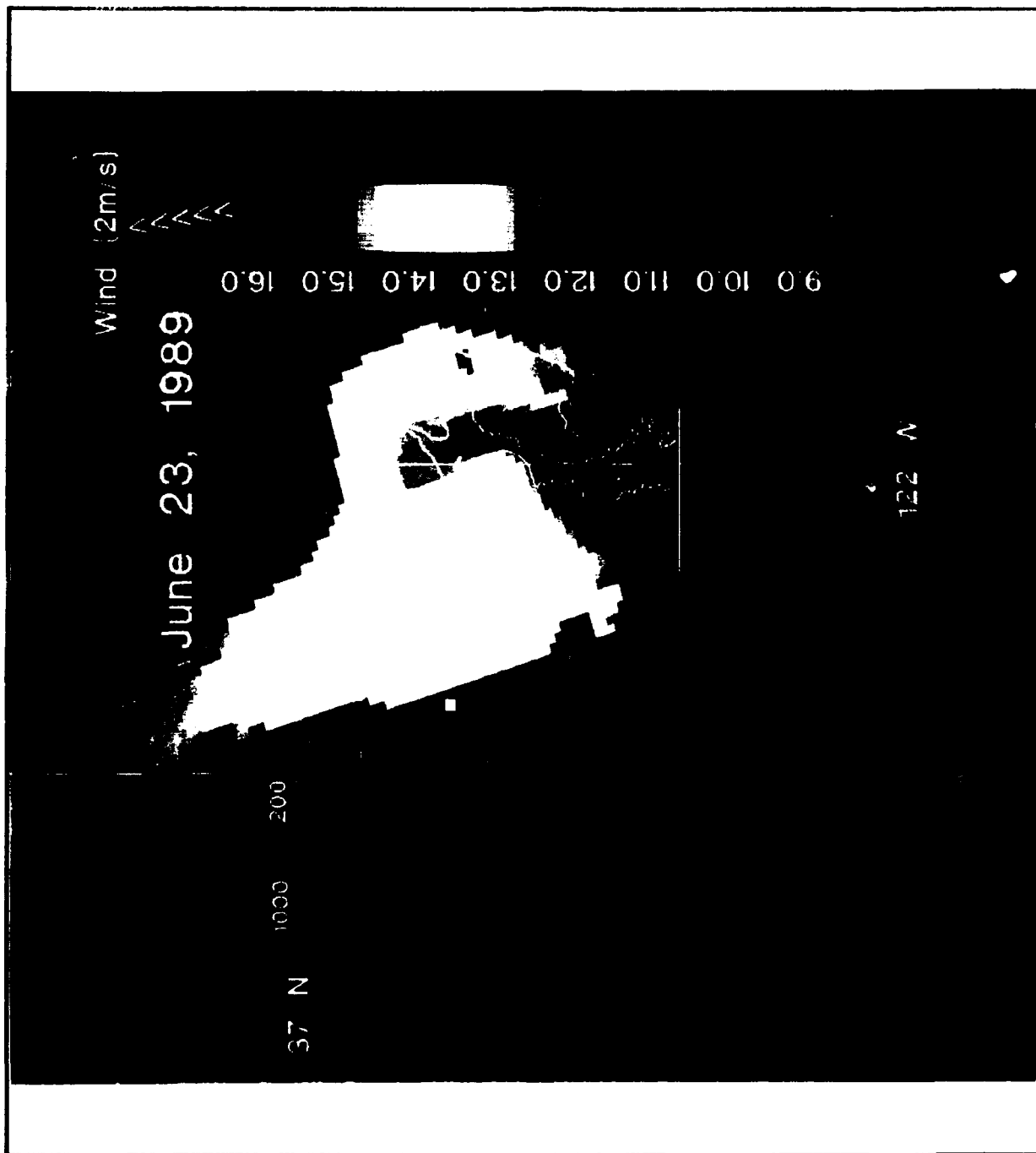
THIS PAGE INTENTIONALLY LEFT BLANK

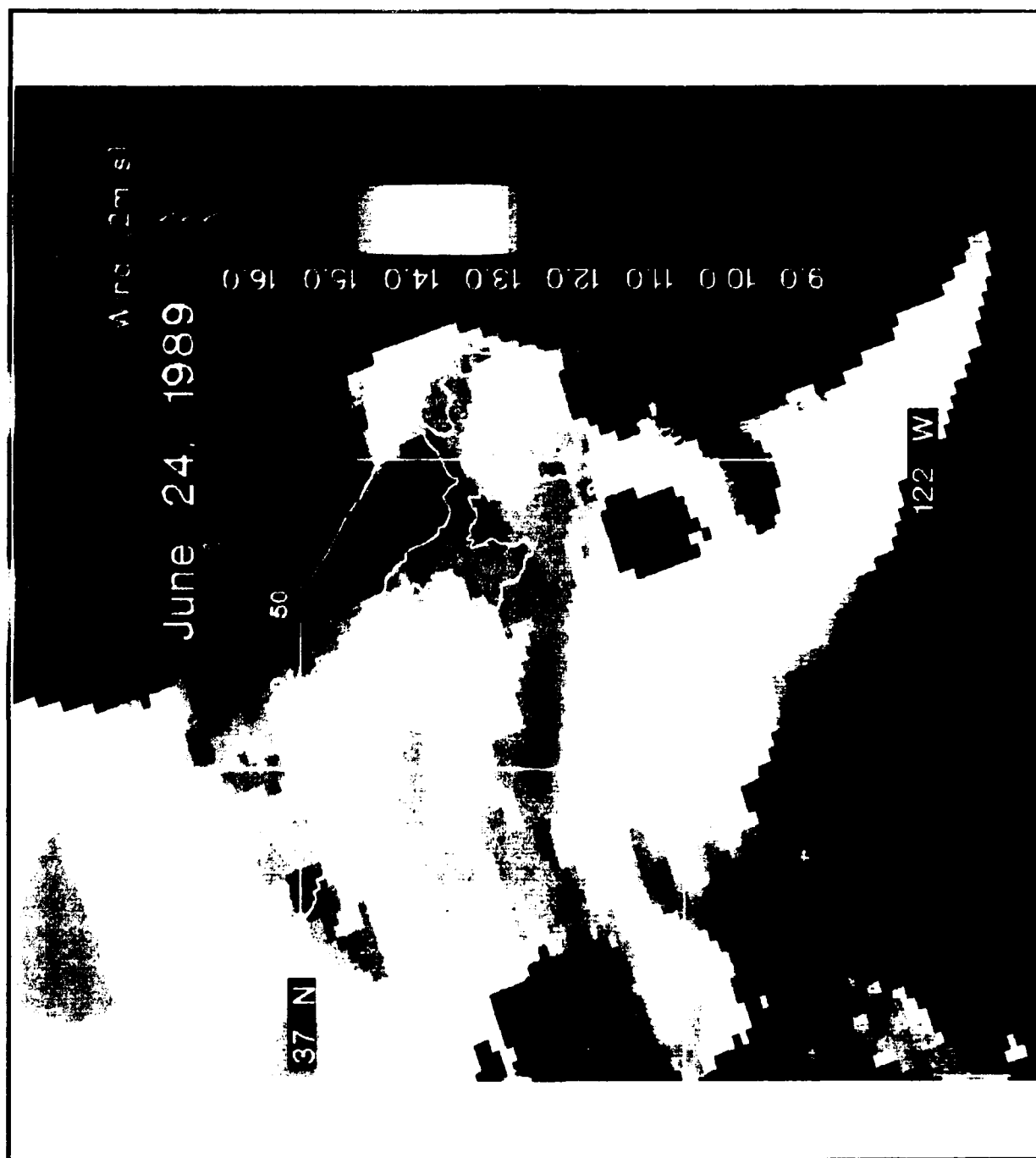Figure 29. AVHRR satellite image of Monterey Bay on 6/23/89.

BLANK PAGE

Figure 30. AVHRR satellite image of Monterey Bay on 6/24/89

BLANK PAGE

groundfish recruitment program. Near-surface temperatures from this cruise agree very closely with the results of satellite imagery and USNS DeSTEIGUER transections. In fact, the surface temperature contours are in close quantitative agreement with the satellite image of 5/25 (Figure 31). The cold upwelling water near Año Nuevo is well defined along with the cool plume across the mouth of the Bay. Warm water is seen both inside the Bay and offshore in the anticyclonic eddy.

The satellite pass on 5/25 was an instantaneous measurement of SST while the CTD surface contour was acquired over several days. Even though there is significant variability in the nearshore processes, the excellent quantitative agreement of the two independent observations in both amplitude and spatial structure of the thermal field provides good justification for allowing data intercomparison between satellite MCSST and shipboard CTD observations.

2. Time Series

MBARI periodically occupies a set of fixed hydrographic stations in Monterey Bay; including C1, H3, C7, M1, H1, and H3 whose locations are shown on Figure 18. During the May - June period, most of these stations were occupied on 5/4, 6/14, 6/20 and 6/29. This sampling allows temporal variation of the vertical temperature structure to be estimated. Station C1 (Figure 32) lies inside the Bay at the head of the Canyon. The sequence began on 5/4 with warm, 14.9 °C surface water. The surface water was significantly cooler by 6/14 and cooled further to 12.6 °C by 6/20. However, on 6/29 the surface temperature was over 14.6 °C. The warm temperatures on 6/29 followed the relaxation event mentioned earlier. The warming of the entire water column down to at least 200 m indicates onshore advection of warm oceanic water, as opposed to just surface heating effects. This advection progressed at least as far as the head of the Canyon at station C1.

Station H3 (Figure 33) is located mid-Bay and, similar to station C1, showed warming throughout the water column down to at least 200 m between 6/20 and 6/29. (No data were available for this station on 5/4.) Station C7 (Figure 34), located further offshore over the Canyon axis, was in the warm oceanic water prior to the relaxation event and exhibited a similar surface warming, but a reduced amount of warming at depth between 6/20 and 6/29, with considerably more heating near the surface. Stations M1 (Figure 35) and H1 (Figure 36) are located in the south Bay. These stations both showed the cooling trend from the beginning of May to mid-June and the warming event throughout the water column between 6/20 and 6/29. Station H5 (Figure 37) in the north Bay also warmed between 6/20 and 6/29.

3. Station Profiles

Vertical profiles of temperature were compared for the six MBARI stations for the observation dates 5/4, 6/14, 6/20, and 6/29. On 5/4 (Figure 38), all stations inside the Bay, with the exception of H3 for which no data were available, showed warm surface water in the Bay, in agreement with the satellite image of 5/3 (Figure 39). The apparently southward-flowing cold water jet envelops station C7 which shows near surface temperatures 2-3 °C cooler than the stations inside the Bay. On June 14 (Figure 40) (for which no data is available at station H5), the warmest water appeared nearshore at C1, with colder water from the southward flowing jet being seen at H3 and C7. On June 20 (Figure 41), the well established cold jet was seen in satellite imagery and at all stations, except the nearshore station C1 and the northern station H5, where warming had occurred. The shallow warm layer in the north Bay at H5 indicates high surface solar heating and low vertical mixing. Assuming equal surface heating at all stations, the 10 m mixed layer depth suggests lighter winds than at the other stations, which have mixed layer depths of 20-30 m.

78
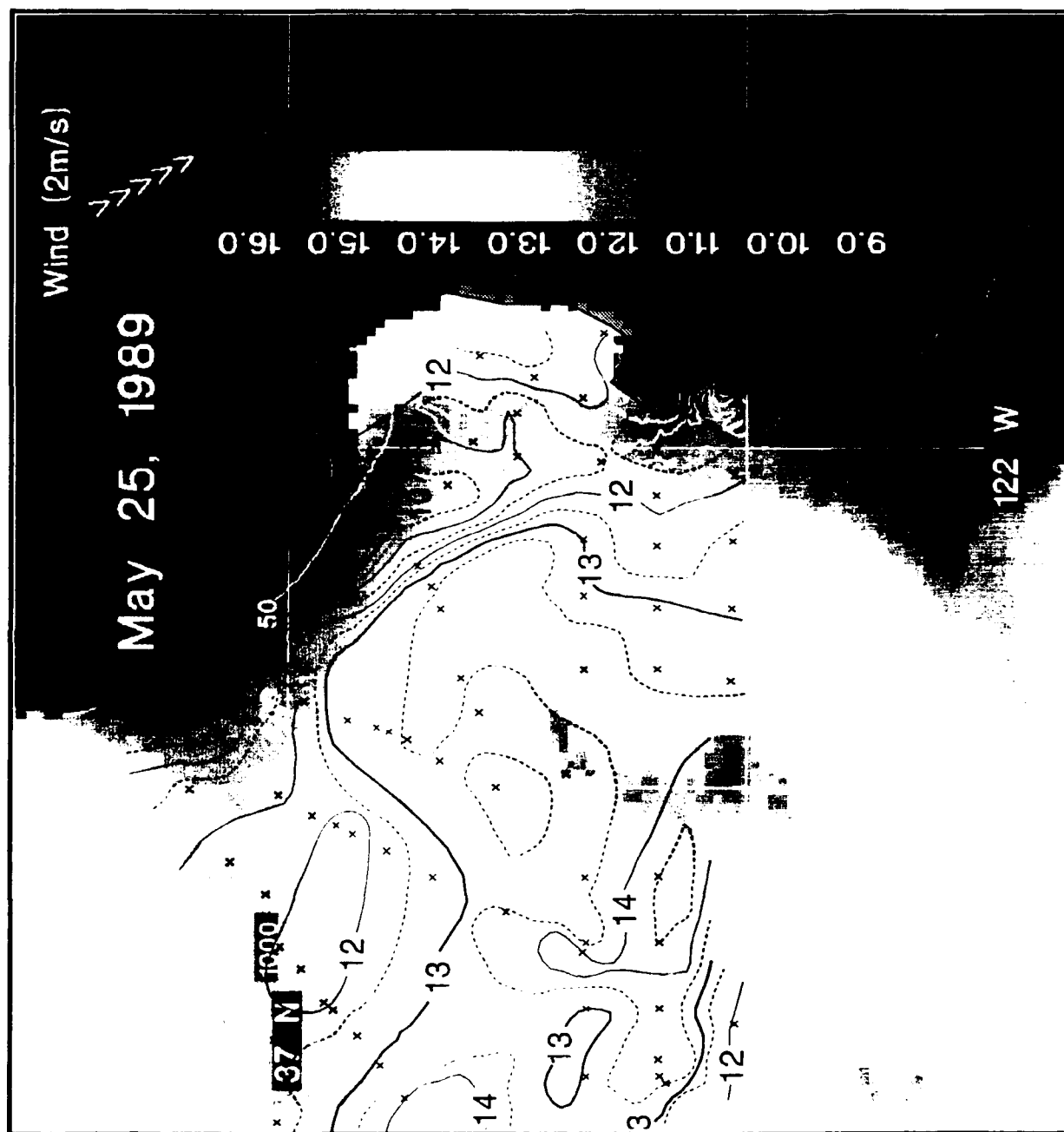
Figure 31. AVHRR satellite image of Monterey Bay on 5/25/89. Surface temperature contours from CTD stations collected between 5/23-5/25 by DeSTEIGUER and DAVID STARR JORDAN were laid over the satellite image. There is good qualitative agreement between ship observations and satellite

79

BLANK PAGE

Figure 32. Time series profiles of temperature at MBARI station C1.

Figure 33. Time series profiles of temperature at MBARI station H3.

Figure 34. Time series profiles of temperature at MBARI station C7.

83

Figure 35. Time series profiles of temperature at MBARI station M1.

84

Figure 36. Time series profiles of temperature at MBARI station H1.
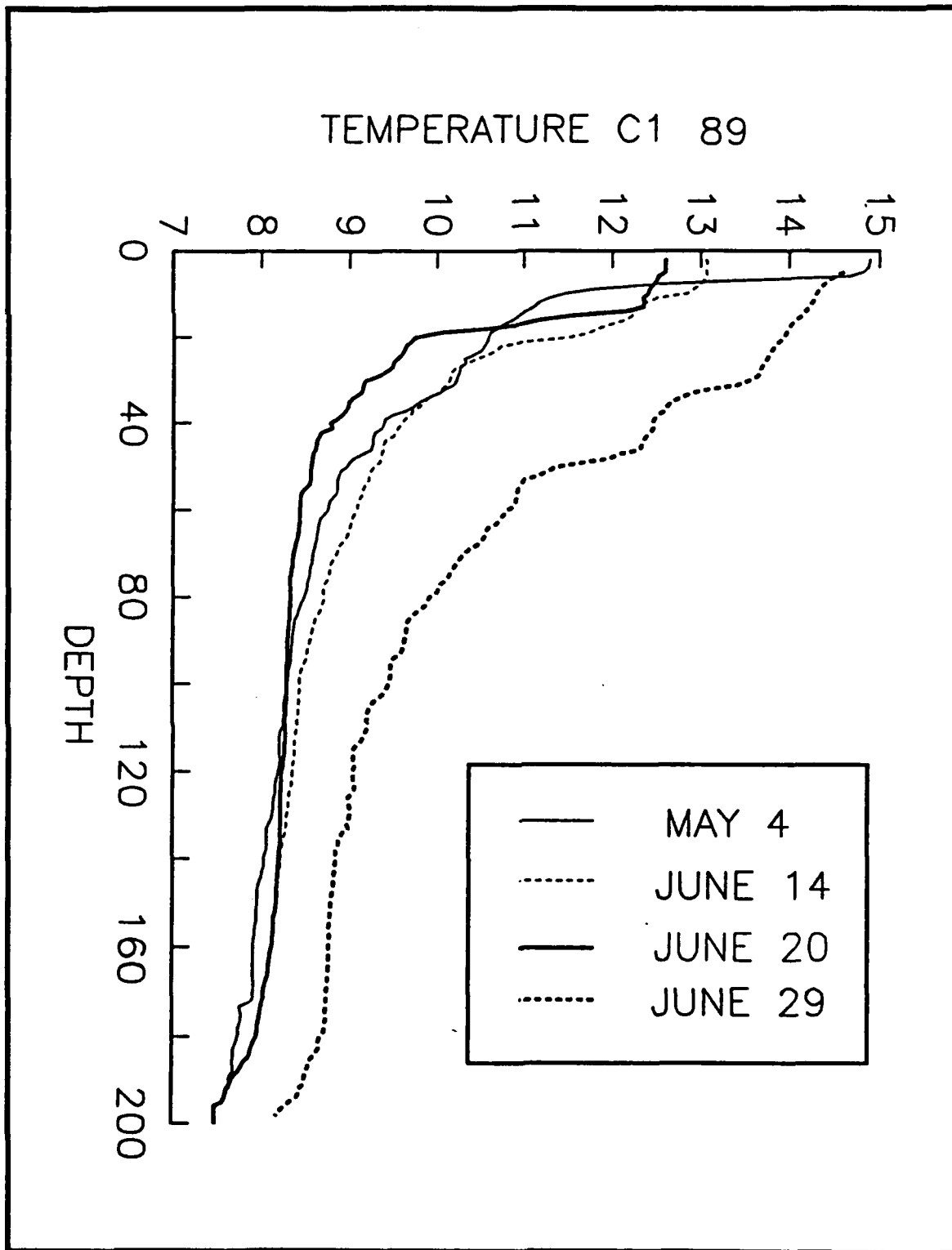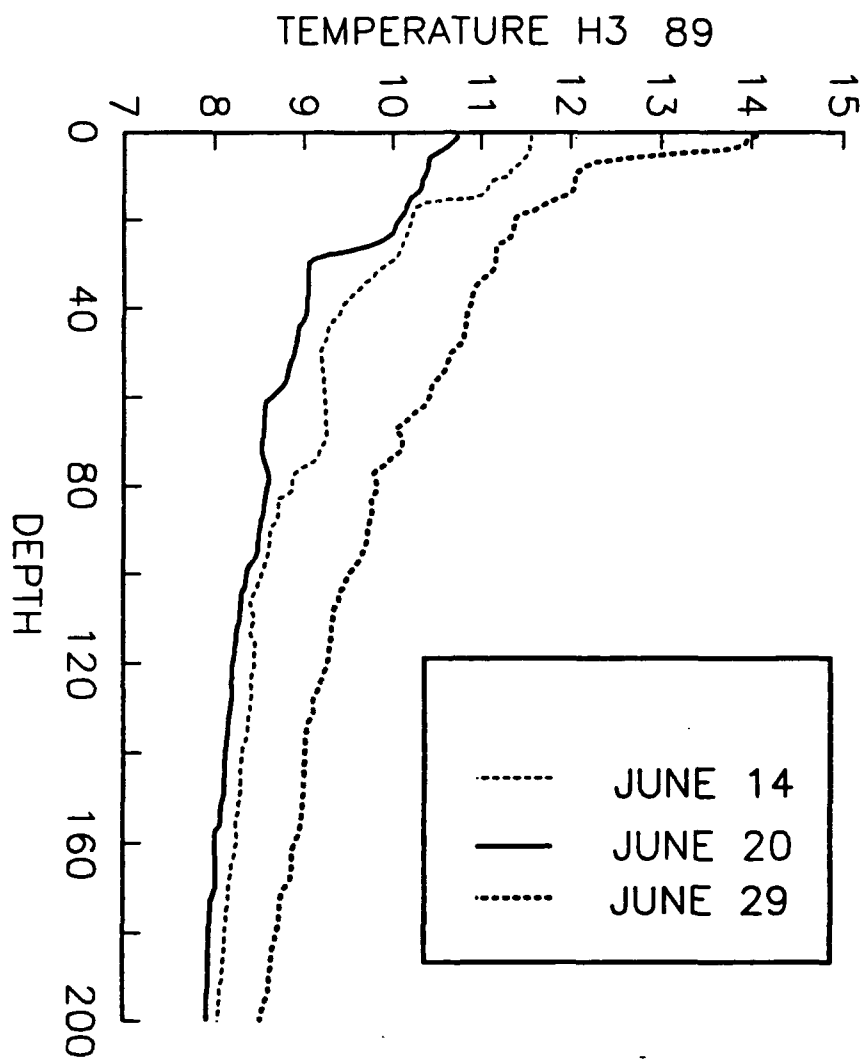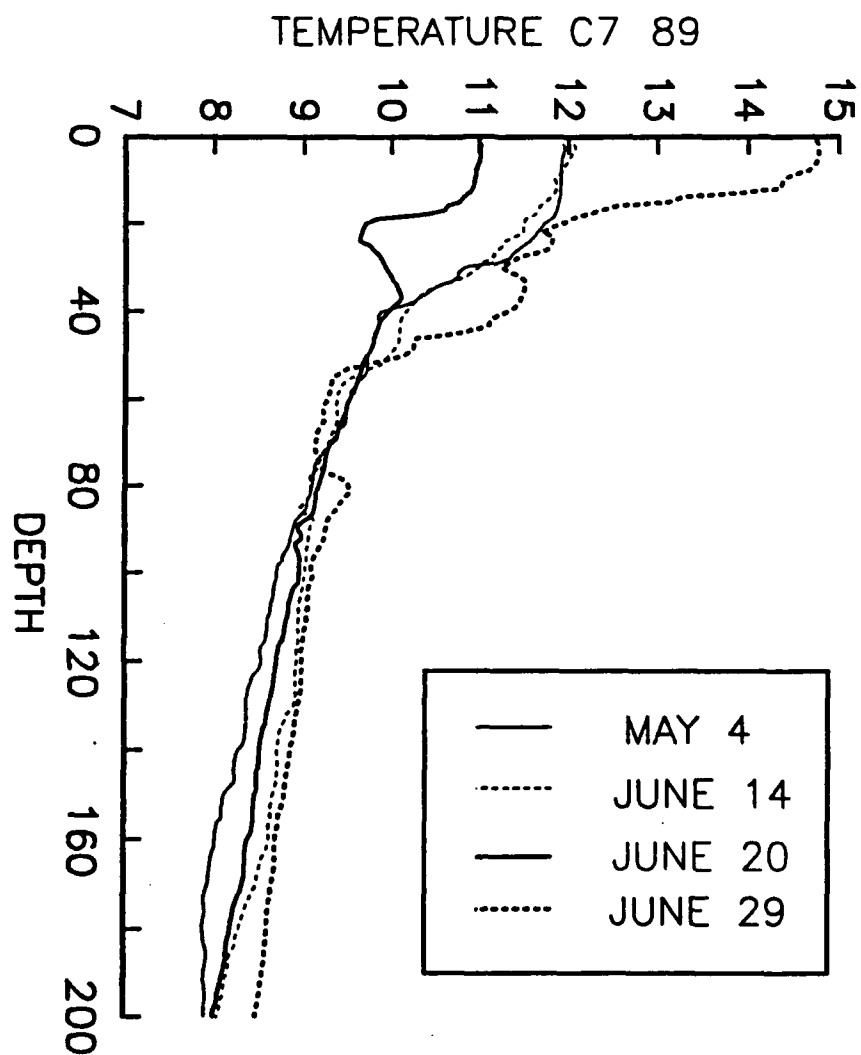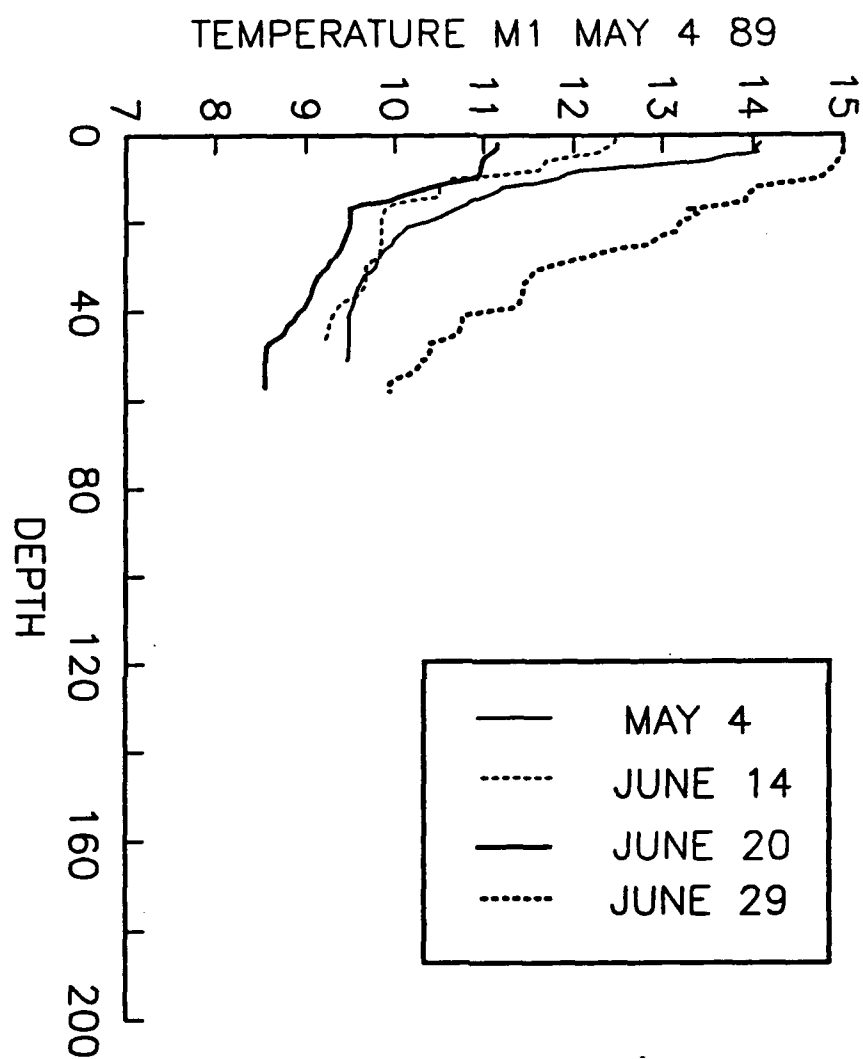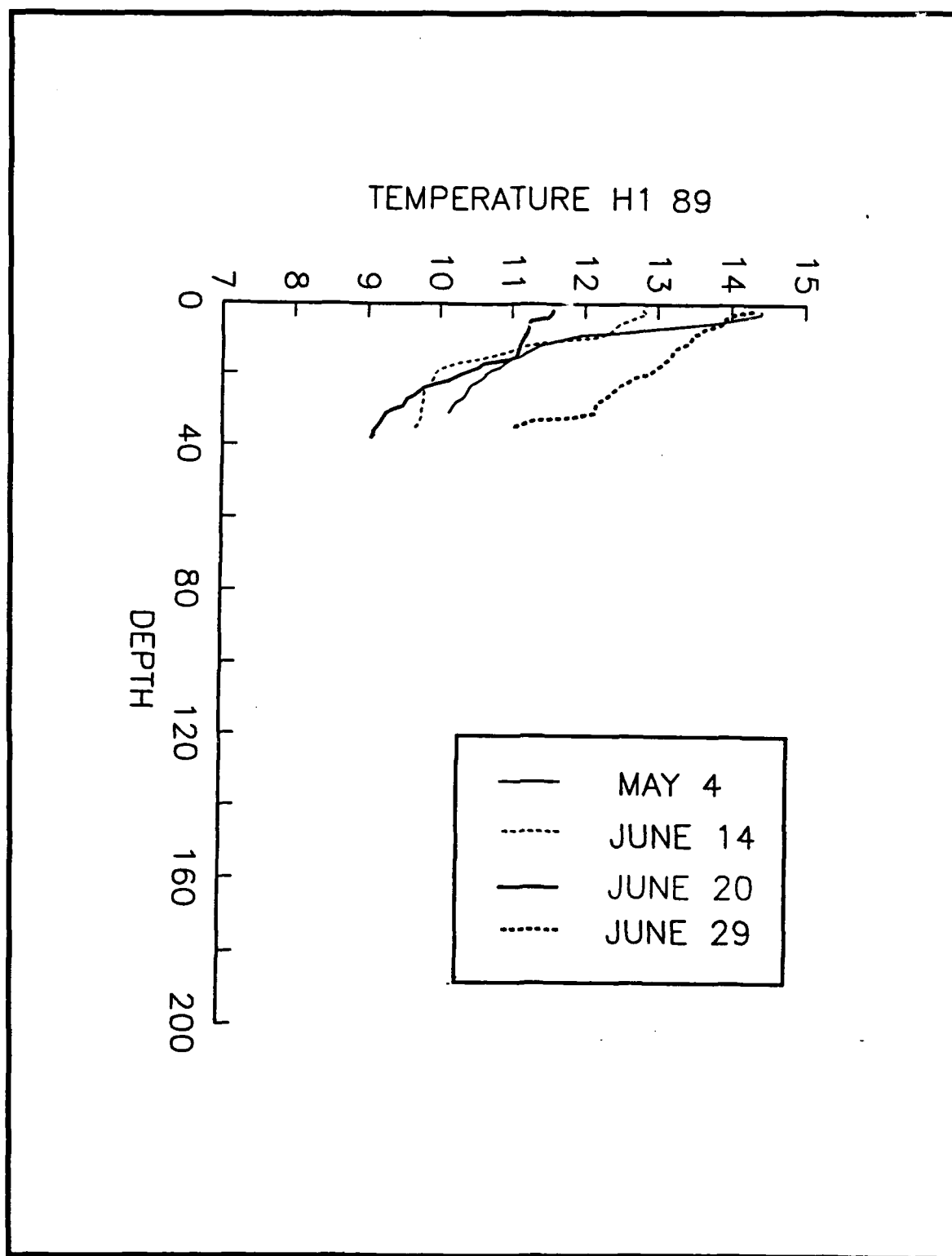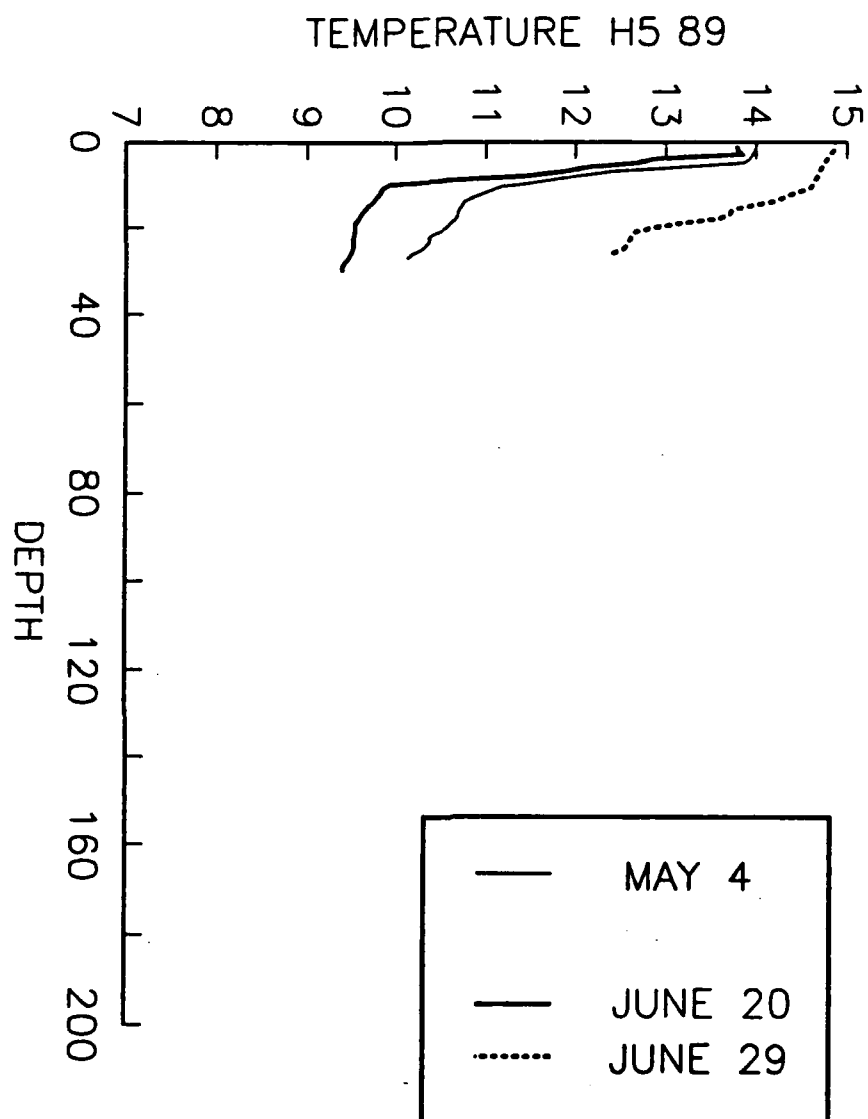
Figure 37. Time series profiles of temperature at MBARI station H5.
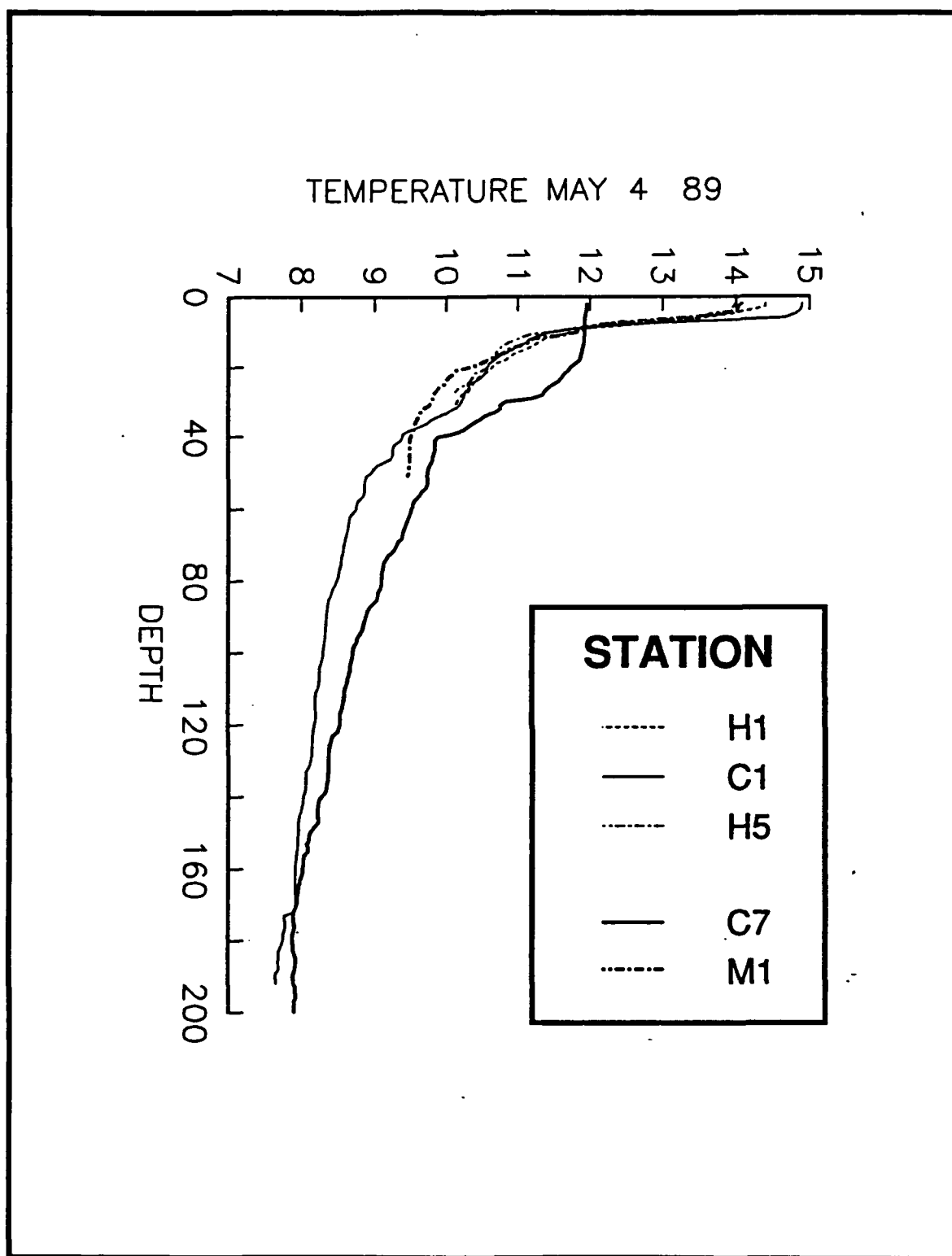
86

Figure 38. May 4, 1989 profiles of temperature at MBARI stations.

On June 29 (Figure 42) following the relaxation event, all stations have warmed throughout the water column. This warming indicated a complete exchange in water mass throughout the Bay with oceanic water.

4. CTD Transections

Locations of CTD stations are identified in Figure 18. Contoured vertical sections of the May 20-25, temperature data help to identify the upwelling locations. For example, the Santa Cruz section (Figure 43) including the nearshore station 42 out to station 92 shows nearshore upwelling down to the 9 degree isotherm (about 100 m depth). The 8.5 °C isotherm is nearly level at about 150 m which suggests that the surface flow is decoupled from the deeper circulation. A thermal front appears to be located between stations 44 and 72. Assuming a level of no motion at the reference level of 150 m, the geostrophic flow is equatorward (out of the page) which is in agreement with the warm core eddy seen offshore. Surface warming occurred reaching a maximum over 14.5 °C offshore in this warm core eddy.

The Moss Landing (Figure 44) section including the nearshore station 30 out to station 94 shows warm water centered on station 77, the center of the offshore eddy, with cooler water toward the shore. It is only the isotherms warmer than 11 °C (above 40 m) that bend upward to form a cool front between stations 68 and 28. There is no indication of nearshore upwelling as seen in the Santa Cruz section. The Canyon Axis (Figure 45) section includes the nearshore station 30 out to station 14. Warm surface water centered on station 24 had a mixed layer depth of 30 m. The surface water cooled toward the shore with a cold front between stations 29 and 35 which agrees with the cool tongue seen in the AVHRR imagery. The 8.5 °C isotherm again is nearly level at about 125 m.
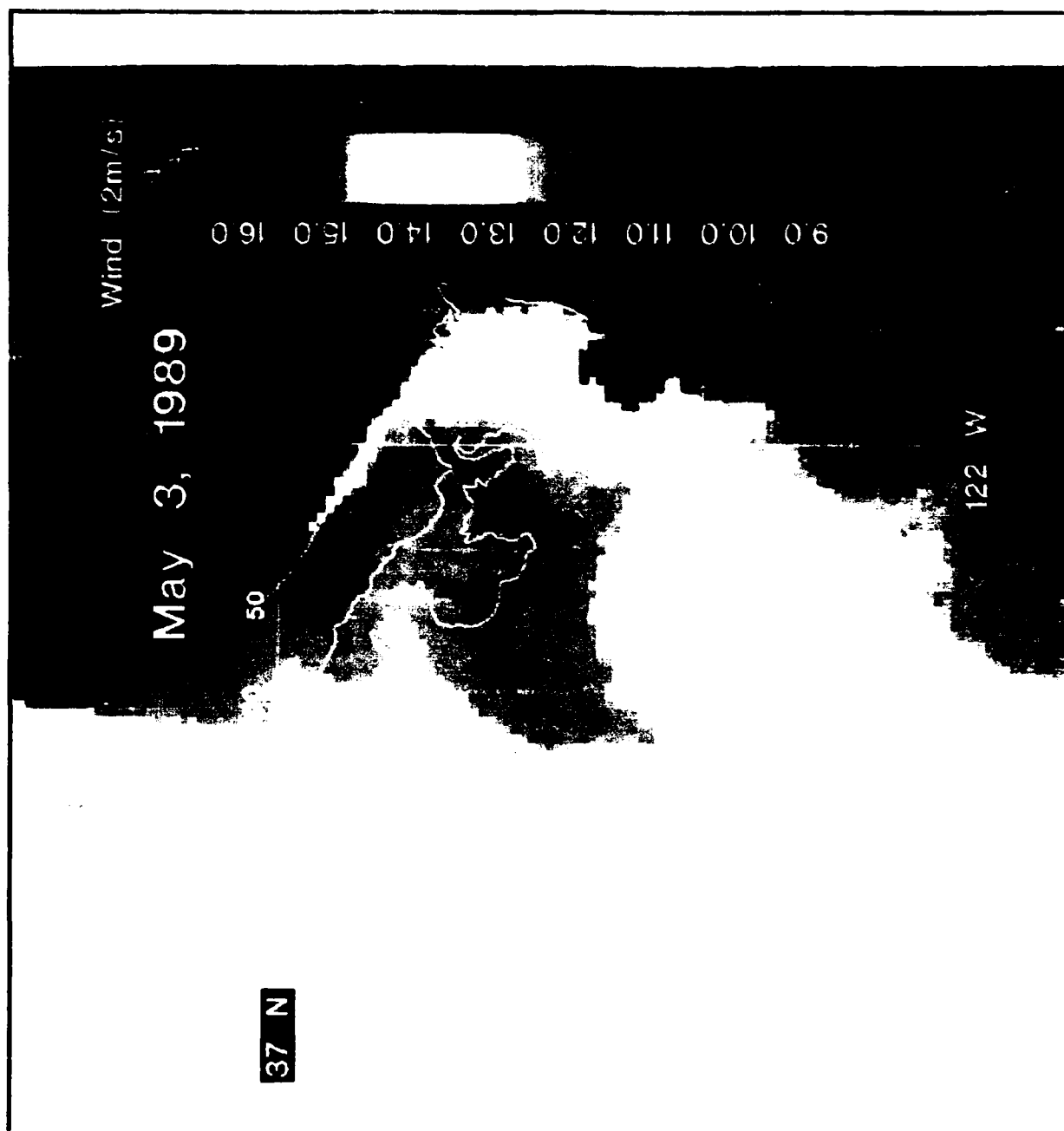
Figure 39. AVHRR satellite image of Monterey Bay on 5/3/89. There is good agreement between the satellite MCSST and Figure 38. Station C7 is cool at the surface. The remaining stations are warm at the surface as seen by both the satellite and the temperature profiles for 5/4/89.

BLANK PAGE
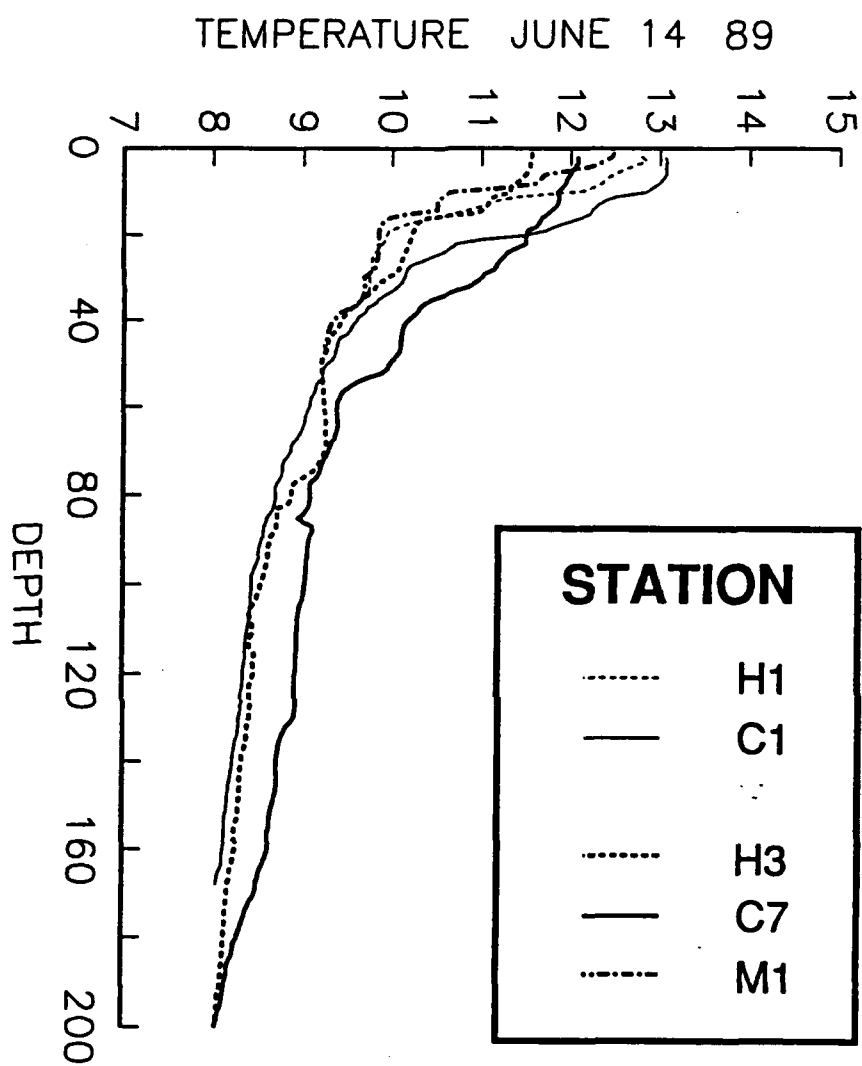
Figure 40. June 14, 1989 profiles of temperature at MBARI stations.
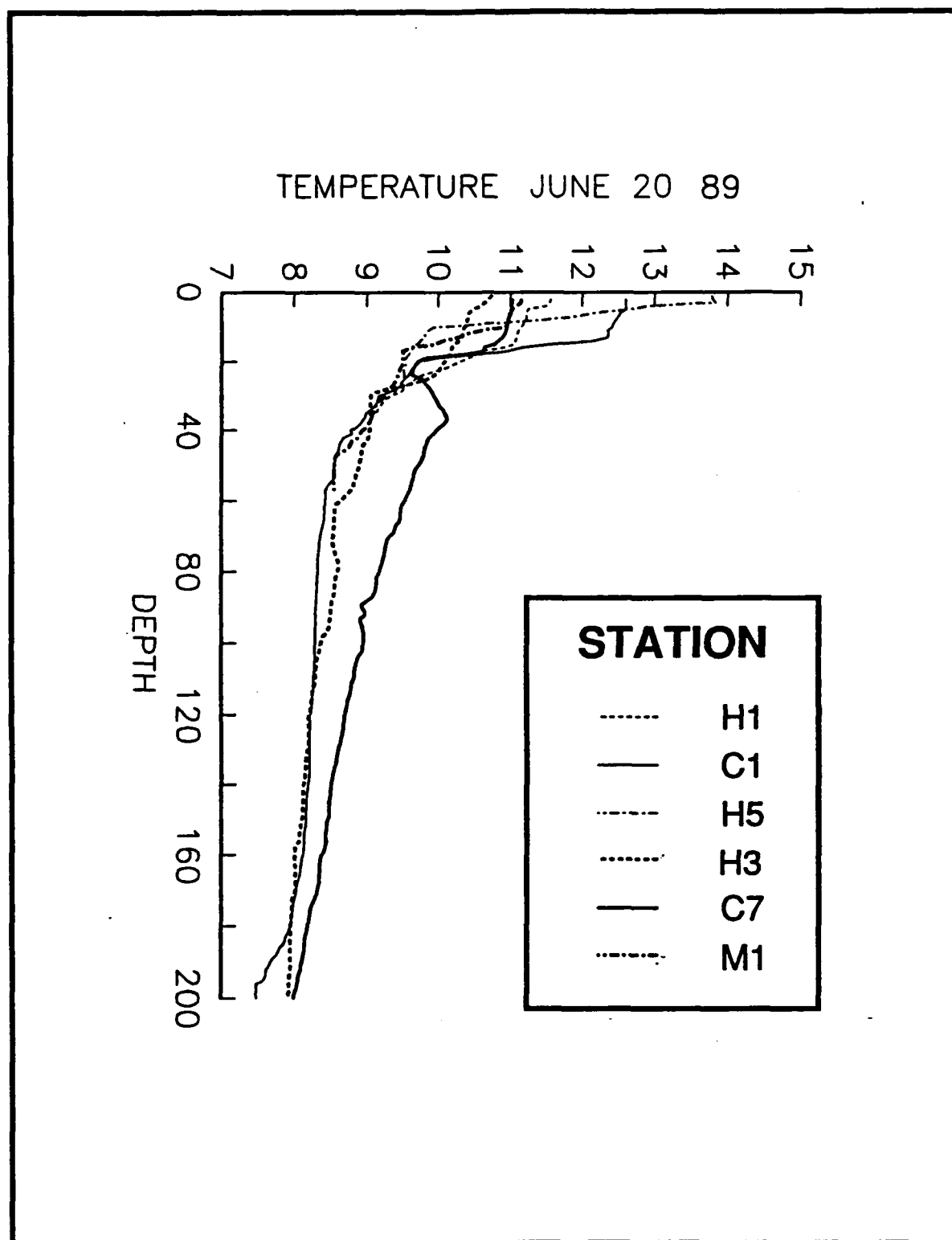
Figure 41. June 20, 1989 profiles of temperature at MBARI stations.
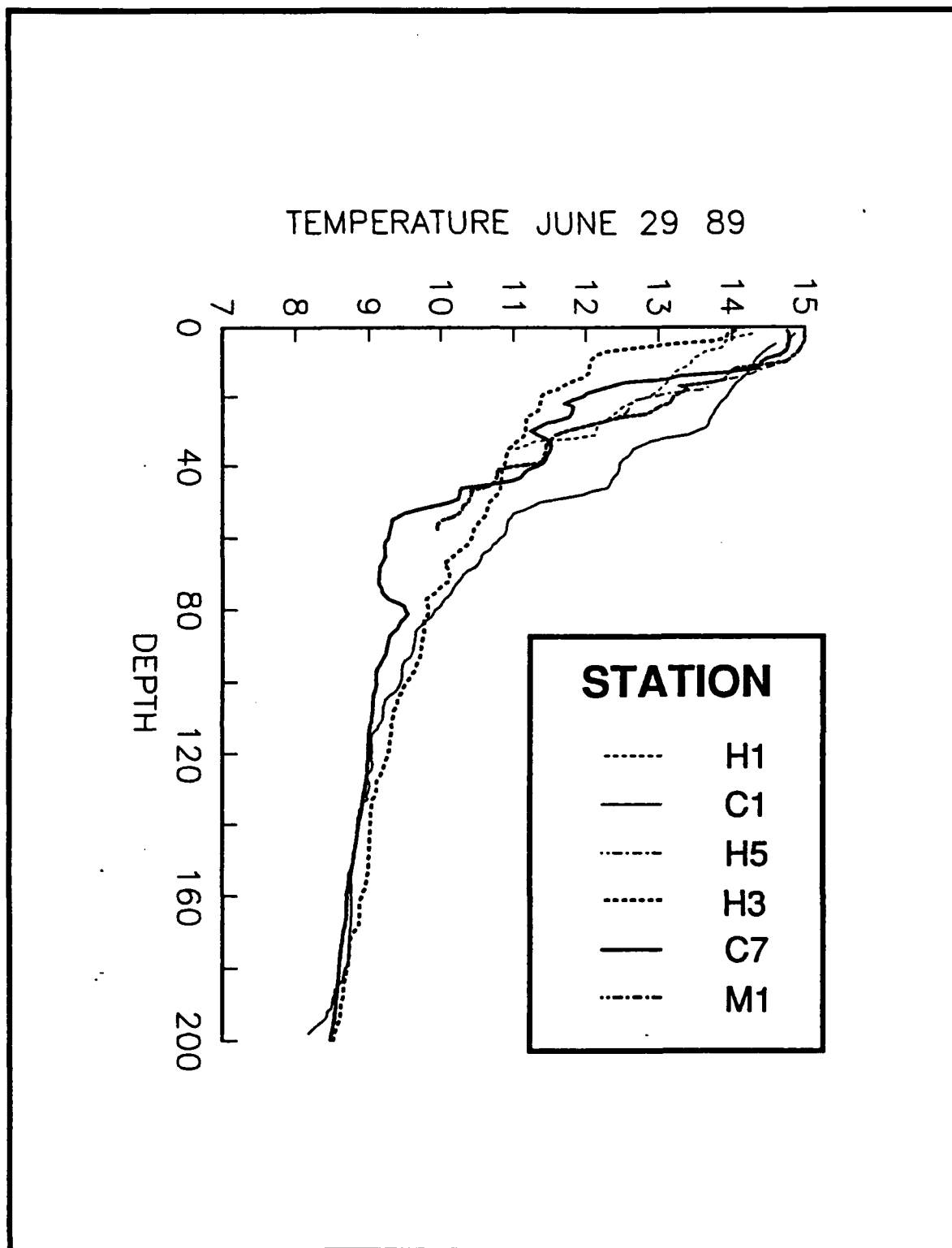
Figure 42. June 29, 1989 profiles of temperature at MBARI stations.
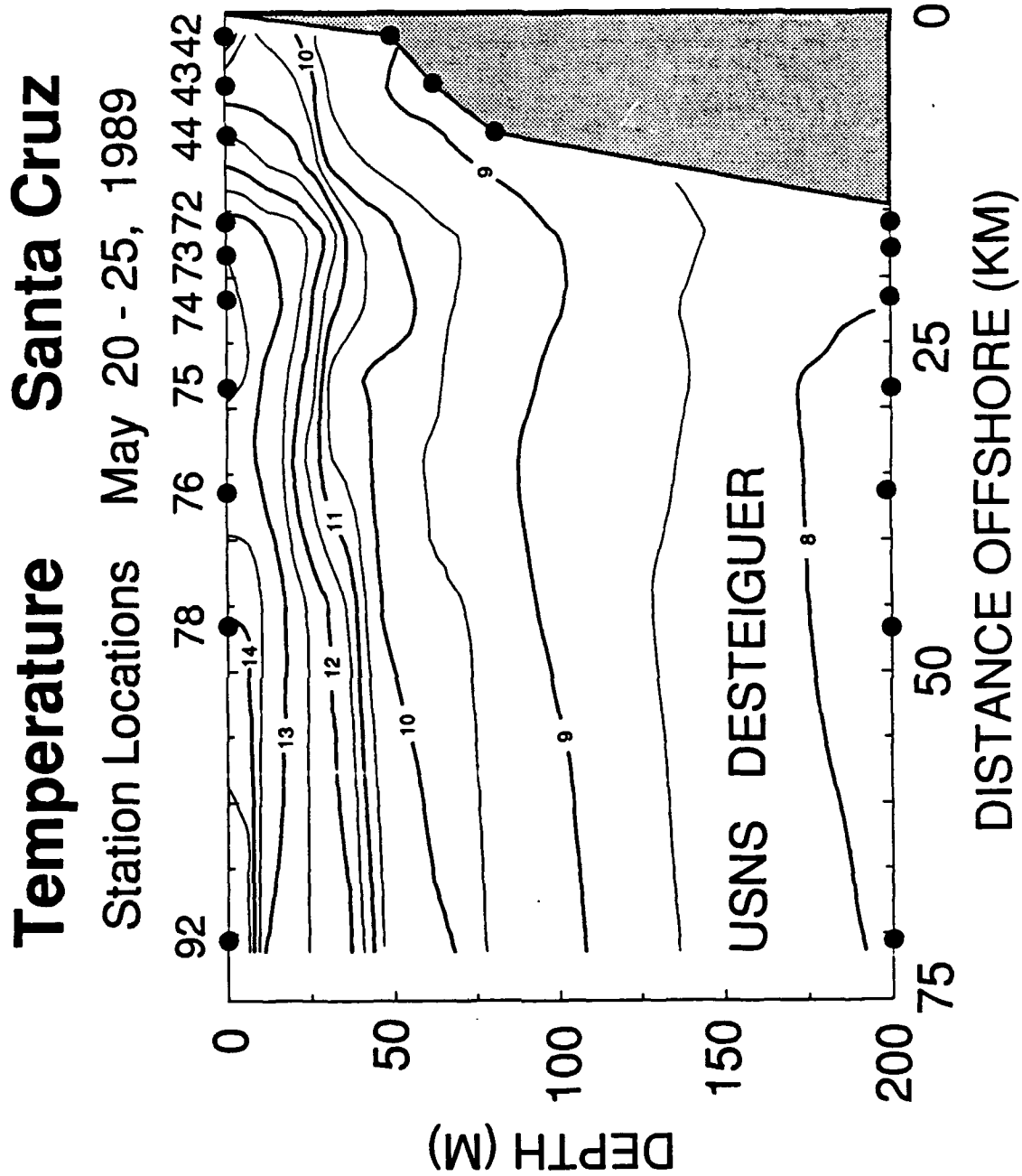
Figure 43. Santa Cruz temperature section. Water appears to upwell along shore to the right (station 42).

94
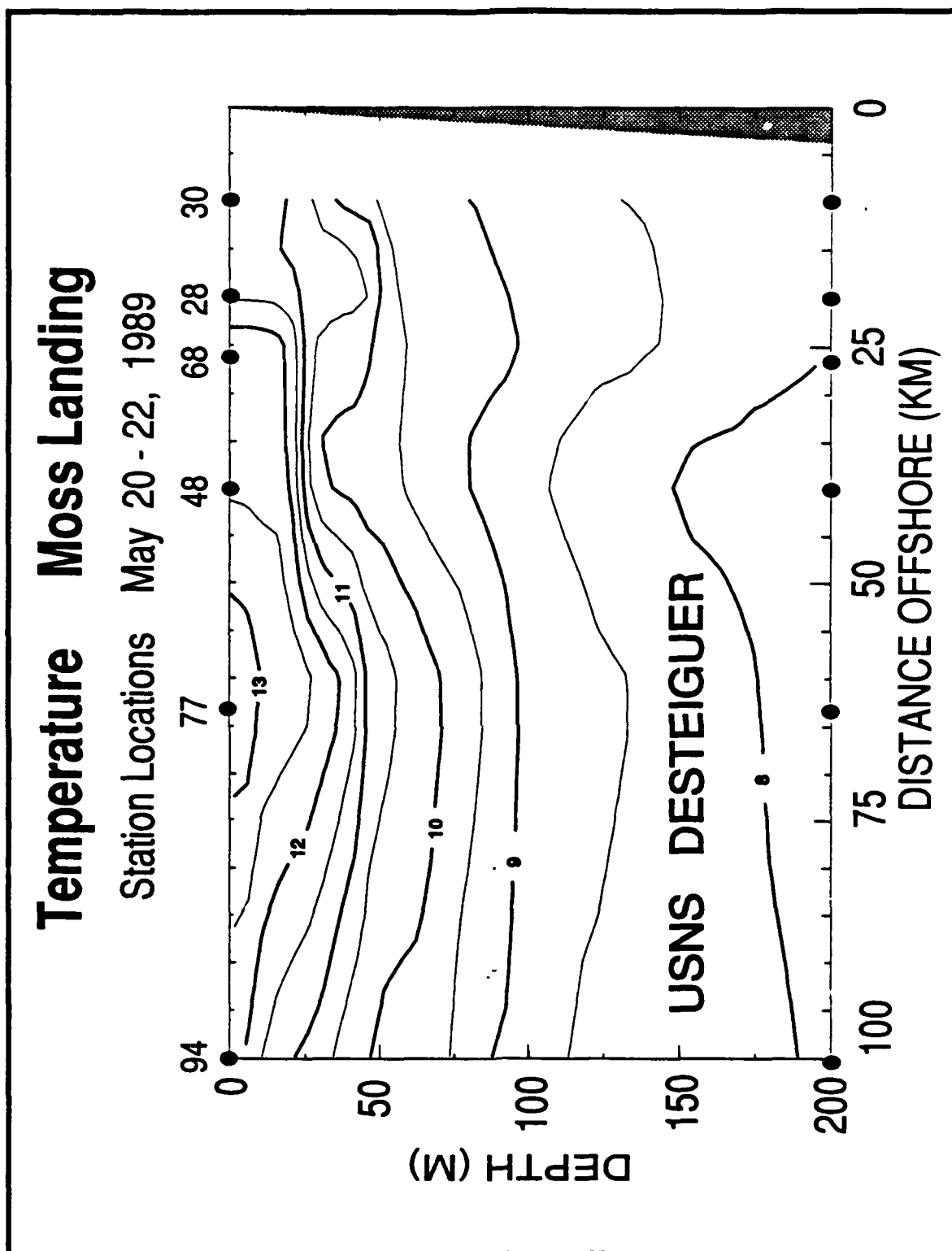
Figure 44. Moss Landing temperature section. Cold water which is found in mid-Bay between station 68 and 30 does not appear to be upwelling locally.

95

The UCSC (Figure 46) section runs from north (station S1, located just south of Terrace Point) along longitude 122° W to south (station S5 located in mid-Bay.) This transection shows warm water nearshore at the north end of the Bay and colder surface water southward toward station S5. This suggests a geostrophic flow toward the west in the north Bay. Since the isotherms above 40 m are rising toward the surface at station S5, this may be the depth of the southward advection of cold, upwelled water from Año Nuevo.
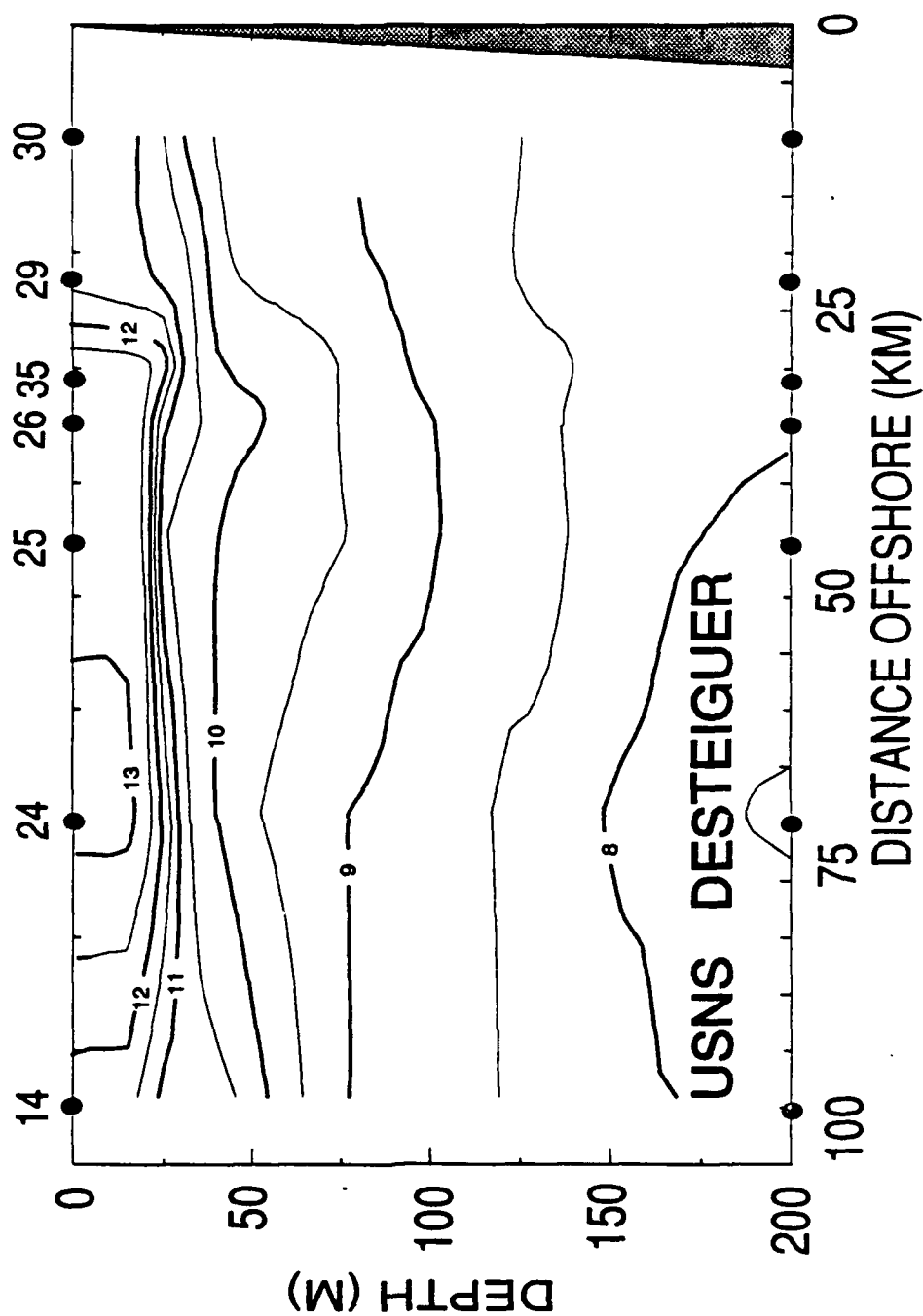
Figure 45. Canyon Axis temperature section. Cold water is found at mid-Bay, but there doesn't appear to be any local upwelling since the 11°C isotherm is almost level.
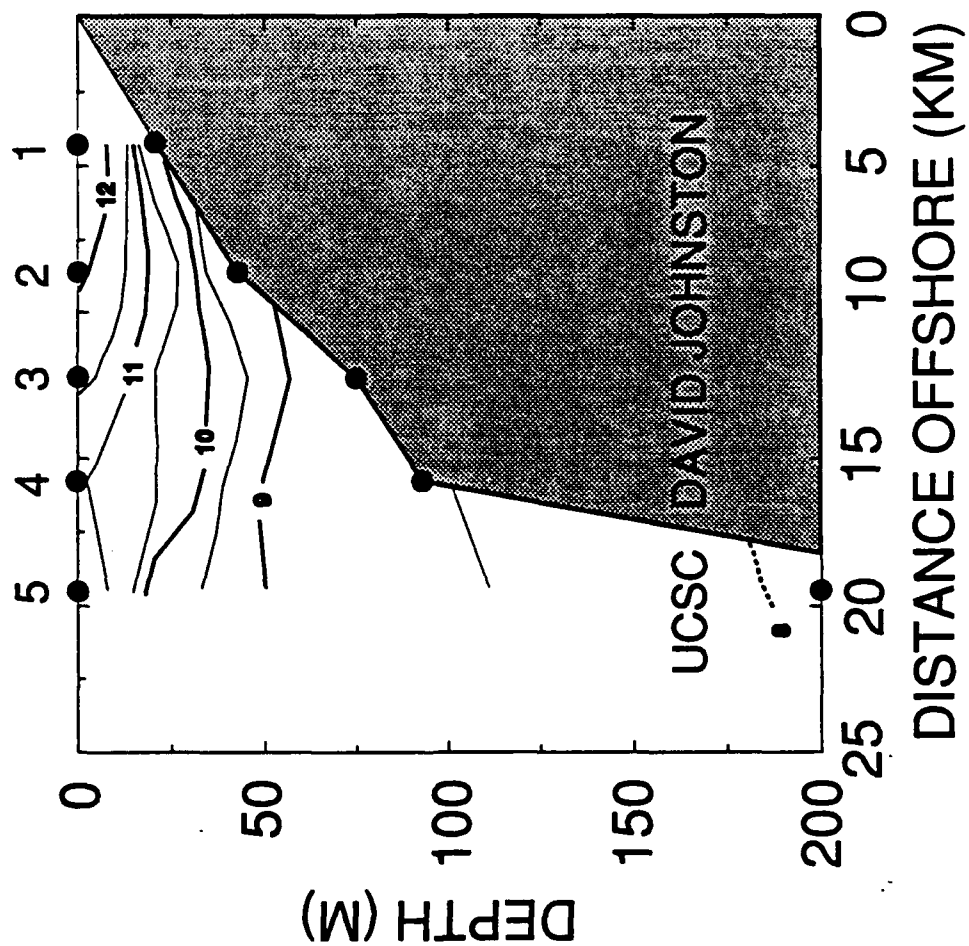
Figure 46. UCSC temperature section. There doesn't appear to be any upwelling over the Canyon, but there is some warmer water on the northern shelf.

98

VI. DISCUSSION

There never seems to be enough information to completely characterize the oceanic environment. This is especially true of a coastal environment like Monterey Bay where there is great temporal and spatial variability. The time scales of thermal variations occur in a broad spectrum from supertidal, caused by processes such as local internal waves, to multi-year changes due to distant events such as El Niño. Intermediate periods of interest are tidal, inertial, synoptic, seasonal and annual.

Frequent modifications to the thermal structure are caused by a complex set of dynamic forces which affect circulation in the Bay. These forces may act in concert or, on occasion, a single or a balanced pair of forces may dominate the circulation. According to Breaker and Broenkow (1989), many processes affect circulation of Monterey Bay, including: winds, upwelling, interaction with Monterey Submarine Canyon, bottom friction, tides, local heating, river discharge, offshore circulation, oceanic fronts, and spring transition events. The focus of this research was to investigate the source of cold water often seen in Monterey Bay using AVHRR satellite imagery.

A. HISTORICAL PERSPECTIVE

Historically, the cold water was thought to upwell over the Canyon walls (Bigelow and Leslie 1930). If this were true, satellite images should indicate an isolated cold water cell located over the mid-Bay. Another source of cold water was purported to be upwelled at Point Sur and transported northward into the Bay around Point Piños (Lasley 1977) and (Broenkow and Smethie 1987). From imagery, cold water should be seen at Point Sur with a northward plume traveling into the south Bay.

After viewing a one-year record of 112 satellite images, I did not find sufficient evidence to substantiate the above hypotheses. To be fair, during the winter, when the sea

surface was uniformly cold both inside and outside the Bay, satellite imagery was not the best tool to determine the signature of upwelling. Also, a complete set of images was not available because fog often obscured the sea surface in and near Monterey Bay. However, if one of these two hypotheses explained the dominant source of cold water observed in the Bay, then that source should have been visible frequently throughout a one-year record of MCSST. These processes may occur, but they do not appear to be primary mechanisms for providing nutrient-rich upwelled water in Monterey Bay.

My hypothesis is that circulation in Monterey Bay is closely coupled to the coastal wind. Historical drogue and current meter data were difficult to evaluate because the coastal wind data, which is critical, were never measured. Without wind measurements, it is impossible to determine whether historical observations were made during an upwelling or a relaxation event. However, northwesterly winds were dominant so it is assumed most observations were made during upwelling events. Relaxation events occur frequently so that changes in the dominant circulation regime were expected.

B. OBSERVATIONS

The winds were primarily northwesterly during the entire period of study, 10/1/88 - 9/30/89 (Figure 13), with relaxation or reversals every week or two. These appear to be normal conditions in the vicinity of Monterey Bay (Nelson 1977). During the fall and winter, northwesterly winds are less strong and reversals more are frequent than during the spring and summer. In particular, during May - June, 1989, the winds were northwesterly and strong with occasional relaxation or reversal. This was an ideal evaluation period, since several consecutive satellite cloud-free images of the Bay were available for observing the surface temperature distribution near the Bay. Also, several research ships were collecting CTD data in the vicinity of Monterey Bay, which proved essential in determining the vertical thermal structure. Since the winds were favorable to upwelling during the May

100

observation period, the CTD transections were considered synoptic. However, if a relaxation or reversal should occur, major changes in Bay circulation occur as seen during the June period.

With this comprehensive set of data, two series of satellite images were considered. The first period, 5/23 - 5/26, was primarily an upwelling period. Numerous CTD transections were completed during this period. The second series began during strong, upwelling favorable winds on 6/17 and continued until relaxation on 6/22 with full wind reversal on 6/23 and 6/24.

The close agreement between the MCSST from satellite and the SST field from the CTD observations is very reassuring. The overall agreement in SST pattern and absolute temperature lends credibility to using AVHRR satellite imagery as a tool for observing and quantifying SST. When surface temperature gradients occur, MCSST may also indicate surface currents. This must be supported by vertical temperature profiles, hydrographic transections and ultimately in situ current observations. Unfortunately, during the May - June observation period, the only current measurements made in the Bay were at a very shallow nearshore location off the Monterey Bay Aquarium.

Without actual current observations, a certain amount of intuition must be employed to develop a conceptual model of circulation in Monterey Bay. Using satellite imagery, CTD sections, and historical observations there are, in some cases, a clear indication of circulation patterns. In other cases, there are reasonable estimates of circulation that are plausible and self-consistent.

I want to reiterate that significant variability has been observed in the Bay. Occasionally, events other than wind-forced upwelling may dominate the circulation pattern in the Bay. The data examined as part of this investigation do not support the Point Sur upwelling center as a significant source of cold water for the Bay, although this does not

rule out the possibility of occasional northward advection from this area. An occasional image may contain isolated cold water in the Bay or a cold plume connected to Point Sur (Figures 28 and 29), but previous sequential images indicate this cold water to be a residual from upwelling at Año Nuevo that advected southward into the Bay.

1. Upwelling Centers

During northwesterly wind events, an upwelling center has been identified north of Monterey Bay at Año Nuevo, another south of the Bay at Point Sur. These upwelling centers are seen frequently throughout the year in satellite imagery (Breaker 1973, Breaker and Broenkow 1989). At these two locations, satellite imagery shows plumes of cold surface water extending offshore consistent with Ekman transport. Cold water is also seen extending southward at these two locations. Surface intensified southward flow is consistent with geostrophic balance for isotherms sloping upward toward the coast. The depth of the southward-flowing jet appears to be about 30 m, as seen in the Santa Cruz CTD Section (Figure 43).

2. Circulation in the Bay

This section develops a conceptual model for circulation inside the Bay, which is based on historical observations and MCSST data that has been presented in Chapter 5. Cold water is upwelled at Año Nuevo, and flows southward in geostrophic balance with isopycnals that slope upward toward the coast during upwelling. This southward flow is about 10 km wide and creates a western boundary for the Bay which effectively isolates the interior Bay from the intrusion of the oceanic water mass. Water from inside the Bay is entrained with the southward flow along its western boundary. This in turn creates a low pressure area at the northwest corner of the Bay which draws water from shallow areas along the northern boundary toward the west. Westward flow is inferred by the satellite image for 6/18 (Figure 24) when compared to 6/17 (Figure 23),

102

where the warm water of the north Bay is seen west of Terrace Point. Direct observations show predominant westward flow off Terrace Point (Brown and Caldwell 1977).

By continuity with the westward flow along the northern boundary, a northward flow must occur along the eastern boundary. Satellite observations for 6/17, 6/18, and 6/19 (Figures 23, 24, and 25) show a northward propagation of a warm water cell along the eastern boundary beginning at the south Bay. Direct current measurements from the eastern edge of the Bay show predominantly northward flow (ESI 1978; ECOMAR, Inc. 1981). Also, the water in the northern bight is considerably warmer which could be due to a longer period of solar heating as the water circulates in a cyclonic manner along the shallow portions of the Bay. However, the warming in the northeastern bight may also be the result of reduced vertical mixing due to lighter winds in the lee of Santa Cruz. This area is shallower, thus there is no cool water at depth to mix vertically with warm surface water.

To supply this northward-flowing current along the eastern boundary, some portion of the water flowing southward across the mouth of the Bay must be injected onshore near the middle of the Bay and the south end near Pacific Grove. Recall that one historical justification for northward flow from Point Sur around Point Piños into the southern bight of the Bay came from the observation of cold surface water at Pacific Grove five days after the appearance of cold water at Granite Canyon (Breaker and Broenkow 1989). Upwelling occurs simultaneously at Año Nuevo and Point Sur with the onset of northwesterly winds. Rudimentary feature tracking of a cold cell from Año Nuevo along the southward jet shows the feature traveled at 33 cm/sec and arrived off Pacific Grove about five days after the commencement of upwelling. Thus the five-day time lag is consistent with southward flow of cold upwelled water into the Bay from Año Nuevo.

103

Other evidence for northward flow along the eastern boundary comes from the distribution of barnacle larvae, which have a source in the Elkhorn Slough. Large populations were observed along the eastern shore from Moss Landing northward to Santa Cruz. No larvae were found to the south of Moss Landing, although a separate population does exist near Pacific Grove. (Miller, Ph.D. Dissertation 1990).

Surface circulation in the southern bight is difficult to interpret and satellite imagery doesn't provide much information. Drogue measurements indicate generally a large cyclonic gyre in the Bay (Moomy 1973). Current observations from Monterey Bay Aquarium indicate a westward flow alongshore in the south Bay. However, this measurement is within 300 m of shore and may be a lee eddy that does not indicate the larger scale circulation in the southern Bay.

Modeling efforts by Garcia (1971) indicate cyclonic flow occurs in the Bay when water flows south across the mouth of the Bay. This single-layer, cavity model indicates cyclonic circulation in Monterey Bay. However, the Bay is not homogeneous, as assumed by Garcia, and the results should be evaluated further. Using a three layer model, Klinck (1989) found that a 10 cm/sec cross-canyon current flow could cause vortex stretching and cyclonic flow. However, Klinck remarked that, if a canyon was narrower then one-half the first internal Rossby radius there would be reduced perturbation effects on shelf flow. Koehler (1990) calculated the Rossby radii at different locations around Monterey Bay and found that the Monterey Canyon could be defined as "narrow" in both the barotropic and the baroclinic sense. Both modeling efforts suggest that a basis for cyclonic flow may exist.

Satellite images do not demonstrate evidence of bathymetric effects from the Submarine Canyon. Neither cold nor warm water appear to be isolated over the Canyon.

104

However, nearshore flow inside the Bay apparently is preferential along bathymetry. The satellite image for 6/19 (Figure 25) indicates warm water inshore of the 50 m isobath.

3. Offshore Circulation

Directly offshore of Monterey Bay, a warm core anticyclonic eddy is quite persistent. This feature is bounded on the north and south by the offshore plumes from Año Nuevo and Point Sur. The eastern boundary of this eddy is the southward jet from Año Nuevo across the mouth of the Bay. This feature is seen often in satellite images during this research period and has been described in the literature by Broenkow and Smethie (1973), Pirie and Stellar (1977), Breaker (1983), and Breaker and Broenkow (1989). The eddy radius is about 25 km, which is nearly the first internal Rossby radius at this location. This size is a natural scale of the system and perhaps a reason for the eddy's persistence. The depth of this warm core feature is observed to be about 800 m (Tisch 1990).

The mechanisms for production and maintenance of this eddy are not clear. The open eddy may be a meander from the California Current System which may enhance the southward-flowing jet from Año Nuevo and the westward-flowing jet from Point Sur. The eddy could be the result of current shear instabilities in lower layers of the ocean due to the California Undercurrent. Another strong possibility is that the eddy's negative vorticity may be initiated and maintained by the current shear from the southward flowing jet to the east and the westward flowing plume to the south.

4. Wind Reversal Events

An intriguing ocean response occurred during relaxation and reversal of the upwelling favorable winds on 6/22/89. The rapid warming of 2 °C of the surface water observed from satellite imagery was consistent with solar heating during light winds which provide little mixing (Appendix B). Upwelling ceases at Año Nuevo during southerly

winds. The southward jet ceased resulting in an unbalanced pressure gradient force that allowed the eddy/meander to rapidly move shoreward. An example of this shoreward movement is seen by comparing the position of the retroflection just offshore of Point Sur on the 6/21 satellite image (Figure 27) to the same feature on 6/22 (Figure 28). It moved northeastward implying an average velocity of 19 cm/s.

The offshore feature appears to move toward the northeast and impact the northern boundary of the Bay. It is hard to determine from the satellite image on 6/22 if the clockwise rotation of the eddy forces warm water into the Bay immediately. However, on the following days, 6/23-6/24, a clockwise flow pattern of warm water inside the Bay can be inferred from the satellite images. Southward episodes of nearshore flow have been observed in Monterey Bay (ESI 1978 and ECOMAR 1981). It is conceivable these historical current reversals may have been associated with relaxation or reversal of upwelling favorable winds. At any rate, the character of the Bay has been completely altered in one day. Temperatures have warmed throughout the water column as observed by vertical temperature profiles (See Figures 31 and 32).

VII. CONCLUSIONS AND RECOMMENDATIONS

A. CONCLUSIONS

AVHRR satellite imagery has proven to be an excellent tool for observation of surface thermal gradients. Satellite imagery provides synoptic observations of sea surface temperature with high spatial resolution. In the case of Monterey Bay, large thermal gradients were used to infer surface circulation. The addition of vertical temperature profiles provided greater confidence for the inferred circulation scheme. However, in situ current measurements are needed to validate the circulation model developed from satellite imagery.

The historical perspective of circulation in Monterey Bay has been the result of numerous surveys which have focussed on one aspect or another. These surveys have not had the luxury of high density spatial or temporal resolution. Current meter stations have measured circulation continuously in time, but only at a few locations; hydrographic surveys have been broader in spatial coverage, but at intermittent intervals in time.

This research combines, for the first time, nearshore wind data with high spatial and temporal density satellite imagery and large-scale hydrographic surveys to infer wind-driven circulation. There is sufficient evidence to conclude that during a northwesterly wind regime, upwelling occurs at Año Nuevo as a result of Ekman transport. The cold nutrient-rich upwelled water is then advected southward across the mouth of Monterey Bay with a portion entering the middle and south Bay. It is suspected that northward currents along the eastern boundary and westward flow along the northern boundary are produced in response to the southward jet across the mouth of the Bay (Figure 47).

When upwelling favorable winds relax and/or reverse, extremely rapid changes can occur inside the Bay. With light winds and low mixing, the surface temperature can
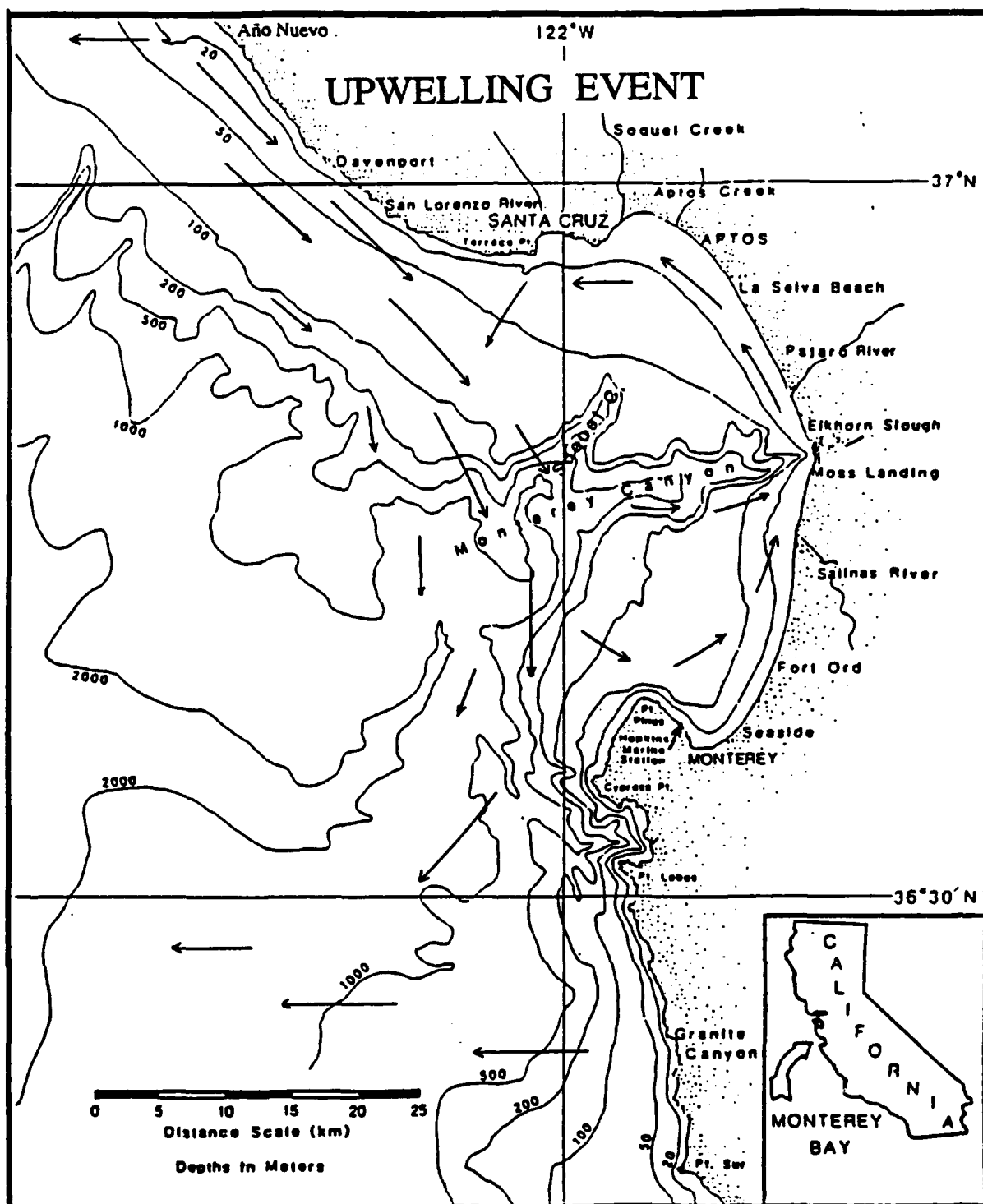
107

Figure 47. Sketch of Monterey Bay circulation scheme during spring upwelling favorable winds. Current directions are estimates inferred from satellite images obtained during upwelling events.

108

increase dramatically; a 2°C rise was observed in one day (6/21-6/22). The warm core, anticyclonic eddy usually located just offshore of the Bay can move rapidly shoreward during wind relaxations. During these events, "oceanic" water enters Monterey Bay and a complete exchange of the upper waters can occur inside the Bay. The clockwise rotation of the eddy may influence nearshore circulation which appears to become southward along the eastern boundary (Figure 48). Unfortunately, the June sequence was terminated due to cloud cover and the subsequent establishment of upwelling was not observed.

During the one-year period covered by this research, there were no satellite images which indicate spontaneous or isolated upwelling over the Monterey Submarine Canyon. If upcanyon flow or internal tides produce upwelling in the Canyon, it is a minor effect compared to advection into the Bay of upwelled water from Año Nuevo.

During upwelling favorable winds, there appears to be southward transport of cold upwelled water from Point Sur. During relaxation or reversal events, the water at Point Sur may have a northward component of flow. This northward current quickly loses its upwelled character and is not a major source of upwelled water for the Bay.

B. RECOMMENDATIONS

Historical drogue, current meter, and hydrographic observations in Monterey Bay have indicated considerable variability in circulation, but for the most part, the forcing mechanisms were not identified. Future research in the Bay must consider wind events and place their measurements in the context of coastal upwelling forcing the circulation in the Bay.

Historical surveys near Monterey Bay have mainly been conducted completely inside the Bay. The few, such as CALCOFI, conducted outside the Bay with some ancillary measurements inside the Bay have been generally coarse in horizontal resolution and confined well off the shelf. Future surveys must consider the offshore circulation as
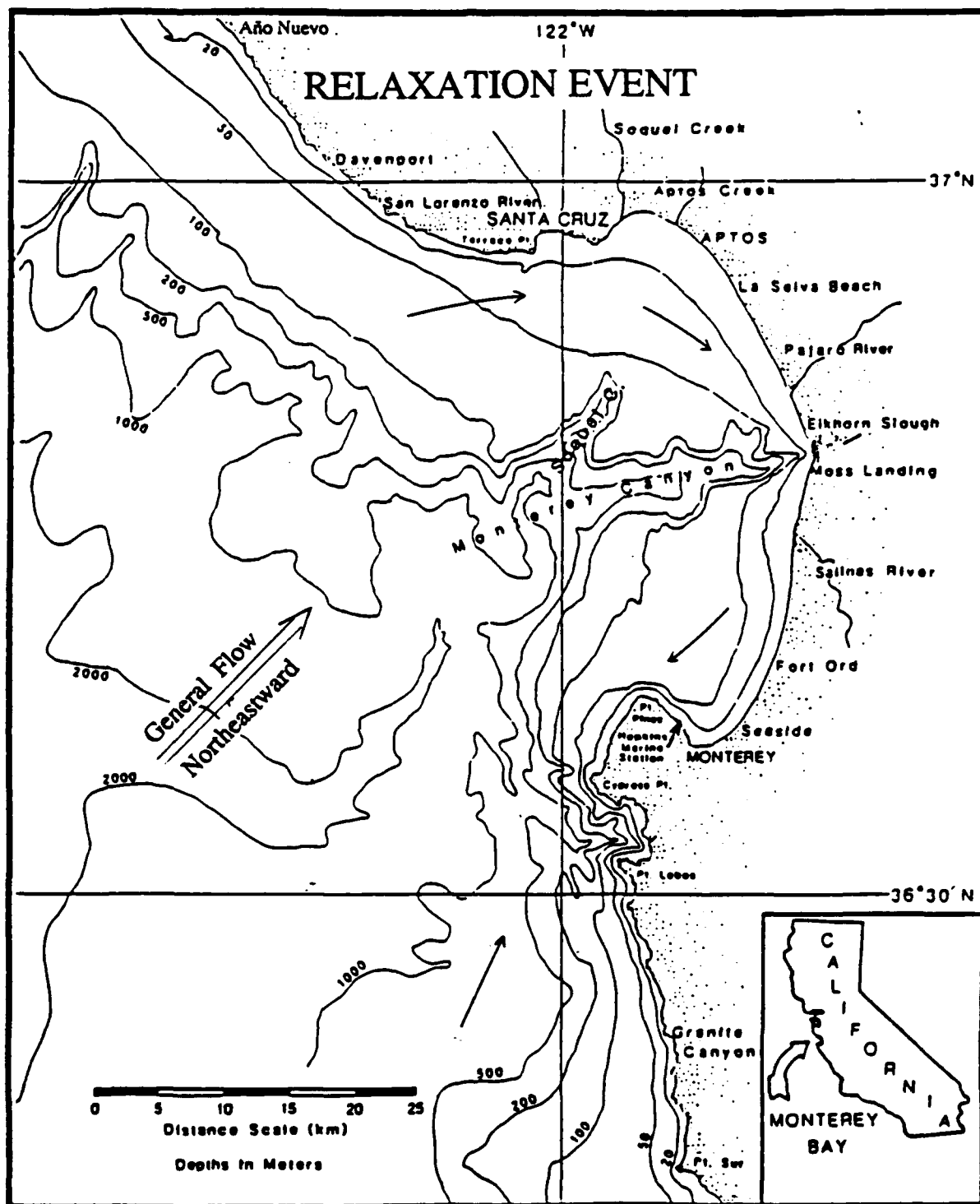
Figure 48. Sketch of Monterey Bay circulation scheme during spring relaxation or reversal of upwelling favorable winds. Currents directions are estimated from a short series of satellite images during a wind reversal event. The general flow is toward the northeast.

well as the circulation inside the Bay. The primary consideration is the linkage between circulation outside the Bay and the circulation inside.

A field experiment should be conducted to validate the proposed surface circulation model of Monterey Bay. A number of current meter moorings with thermistor chains should be installed to observe the major features of the circulation model including: the upwelling jet across the mouth of the Bay; the current flow inside the north, south, and middle Bay; the offshore eddy; and the possibility of northward flow of upwelled water from Point Sur.

Long-term, high spatial density current measurements should be the highest priority. Circulation in the Bay must be understood in order to protect the environment from thermal and chemical waste; respond to an oil spill; manage the fisheries; anticipate sediment erosion; plan for coastal development; and further understand the coastal impact on Monterey Bay.

There are five major oceanographic institutions located near the Bay. Resources for in situ current measurement must be identified and institutions must coordinate their efforts to validate a comprehensive model for circulation in Monterey Bay.

LIST OF REFERENCES

Anderson, R.C., 1971: Thermal conditions in Monterey Bay during 9/1966-9/1967 and 1/1970-6/1971. M.S. Thesis, Naval Postgraduate School, Monterey, CA. 77 pp.

Arthur, R.S., 1965: On the calculation of vertical motion in eastern boundary currents from determinations of horizontal motion. J. Geophys. Res., 70, 2799-2803.

Bernstein, R.L., 1982: Sea surface temperature estimation using the NOAA 6 satellite advanced very high resolution radiometer. J. Geophys. Res., 87, 9455-9465.

Bigelow, H.B. and M. Leslie, 1930: Reconnaissance of the waters and plankton of Monterey Bay, July, 1928. Bulletin of the Museum of Comparative Zoology, Harvard College, 70, 427-581.

Bolin, R.L. and D.P. Abbott, 1963: Studies on the marine climate and phytoplankton of the central coastal area of California, 1954-1960. California Cooperative Oceanic Fisheries Investigations Progress Report, IX, 1 July 1960 to 30 June 1962, Marine Research Committee, California Department of Fish and Game, Sacramento, CA, pp. 23-45.

Breaker, L.C., 1983: The space-time scales of variability in oceanic thermal structure off the Central California coast. Ph.D. Dissertation, Naval Postgraduate School, Monterey, CA. 483 pp.

Breaker, L.C. and W.W. Broenkow, 1989: The circulation of Monterey Bay and related processes. Moss Landing Marine Laboratory Technical Publication 89-1.

Brink, K.H., 1983: The near surface dynamics of coastal upwelling. Prog. Oceanogr., 12, 223-257.

Broenkow W.W. and W.M. Smethie, Jr., 1978: Surface circulation and replacement of water in Monterey Bay. Estuarine and Coastal Marine Science, 6, 583-603.

Brown and Caldwell, 1977: Wind and current data, June 1976 - January 1977, Santa Cruz wastewater facility planning study, Brown and Caldwell, Walnut Creek, CA

CALCOFI, 1956: State of California Marine Research Committee, CALCOFI Progress Report. 1 April 1955 - 30 June 1956., pp. 15-18.

Chelton, D.B., A.W. Bratkovich, R.L. Bernstein, and P.M. Kosro, 1988: Poleward flow off central California during the spring and summer of 1981 and 1984. J. Geophys. Res., 93, 10604-10620.

Crowe, F.J. and R.A. Schwartzlose, 1972: Release and recovery of drift bottles in the California region, 1955 through 1971. California Cooperative Oceanic Fisheries Atlas #16, Marine Research Committee, State of California.

Deschamps, P.Y., and T. Phulpin, 1980: Atmospheric correction of infrared measurements of sea surface temperature using channels at 3.7, 11, and 12 μm. Boundary-Layer Meteorology, 18, 131-143.

Ecomar, Inc., 1981: Final oceanographic studies report (November, 1979 to December 1980), Volume 1. For J.M. Montgomery Consulting Engineers, Inc. 273 pp.

Ekman, V.W., 1905: On the influence of the earth's rotation on ocean currents. Ark. F. Mat., Astron. och Fysik, Vol. 2, No. 11, pp. 1-53.

Engineering Science, Inc., 1978: Facilities plan for north Monterey County, draft oceanographic pre-design report. 1, Engineering Science, Inc., Berkeley, California.

Farrell, T.M., D. Bracher, and J. Roughgarden, 1990: Cross-shelf transport causes recruitment to intertidal populations in central California, (Limnol. Oceanogr., in press.)

Garcia, R.A., 1971: Numerical simulation of currents in Monterey Bay. M.S. Thesis, Naval Postgraduate School, Monterey Bay, CA. 154 pp.

Garwood, R.W., 1977: An oceanic mixed layer model capable of simulating cyclic states., J. Phys. Oceanogr., 7, 455-468

Hickey, B.M., 1979: The California Current System - hypotheses and facts. Prog. in Oceanogr., 8, 191-279.

Hunthnance, J.M., 1981: Waves and currents near the continental shelf edge. Prog. Oceanogr., 10, 193-226.

Klinck, J.M., 1989: Geostrophic adjustment over submarine canyons., J. Geophys. Res., 94, 6133-6144.

Koehler, K.A., 1990: Observations and modeling of currents within the Monterey Bay during May, 1988. M.S. Thesis, Monterey, CA. 110 pp.

Lammers, L.L., 1971: A study of mean monthly thermal conditions and inferred currents in Monterey Bay. M.S. Thesis, Naval Postgraduate School, Monterey, CA. 160 pp.

Lasley, S.R., 1977: Hydrographic changes in Monterey Bay surface waters in relation to nearshore circulation. M.A. Thesis, San Jose State University, San Jose, CA. 75 pp.

McClain, 1985: Comparative performance of AVHRR-based multichannel sea surface temperatures. J. Geophys. Res., 90, 11,587-11,601.

Miller, K., 1990: Ph.D. Dissertation, Stanford University, John Hopkins Marine Station, Monterey, CA.

Moomy, D. H., 1973: Temperature variations throughout Monterey Bay, September 1971 - October 1972. Master of Science Thesis, Naval Postgraduate School, Monterey, CA. 166 pp.

Nelson, C.S., 1977: Wind stress and wind stress curl over the California Current. NOAA Technical Report NMFS SSRF-714, U.S. Department of Commerce, 89 pp.

Peffley, M.B. and J.J. O'Brien, 1976: A three-dimensional simulation of coastal upwelling off Oregon. J. Phys. Oceanogr., 6, 164-180.

Pickard, G.L., and W.J. Emery, 1982: *Descriptive Physical Oceanography, an Introduction*, Pergamon Press, NY, 249 pp.

Pirie, D.M. and D.D. Steller, 1974: California Coast Nearshore Processes Study Final Report - ERTS-A. Goddard Space Flight Center, Greenbelt, Maryland, 164 pp.

Pirie, D.M. and D.D. Steller, 1977: California Coastal Processes Study - Landsat II Final Report, LANDSAT investigation #22200. Goddard Space Flight Center, Greenbelt, Maryland.

Preller, R. and J.J. O'Brien, 1980: The influence of bottom topography on upwelling off Peru. J. Phys. Oceanogr., 10, 1377-1398.

Reid, J.L., Jr., G.I. Roden and J.G. Wyllie, 1958: Studies of the California Current System. CALCOFI Progress Report, 7.1.56 to 1/1/58, Marine Resources Committee, California Department of Fish and Game, Sacramento, CA, pp. 27-56.

Reise, J.A., 1973: A drift bottle study of the southern Monterey Bay. M.S. Thesis, Naval Postgraduate School, Monterey, CA. 113 pp.

Schwartzlose, R.A., 1963: Nearshore currents of the western United States and Baja California as measured by drift bottles. California Cooperative Oceanic Fisheries Investigations Progress Report, 7-1-60 to 6-3-62, Marine Research Committee, California Department of Fish and Game, Sacramento, CA. pp. 15-22.

SeaSpace, 1989: TerraScan user documentation, San Diego, CA 135 pp.

Shea, R.E., and W.W. Broenkow, 1982: The role of internal tides in the nutrient enrichment of Monterey Bay, California. Estuarine, Coastal and Shelf Science, 15, 57-66.

Shepard, F.P. and R.F. Dill, 1966: Submarine Canyons and other Sea Floor Valleys. Rand McNally & Co. Chicago IL. 381 pp.

Shomaker, C.W., 1983: A model for tidal circulation adapted to Monterey Bay, M.S. Thesis, Naval Postgraduate School, Monterey, CA. 99 pp.

Skogsberg, T. and A. Phelps, 1946: Hydrography of Monterey Bay, California. Thermal Conditions, part II (1934-1937). Proceedings of the American Philosophical Society, 90, 350-386.

Skogsberg, T., 1936: Hydrography of Monterey Bay, California. Thermal conditions, 1929-1933. Transactions of the American Philosophical Society, 29, 152 pp.

Stoddard, H.S., 1971: Feasibility study on the utilization of parachute drogues and shore-based radar to investigate surface circulation in Monterey Bay. Master of Science Thesis, Naval Postgraduate School, Monterey, CA.

Stull, R.B.1988: *Boundary Layer Meteorology*. Kluwer Academic Publishers, Boston, MA. 666 pp.

Tisch, T.D., 1990: Seasonal variability of the geostrophic velocity and water mass structure off Point Sur, California. Master of Science Thesis, Naval Postgraduate School, Monterey CA. 163 pp.

Wickham, J.B., A.A. Bird, and C.N.K. Mooers, 1987: Mean and variable flow over the central California continental margin, 1978-1980. Continental Shelf Research, 7, 827-849.

Wyllie, J.G., 1966: Geostrophic flow of the California Current at the surface and at 200 m. California Cooperative Oceanic Fisheries Investigations Atlas #4, xiii pp. and 288 charts.

APPENDIX A: SATELLITE IMAGE PROCESSING

The TeraScan image processing system was developed by Sea Space and is installed at the Naval Oceanographic and Atmospheric Research Laboratory (NOARL) - West in Monterey, CA. The TeraScan system runs on a Hewlett-Packard minicomputer using the UNIX operating system allowing the user to manipulate files with UNIX commands.

A. PROCESSING HARDWARE

The Hewlett-Packard HP(000/835 Turbo SRX Graphics Computer is a 32-bit machine with 80 Mbytes of memory running at 14 MIPS. The graphics library and hardware microcode support powerful primitive commands to accelerate an image through the four-stage graphics pipeline. Quick access data is stored on four 571 Mbyte hard disks with 20 msec cycle time. Data archival is on an HP-7978 9-track, 6250 BPI, digital tape drive.

Images are displayed on HP-9735 Color Graphics Display Systems which are directly interfaced to a Mitsubishi 8650-10 Color Line Printer using the Gammacolor 100 Video-Interface. Photographic images can be made in 35 mm slides, prints or 8x10 in positive, negative or print format.

B. PROCESSING SOFTWARE

TeraScan processing accepts the most common HRPT data formats. The level 1b data is first calibrated and navigated to Earth coordinates. Then, multi-channel sea surface temperatures are computed pixel by pixel with any detected clouds or land removed. Finally, each image is co-registered to an identical coordinate map and recorded digitally on magnetic tape and as a hardcopy color image. The following information was abstracted from the *TerraScan User Documentation*.

1. AVIN - Data Ingest

Raw data (10 bits) are extracted from magnetic tape along with the header necessary to convert the data to radiometric temperatures. A master file is used to identify the specific area of interest so the subsampled image reduces the file storage requirement to one tenth of the full pass. AVIN can ingest multiple images from one tape or disk. Since the header information does not include the year, it must be added so the satellite position can be calculated from the ephemeris during processing.

2. AVCAL - Calibration

Calibration information is extracted from HRPT header records which are stored along with the raw AVHRR counts. The engineering units of percent albedo (channels 1 and 2) and brightness temperatures (channels 3, 4, and 5) are computed and stored on disk.

3. NAV - Earth Location

The Earth reference data is computed from the Department of Defense orbital elements, spacecraft clock time, and the pointing angle of the AVHRR scanner. The image is generally navigated within several kilometers of the actual location. The spacecraft clock time can be in error by 1 second or the equivalent of 6.6 km location error along the satellite track. The attitude (pitch, roll, and yaw) are maintained within 0.2 degrees, which translates to 2 pixels in the AVHRR image.

The known coastline from the 1975 CIA database is aligned with the image coastline using interactive commands to adjust the satellite attitude, clock time, and sensor tilt. By adjusting the coastline overlay to match the image coastline using either channel 2 or 4, the image agreement with the coastline lies within half of the pixel width or within 0.6 km directly under the satellite.

4. NITPIX - MCSST Computation and Cloud Mask

A number of sequential tests are performed to eliminate unacceptable data. Only those pixels that pass all tests are judged to be cloud-free and converted to MCSST. The AVHRR scanner sweeps the Earth from -72° to 72°; only data with zenith angles less than 60° are retained.

The "art" of image processing is determining the appropriate limits of sun glint (albedo), ocean front gradients (temperature), shoreline, and clouds. On one hand, all clouds can be eliminated, but actual thermal gradients may be removed as well. On the other hand, if all real thermal gradients are allowed, some clouds may also be admitted. So the channel 2 and 4 maximum and differential limits affect the MCSST calculation. Since the images were initially chosen to be mostly cloud-free, loose limits were chosen which allowed actual thermal gradients to be observed.

In general, the ocean albedo is less than the threshold value of 3.0%. Higher values are usually land or clouds and are given pixel values of zero. Sun glint may raise the ocean albedo and require a change of threshold. If a 3x3 pixel array has an average albedo (channel 2) that is 0.25% lower than the central pixel, the central pixel is contaminated and given the value zero.

Since cloud temperatures are colder than the sea surface, sub-resolution clouds cause a pixel to be colder than the surrounding pixels. If a 3x3 pixel array has an average pixel brightness temperature (channel 4) 0.5 degrees warmer than the central pixel, the central pixel is considered contaminated and given the value zero. However, a thermal front may have similar characteristics, so a trade-off exists between cloud removal and observation of thermal fronts.

For those remaining pixels, SST may be calculated using the correct algorithm for the satellite sensor which collected the data. Observations from NOAA 10 do not include

118

channel 5 and are not as accurate as those from NOAA 9 and NOAA 11 which do have five channels of HRPT. The National Environmental Satellite and Data Information Service (NESDIS) provided the following bulk temperature algorithms for daytime MCSST:

NOAA 9: $T(4/5) = 3.4317 * T(4) - 2.5062 \ T(5) - 251.24$ (A.1)

NOAA 11: $T(4/5) = 1.01345 * T(4) + 2.659762 * (T(4) - T(5))$

$$+ 0.526548 * (T(4) - T(5)) * (SEC(sza) - 1) - 277.742 \qquad (A.2)$$

5.   FASTREG - Image co-registration

To intercompare sequential images, both scenes must identically contain the same spatial information. FASTREG allows the user to create a master file which again identifies the center latitude and longitude along with the range of pixel lines and samples. All Monterey Bay hardcopy images are registered to 130 lines by 130 samples centered at 36.7°N and 122°W.

6.   Image Enhancement

The temperature range of the images was fixed between 9°C and 16°C. This temperature range appeared to be the annual minimum and maximum values for Monterey Bay (Breaker and Broenkow 1989). The color scale was divided into 64 values and distributed in a linear stretch from violet to red. A color bar was added to the hardcopy image for reference from color to the temperature scale.

The coastline was identified on the graphics overlay of the image along with the latitude and longitude grid at a 30' increment. The final touch to the hardcopy image was text to identify the date and time of the satellite pass. Several other techniques are available to operate on individual pixels. Two or more images can be composited by averaging each pixel value on a set if co-registered images. A rudimentary feature tracking can be performed by looking at the pixel by pixel difference between two coregistered image... On occasion, noise can be eliminated from an image by SMEARING (TeraScan

119

command) or using the median value at the center of a 3 x 3 array. Care is necessary because information is lost when smearing an image. Smearing should only be used on bad data points and not throughout the image.

APPENDIX B. CALCULATION FOR SURFACE WARMING

As mentioned in Chapter III.D, when the surface wind is light and solar heating is high, the mixed layer depth can be shallow. In fact the mixed layer turbulent kinetic energy (TKE) budget can approach equilibrium when wind induced shear production of TKE balances the buoyant damping due to thermal heating. The depth scale at which this balance occurs is known as the Monin-Obukhov length (L). This similarity theory has been presented from the atmospheric perspective by Stull (1988) and from the ocean mixed layer perspective by Garwood (1977).

By assuming no entrainment at the bottom of the mixed layer, a constant mixed layer depth, horizontally uniform surface heat flux and wind stress, no advection, and negligible salinity effects, the prognostic heat equation can be solved for a daily temperature change when wind speed and solar heat flux are known. By measuring the wind at the NDBC Buoy 46042 and using a climatological heat flux, it is possible to estimate the temperature increase that is observed under the light wind conditions.

The NDBC Buoy 46042 measures wind (U_5) at five meters above the ocean surface. An iterative scheme was used to find the atmospheric friction velocity U_* for U_5 = 2 and 4 m/s. The smooth form of neutral drag was used for light winds. For example the computation for 2 m/s yields:

$$U_* = C_{Dn_5}^{1/2} U_5 = (.00142)^{1/2} (2 \text{ m/s}) = .075 \text{ m/s} \tag{B1}$$

where C_{DN_5} is the drag coefficient for neutral conditions,

$$C_{DN_5} = \left[\frac{k}{1 + \ln\left(\frac{k \, z \, U_*}{v}\right)} \right]^2 \tag{B2}$$

121

$$C_{DN_5} = \left[\frac{0.4}{1+\ln\left(\frac{(0.4)\ (5\,m)\ (.075\,m/s)}{(10^{-5}\ m^2/s)}\right)} \right]^2 = 0.00142 \qquad (B3)$$

and ($k = 0.4$) is the von Karman constant, z is the height of wind measurement above the sea surface, and v is the molecular viscosity. Now converting the atmospheric friction velocity U_* to that for water w_*:

$$w_* = U_* \left[\frac{\rho_a}{\rho_o} \right]^{1/2} \qquad (B4)$$

$$w_* = (7.5\ \frac{cm}{s}) \left[\frac{.00125\frac{g}{cm^3}}{1.0\ \frac{g}{cm^3}} \right]^{1/2} \approx 0.27\ \frac{cm}{s} \qquad (B5)$$

where ρ_a is the density of air and ρ_o is the density of water. From the turbulent kinetic energy equations, the rate of entrainment by the mixed layer $\partial h/\partial t$ is zero when there is no entrainment.

$$\frac{\partial h}{\partial t} \Lambda = \frac{C_1\ w_*^3}{\alpha\ g\ h\ \Delta T} - \frac{C_2 \frac{Q_0}{\rho_o C_p}}{\Delta T} = 0 \qquad (B6)$$

where Q_0 is the heat flux; Λ is the Heavyside step function, which equals 1 when $\frac{\partial h}{\partial t}$ is increasing and 0 otherwise; C_p is the heat capacity of sea water; α is the thermal expansion coefficient; and g is the acceleration of gravity.

122

Now a solution can be found for the mixed layer depth (h) in terms of heat flux and wind stress. Physically, when there is no entrainment, the shear production term exactly balances the buoyancy flux term. With this balance, the mixed layer depth (h) is equal to the Obukov length scale (L). In this case the heat flux is negative (downward). Solving for the depth when the tuning constants are C1/C2 = 2 (Garwood, personal communication).

$$h = \frac{C_1 \, \rho_0 \, C_p \, w_*^3}{C_2 \, \alpha \, g \, Q_0} = L \qquad (B7)$$

$$L = \frac{2 \, (1\frac{g}{cm^3}) \, (1\frac{cal}{g \cdot {}^\circ C}) \, (.27\frac{cm}{s})^3}{(2.5 \times 10^{-4} {}^\circ C^{-1})(10^3 \frac{cm}{s^2})(100 \frac{W}{m^2}) \, (2.39 \times 10^{-5} \frac{cal \quad m^2}{s \cdot cm^2 \, W})} \qquad (B8)$$

$$L = 66 \text{ cm.}$$

A climatological value for heat flux is 100 - 150 W/m^2 (Pickard and Emery 1982), even a value of 200 W/m^2 is reasonable for a clear summer day. The prognostic equation for temperature ($\frac{\partial T}{\partial t}$) can now be solved.

$$\frac{\partial T}{\partial t} = \frac{Q_0}{\rho_0 \, c_p \, L} \qquad (B9)$$

Substituting B7 into B9, we can estimate for ΔT per day:

$$\Delta T = \frac{\alpha \, g \, Q_0^2}{2(\rho_0 c_p)^2 w_*^3} \, \Delta t \qquad \qquad \text{(B10)}$$

$$\frac{\Delta T}{\Delta t} = \frac{(2.5 \times 10^{-4} \, ^\circ C^{-1}) \, (10^3 \frac{cm}{s^2}) \, (100 \frac{W}{m^2})^2 \, (2.39 \times 10^{-5} \frac{cal \; m^2}{s\text{-}cm^2 W})^2}{2 \, (1 \frac{g}{cm^3})^2 \, (1 \frac{cal}{g\text{-}^\circ C})^2 \, (0.27 \frac{cm}{s})^3} \qquad \text{(B11)}$$

$$\frac{\Delta T}{\Delta t} = 3.627 \times 10^{-5} \, ^\circ C/s = 3.1 \, ^\circ C/day$$

In summary, for a measurement height of 5 meters, wind velocities of 2 and 4 m/s; and heat flux of 100 and 200 W/m^2 the values were calculated for U_*, w_*, L, and $\Delta T/\Delta t$. For light winds, it is not unreasonable to expect the sea surface temperature to increase by 2°C in one day as was seen from 6/21 to 6/22 (Figures 27 and 28).

Summary of Calculation (Smooth Sea)

Q_0 W/m^2	U_5 m/s	U_* cm/s	w_* cm/s	L cm	$\Delta T/\Delta t$ °C/day
100	2	7.5	0.27	66	3.10
200	2	7.5	0.27	33	12.50

INITIAL DISTRIBUTION LIST

No. Copies

1. Defense Technical Information Center   2
   Cameron Station
   Alexandria, Virginia 22314

2. Library, Code 52   2
   Naval Postgraduate School
   Monterey, CA 93943-5000

3. Chairman (CodeOC/Co)   1
   Department of Oceanography
   Naval Postgraduate School
   Monterey, CA 93943-5000

4. Professor Leslie K. Rosenfeld (OC/Ro)   1
   Department of Oceanography
   Naval Postgraduate School
   Monterey, CA 93943-5000

5. Professor Newell Garfield (OC/Ga)   1
   Department of Oceanography
   Naval Postgraduate School
   Monterey, CA 93943-5000

6. Dr. Frank B. Schwing   1
   NMFS, NOAA
   P.O. Box 831
   Monterey, CA 93942

7. CDR Dan E. Tracy   1
   Department of Oceanography
   Naval Postgraduate School
   Monterey, CA 93943-5000

8. Director Naval Oceanography Division   1
   Naval Observatory
   34th and Massachusetts Avenue NW
   Washington, DC 20390

9. Commander   1
   Naval Oceanography Command
   Stennis Space Center
   MS 39529-5000

10. Chief, Ocean Services Division   1
    National Atmospheric and Oceanic
     Administration
    8060 Thirteenth Street
    Silver Springs, MD 20910

11. Chief, Career Development Div.   1
    Commissioned Personnel Center
    National Atmospheric and Oceanic
     Administration
    Rockville, MD 20852

12. Director, Center for Ocean   1
    Analysis and Prediction
    NOAA,
    Monterey, CA 93940

13. Dr. Nicholas Fofonoff   1
    WHOI
    Woods Hole, MA 02543